Near Infrared Spectroscopy/Imaging and Terahertz Pulsed Spectroscopy/Imaging for the Analysis of Solid Dosage Forms

Inauguraldissertation

zur
Erlangung der Würde eines Doktors der Philosophie
vorgelegt der
Philosophisch-Naturwissenschaftlichen Fakultät
der Universität Basel

von

Lene Maurer
aus Zweibrücken, Deutschland

Basel, 2008

Genehmigt von der Philosophisch-Naturwissenschaftlichen Fakultät
auf Antrag von

Prof. Dr. Hans Leuenberger
PD Dr. Stephan Marrer
Dr. Andrea Kimpfler

Basel, den 20. Mai 2008

Prof. Dr. Hans-Peter Hauri
Dekan

Für meine Eltern

Danksagung

Die Danksagung in einer Doktorarbeit ist eine knifflige Angelegenheit. Man möchte einerseits natürlich niemanden vergessen, kann aber andererseits auch niemals alle nennen denen man danken möchte; es soll persönlich sein, aber die Sprache bringt es mit sich dass es dann doch irgendwie formell klingt. Und dann auch noch den richtigen Anfang zu finden…

Wenn man die Danksagung schreibt, ist normalerweise der grösste Teil der Dissertation vorbei. Natürlich kommt da dann irgendwann noch die Prüfung, aber das Zusammenschreiben hat man so gut wie hinter sich. Man fängt also so langsam an, sich zu freuen (endlich, endlich ist das Schreiben vorbei!) und dann sitzt man schon wieder vor einem leeren Blatt Papier (oder besser gesagt, vor einem grösstenteils weissen Bildschirm).

Man fängt also an, sich Gedanken zu machen, schreibt auf, wem man alles danken möchte… da wären natürlich der Doktorvater und die direkten und weiteren Betreuer, dann diejenigen, die finanziell zum Gelingen beigetragen haben, diejenigen, die einem den Arbeitsplatz zur Verfügung gestellt haben, diejenigen, die erst gegen Ende dazugestossen sind als das Korrigieren und die Prüfung anstanden, diejenigen, mit denen man konstruktive Diskussionen geführt hat, diejenigen, die Korrektur gelesen haben, diejenigen, mit denen man viel gelacht hat, diejenigen, die einen immer wieder aufgemuntert haben wenn mal nicht alles so geklappt hat wie gewünscht, diejenigen, die einen auf andere Weise unterstützt haben… Kurz gesagt: Auch wenn die Hauptarbeit natürlich an einem selbst hängt, stecken noch eine Menge anderer Personen dahinter, wenn eine Doktorarbeit gelingen soll. Diese Personen haben wirklich allen Dank verdient! Einige von ihnen werde ich nennen, andere nicht – sie wissen, dass ich sie nicht vergessen habe und werden nicht böse sein, wenn sie hier nicht namentlich erscheinen. Nun aber zum eigentlichen Danken…

Diese Industriedissertation wurde durch die Zusammenarbeit der galenischen Produktion fester Arzneiformen der F. Hoffmann-La Roche AG in Basel einerseits und des Instituts für Pharmazeutische Technologie der

Universität Basel andererseits ermöglicht. Darum geht mein Dank zunächst in zwei Richtungen.

Von universitärer Seite wurde die Dissertation von Herrn Prof. Dr. Hans Leuenberger als Doktorvater betreut. Er unterstützte mich mit wertvollen Diskussionen, aufbauender Kritik und interessanten Anregungen. Dadurch und durch seine gute Anleitung, wertvolle Hilfe und seinen reichen Erfahrungsschatz hat er massgeblich zum Gelingen dieser Doktorarbeit beigetragen. Hierfür danke ich ihm ganz herzlich.

Auf Seiten Roche möchte ich ganz besonders Herrn Dr. Thomas Polossek und Herrn Dr. Richard Söll danken. Die Dissertation wurde durch die Solidaproduktion ermöglicht – dies zeigt, dass in diesem Bereich innovative Technologien wichtig sind und dass viel Wert darauf gelegt wird. Für die Unterstützung, für den Input, für die Möglichkeit Erfahrungen zu sammeln und sowohl intern als auch extern auf Kursen viel dazuzulernen und dafür, dass ich selbständig arbeiten konnte, möchte ich mich herzlich bedanken. Besonderer Dank gilt Frau Dr. Andrea Kimpfler für ihre ausserordentliche Unterstützung als externe Expertin.

Ich möchte ausserdem Herrn Dr. Rolf Altermatt und Herrn Dr. Anton Fischer von der Abteilung Qualitätskontrolle dafür danken, dass ich während der Dissertation im „Process Robustness Support“-Labor arbeiten konnte. Sie haben mir grosszügig vorhandene Technologien zur Verfügung gestellt. Dank gilt auch meinen Kollegen in dieser Gruppe, speziell Frau Christelle Gendrin für ihre Hilfe beim Programmieren in Matlab.

Ein herzliches Dankeschön möchte ich Herrn PD Dr. Stephan Marrer aussprechen, der die Dissertation als Korreferent betreut hat. Herrn Prof. Dr. Matthias Hamburger danke ich dafür, dass er sich bereit erklärt hat, das Amt des Prüfungsvorsitzenden zu übernehmen.

Ich danke auch meiner Familie und meinen Freunden für die Unterstützung in dieser nicht immer ganz einfachen Doktorandenzeit. Ganz besonders möchte ich meinen Eltern danken. Mein Dank geht auch an Andreas und Sabine, bei denen ich zum ersten Mal „Pharmazieluft“ schnuppern durfte.

Zu guter Letzt möchte ich mich bei Pascal bedanken, der mich seit Beginn der Dissertation begleitet und unterstützt hat, immer viel Geduld aufbrachte und nie den Optimismus verlor.

Table of Contents

Summary

The pharmaceutical industry is highly regulated by health authorities and known for a certain hesitancy to introduce new technologies into the manufacturing sector. However, it is not desirable that on one hand, new and innovative technologies that could bring real benefits are available and on the other hand, such technologies are not implemented. At the beginning of the century, the Food and Drug Administration (FDA) therefore promoted the Process Analytical Technology (PAT) initiative. This initiative, which aims to enhance process understanding and control through different tools, encourages the development and implementation of innovative systems in pharmaceutical development, manufacturing and quality assurance. Analytical technologies are part of those systems; other parts are for example statistical design of experiments or process monitoring strategies.

In this thesis, different analytical technologies that could be valuable in a PAT context were used for the analysis of specific parameters of capsules and tablets. The technologies were evaluated and compared in a laboratory environment. Advantages and disadvantages are discussed and potential at-line or on-line applications are pointed out. One capsule product, two low-dosage tablet products and three film-coated tablet products were used for the evaluation of the following analytical techniques: near infrared (NIR) spectroscopy and imaging, terahertz pulsed spectroscopy (TPS) and imaging (TPI), and laser induced breakdown spectroscopy (LIBS). Additionally, implemented applications of NIR spectroscopy in the full-scale manufacturing of solid pharmaceuticals are presented.

The overview over applications of NIR spectroscopy in solids manufacturing shows that NIR spectroscopy is already used for measurements in nearly all production steps of the manufacturing of solid dosage forms. NIR spectroscopy serves for example for raw-materials identification and moisture determination during drying. Especially at-line analyses are in use, but on-line and in-line measurements also exist. The number of applications is growing and the overview shows that NIR spectroscopy can be a valuable PAT tool.

NIR imaging was applied to investigate hard-gelatin capsules for the presence or absence of a briquette in the capsule shell. The technique allowed detecting the briquette non-destructively. The study could be the basis for the implementation of a fast, non-destructive, near infrared in-process control which could replace the so far used destructive visual in-process controls. A possible way to automation is also shown.

NIR imaging was also applied to study the distribution of active pharmaceutical ingredient (API) in low-dosage tablets. A qualitative comparison of images taken from the tablet surface or from tablet layers was possible. In order to estimate the analyzed sample size, the penetration depth of NIR radiation into the tablets was investigated. This study shows that NIR imaging has potential for analyzing low-dosage tablets. However, quantitative analyses were not possible, and the method is not yet adequate for routine use in a production environment.

Low-dosage tablets were also used to evaluate the ability of TPS and TPI to give information about the API in such tablets. In both cases, determination of the API was not possible. The study indicates that at the moment, neither TPS nor TPI are appropriate to analyze the API in low-dosage tablets.

TPI was used to analyze the coating of film-coated tablets. The fast and non-destructive technique provided direct thickness values. Information about coating uniformity was obtained; and the monitoring of the film-coating process was possible. Limits of the technique due to spatial and depth resolution are discussed. The study shows that the technique has potential for at-line measurements and that it can be a valuable tool for better process understanding.

NIR imaging was applied for analyzing the coating of film-coated tablets, too. The results from this study were compared with TPI results. Both techniques provided useful data to monitor the growth of the coating during the coating process. The advantage of NIR imaging is the higher resolution compared to TPI, but TPI provides direct thickness data. A combination of the

two methods could be very advantageous, and at-line or on-line measurements might be possible.

Film-coated tablets and low-dosage tablets were also analyzed by LIBS. This destructive technique was not in the focus of the thesis; the measurements were therefore just intended as an additional comparison. The study indicates that LIBS is useful for fast estimations of coating thickness or lubricant determination; the analysis of API in low-dosage tablets was not possible in this case. Overall, NIR imaging and TPI were superior for the present questions.

The thesis can be the basis for further development of innovative analytical technologies which could be used in a PAT context, both in a development/up-scaling environment and a solids manufacturing environment.

Zusammenfassung

Die Pharmazeutische Industrie, die strengen Vorschriften und Richtlinien unterliegt, ist dafür bekannt, dass sie neue Technologien nur zögernd in den Herstellungsbereich einführt. Es ist jedoch nicht wünschenswert, dass auf der einen Seite neue und innovative Technologien, die wirklichen Nutzen bringen können, zur Verfügung stehen, dass diese Technologien auf der anderen Seite aber nicht verwendet werden. Zu Beginn dieses Jahrhunderts initiierte daher die Food and Drug Administration (FDA) die Process Analytical Technology (PAT) Initiative. Diese Initiative, die sowohl Prozessverständnis als auch Prozesskontrolle mittels unterschiedlicher Instrumente verbessern möchte, fördert die Entwicklung und Implementierung innovativer Systeme im Bereich der pharmazeutischen Entwicklung, Herstellung und Qualitätssicherung. Analytische Technologien stellen einen Teil dieser Systeme dar, wie zum Beispiel auch statistische Versuchsplanung oder Strategien zur Prozessüberwachung.

In dieser Dissertation wurden verschiedene analytische Technologien, die im Zusammenhang mit PAT nützlich sein können, zur Analyse bestimmter Parameter von Kapseln und Tabletten verwendet. Die Technologien wurden im Labor evaluiert und verglichen. Vor- und Nachteile werden diskutiert und mögliche at-line oder on-line Anwendungen werden aufgezeigt. Ein Kapsel-Produkt, zwei niedrigdosierte Tabletten-Produkte und drei Filmtabletten-Produkte wurden für die Evaluation der folgenden analytischen Technologien verwendet: Nahinfrarot (NIR)-Spektroskopie, Nahinfrarot-Imaging, gepulste Terahertz-Spektroskopie (TPS), gepulstes Terahertz-Imaging (TPI) und Laser Induced Breakdown Spektroskopie (LIBS). Zusätzlich werden bereits implementierte Anwendungen von NIR-Spektroskopie in der Produktion fester Arzneiformen vorgestellt.

Der Überblick darüber, wo Nahinfrarot-Spektroskopie in der Produktion fester Arzneiformen eingesetzt wird, zeigt, dass diese Technologie bereits für Messungen bei fast allen Herstellungsschritten benutzt wird. NIR-Spektroskopie wird zum Beispiel für die Identitätskontrolle von Ausgangsstoffen und zur

Feuchtebestimmung beim Trocknen verwendet. Besonders häufig sind at-line Analysen, es existieren aber auch on-line und in-line Messungen. Die Zahl der Anwendungen nimmt zu und der Überblick zeigt, dass NIR-Spektroskopie ein wertvolles PAT-Instrument sein kann.

Nahinfrarot-Imaging wurde zur Analyse von Hartgelatinekapseln verwendet. Mit dieser Technologie war es möglich, schnell und zerstörungsfrei zu bestimmen, ob in der Kapselhülle ein Formling vorhanden ist oder nicht. Die Studie könnte der Ausgangspunkt für die Implementierung einer schnellen, zerstörungsfreien Nahinfrarot-Inprozesskontrolle sein, die die verwendeten visuellen destruktiven Inprozesskontrollen ersetzen könnte. Ein Weg zu einer möglichen Automatisierung ist aufgezeigt.

NIR-Imaging wurde auch dazu verwendet, die Verteilung des Wirkstoffs in niedrigdosierten Tabletten zu untersuchen. Hyperspektrale Bilder der Tablettenoberfläche und von Tablettenschichten konnten qualitativ verglichen werden. Um die analysierte Probengrösse abzuschätzen, wurde die Eindringtiefe des Lichts in die Tabletten untersucht. Die Studie zeigt, dass Nahinfrarot-Imaging ein gewisses Potential für die Untersuchung niedrigdosierter Tabletten besitzt. Quantitative Analysen waren jedoch nicht möglich, und die Methode ist noch nicht für Routineuntersuchungen in der Produktion geeignet.

Niedrigdosierte Tabletten wurden ebenfalls für die Untersuchung verwendet, ob TPS und TPI Informationen über den Wirkstoff in solchen Tabletten geben können. In beiden Fällen war die Bestimmung des Wirkstoffs nicht möglich. Diese Studie deutet darauf hin, dass im Moment weder TPS noch TPI geeignet sind, den Wirkstoff in niedrigdosierten Tabletten zu analysieren.

TPI wurde weiterhin zur Analyse des Lacküberzugs von Filmtabletten benutzt. Mit der schnellen und zerstörungsfreien Technologie konnte die Schichtdicke der Lackschicht direkt bestimmt werden, und man erhielt Informationen über die Gleichmässigkeit des Überzugs. Weiterhin war die Beobachtung des Coatingprozesses möglich. Grenzen der Technologie aufgrund der Auflösung werden diskutiert. Insgesamt zeigt die Studie, dass die

Methode Potential für at-line Messungen besitzt und dass sie als nützliches Instrument für ein besseres Prozessverständnis dienen kann.

NIR-Imaging wurde ebenfalls zur Analyse des Überzugs von Filmtabletten verwendet. Die Ergebnisse dieser Untersuchung wurden mit den TPI-Ergebnissen verglichen. Beide Technologien gaben nützliche Informationen über das Wachstum des Überzugs während des Coatingprozesses. Der Vorteil des Nahinfrarot-Imaging gegenüber dem gepulsten Terahertz-Imaging ist die bessere Auflösung, wohingegen TPI die Dicke des Überzugs direkt analysiert. Eine Kombination beider Methoden könnte sehr vorteilhaft sein, und at-line oder on-line Messungen könnten möglich sein.

Niedrigdosierte Tabletten und Filmtabletten wurden auch mittels LIBS untersucht. Diese destruktive Technologie war keiner der Schwerpunkte der Arbeit, die Messungen waren lediglich als ein zusätzlicher Vergleich gedacht. Die Untersuchungen deuten darauf hin, dass LIBS zur schnellen Abschätzung der Coatingdicke und Schmiermittelverteilung nützlich sein kann. Die Bestimmung des Wirkstoffs war im Fall der untersuchten niedrigdosierten Tabletten nicht möglich. Insgesamt waren NIR-Imaging und TPI für die vorliegenden Fragestellungen besser geeignet.

Diese Dissertation kann die Grundlage für die weitere Entwicklung innovativer analytischer Technologien, die im Zusammenhang mit PAT verwendet werden können, darstellen, und zwar sowohl in Rahmen der Entwicklung und des Upscalings als auch im Bereich der Produktion fester Arzneiformen.

Abbreviations

AOTF	**A**cousto-**O**ptical **T**unable **F**ilter
API	**A**ctive **P**harmaceutical **I**ngredient
a.u.	**A**rbitrary **U**nits
CCD	**C**harge-**C**oupled **D**evice
FDA	**F**ood and **D**rug **A**dministration
FOV	**F**ield **o**f **V**iew
FPA	**F**ocal **P**lane **A**rray
FT	**F**ourier **T**ransform
GMP	**G**ood **M**anufacturing **P**ractice
HPLC	**H**igh **P**erformance **L**iquid **C**hromatography
IPC	**I**n-**P**rocess **C**ontrol
IR	**I**nfra**r**ed
LCTF	**L**iquid **C**rystal **T**unable **F**ilter
LIBS	**L**aser **I**nduced **B**reakdown **S**pectroscopy
Nd:YAG	**N**eo**d**ymium **D**oped **Y**ttrium **A**luminum **G**arnet
NIR	**N**ear **I**nfra**r**ed
PAT	**P**rocess **A**nalytical **T**echnology
PCA	**P**rincipal **C**omponent **A**nalysis
PLS	**P**artial **L**east **S**quares
PLS-DA	**P**artial **L**east **S**quares **D**iscriminant **A**nalysis
SNV	**S**tandard **N**ormal **V**ariate
THz	**T**era**h**ertz
TPI	**T**erahertz **P**ulsed **I**maging

TPS	**T**erahertz **P**ulsed **S**pectroscopy
UV	**U**ltra**v**iolet part of the electromagnetic spectrum
VIS	**Vis**ible part of the electromagnetic spectrum
(w/w)	(**W**eight/**W**eight)

1

Introduction

1.1 Background

The quality of a pharmaceutical is a very important parameter as it helps to ensure the equally important safety and efficacy of the drug. There are many ways to ensure the quality of a drug; very common is the testing of parameters such as identity or content during the manufacturing process and of the finished product in specialized quality control laboratories. However, such laboratory-based methods, where only a very small amount of the product is tested, have several drawbacks. They are very often environmentally critical due to the required use of solvents; they are generally destructive and often only one parameter is tested at a time, for example the content of the active pharmaceutical ingredient (API) in a tablet, while information about its distribution might be neglected. The fact that measurements are normally time-consuming leads to long cycle times, high inventories and the need for extensive warehouse space as materials and products are normally "quarantined" until the test results are available, thus increasing the costs.

Nowadays, there are modern and innovative technologies available that are able to overcome these disadvantages. Some, like for example near infrared (NIR) spectroscopy, have already been in use for years in other fields; others, like for example terahertz- (THz-) based technologies, are quite new to both the pharmaceutical industry and other fields. They are often able to investigate multiple parameters in one measurement, being fast and non-destructive at the same time, and less pollutant than classical wet-chemical methods.

However, the pharmaceutical industry is heavily regulated by authorities and rather known for its hesitancy to introduce new technologies into the manufacturing sector. Thus, innovative technologies are available but not implemented. To overcome this hesitancy, and to encourage the development and implementation of innovative systems in pharmaceutical development, manufacturing and quality assurance, the Food and Drug Administration (FDA) promoted the Process Analytical Technology (PAT) initiative at the beginning of this century.

PAT can be defined as a "*system for designing, analyzing and controlling manufacturing through timely measurements of critical quality and performance attributes of raw and in-process materials and processes, with the goal of ensuring final product quality*" [1]. It serves to enhance the understanding and control of manufacturing processes, and in this way leads to higher quality. It is consistent with the fact that quality cannot be tested into products, meaning that tests alone are not the correct way to guarantee the quality of a product. In other words, the analytics do not make the quality, they only check it. Instead, the quality has to be built into the product or it has to be by design. This can be achieved by identifying key performance parameters early in the development phase of a product, and then scientifically designing the product and the manufacturing process in such a way that they are robust for these parameters. PAT is not the testing of the final product, but the understanding and controlling of the way to the final product. The designing of well understood processes ensures that the process will yield a product of a predefined quality. PAT attempts to shift pharmaceutical drug development and manufacturing from an art to a science; there should be a mechanistic understanding of how product performance is affected by formulation and process factors. This is illustrated by the knowledge pyramid (figure 1.1). The goal is to reach the top, to understand processes better, and in this way ensure quality through the design of the processes and products itself.

By applying PAT, risks to quality can be reduced and efficiency can be improved. It can for example reduce costs by preventing rejects or scraps, production cycle times can be reduced by in-, on- or at-line measurements,

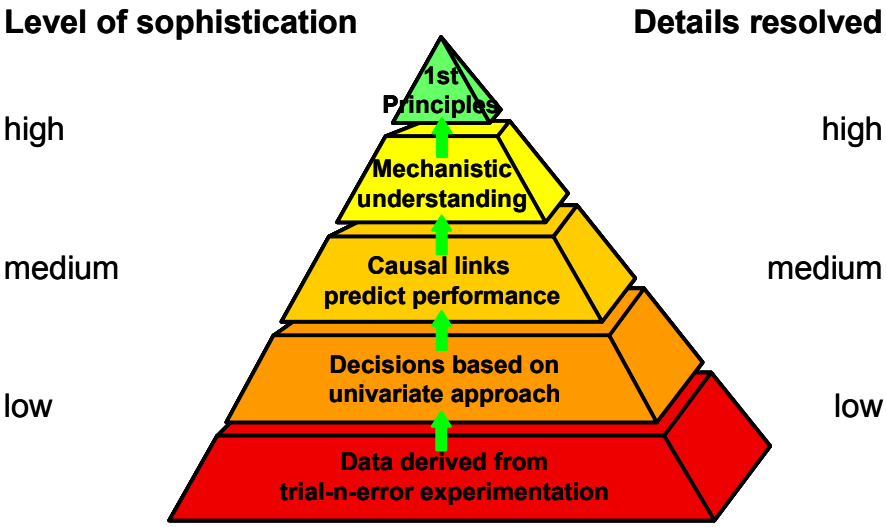

Figure 1.1 Product and process quality knowledge pyramid (source: Dr. A. S. Hussain, formerly FDA).

human errors can be minimized by increasing automation and real-time release can be possible. Four different tools are applied in PAT; several or all can be combined to reach the goals. These are multivariate tools for design, data acquisition and analysis, process analyzers, process control tools and continuous improvement/knowledge management tools. This shows that new analytical technologies, which are part of the process analyzers, are only a part of the strategy.

1.2 Content and Aim of the Thesis

In this work, different new technologies that could possibly be used in a PAT context were investigated in a laboratory environment. Only solid dosage forms, i.e. capsules and tablets, were analyzed. All the products used were marketed products or products in a late development phase. Thus, it was not the goal to investigate different formulations or to decide which process was most suitable for the manufacturing of a product; instead the focus lay on the analytical techniques. Mainly two different technologies were investigated. Those were on one hand near infrared spectroscopy and imaging and on the other hand terahertz pulsed spectroscopy (TPS) and imaging (TPI). Additionally laser induced breakdown spectroscopy (LIBS) was investigated, but being a

destructive technique it was not the focus of this work and was mainly looked at for a comparison with NIR imaging and TPI. All LIBS- and terahertz-based analyses were commissioned work and conducted in specialized laboratories; all NIR-based experiments were conducted at F. Hoffmann-La Roche Ltd.

The aim of the work was to evaluate and compare the different technologies for their ability to analyze solid dosage forms for defined parameters. In the context of the PAT initiative, it is necessary to investigate new technologies in order to see if they can possibly replace classical wet-chemical methods. If non-destructive techniques like TPI could provide the same results as the classical wet-chemical methods, there would be the opportunity to analyze higher amounts of samples. It is important to evaluate if the new technologies would be useful tools in a manufacturing environment to control processes and intermediate products, or if they would be of higher value in an earlier step of the product life cycle, like for example in the development or scale-up phase. Moreover, it should be known if they are able to provide more information than those conventional wet-chemical methods, and if they are helpful for understanding processes better.

Six different products were analyzed. Table 1.1 gives an overview of which product was analyzed by which technique. The chosen products were understood as examples that served to evaluate the analytical techniques.

Product	Characteristic	Analytical technique				
		NIRS	NIRI	TPS	TPI	LIBS
A	Capsule	x	x			
B	Low-dosage tablet		x	x	x	x
C	Low-dosage tablet			x		
D	Film-coated tablet				x	x
E	Film-coated tablet		x		x	
F	Film-coated tablet				x	

Table 1.1 Overview of the products and the applied analytical techniques (NIRS: NIR spectroscopy; NIRI: NIR imaging).

Therefore details about the identity, the composition and the manufacturing of the products were only secondary. For this reason, and also for trade secrecy, detailed information about the products is not given, and the products were

named A, B, C etc.. However, where it is necessary to know more details, they are provided. For example for coating analyses, the composition of the core was not in question and is therefore not given, but information about the coating is available.

The first product which consisted of hard-gelatin capsules was analyzed by NIR imaging and spectroscopy. The aim was to investigate if the presence of a “briquette” in the capsule shell could be detected non-destructively by NIR and possibly replace the so-far applied destructive visual control.

All the other analyzed products were tablets. Two groups could be defined: uncoated low-dosage tablets on the one hand and film-coated tablets on the other. The low-dosage tablets were used to investigate the ability of NIR imaging, TPS/TPI and LIBS to provide information about the distribution of the API and, to some extend, excipients in the samples. It was decided to use low-dosage tablets because, in those products, the distribution of API is more critical and the detection challenge is higher; in this way, it was expected that the limits of the techniques would show up more clearly. The film-coated tablets were mainly used for analysis of coating thickness and uniformity by TPI. One of the products was also analyzed by NIR imaging to allow comparison of this method with TPI. One of the coated products was also analyzed by LIBS. Additionally, the application of NIR spectroscopy in solids manufacturing was investigated, and an overview over such applications is given.

As the focus lay on the analytical techniques and not on the different products, the following chapters 2, 3 and 5 cover one analytical method each. In chapter 4, the comparison of NIR imaging and TPI for coating analysis is presented. Each chapter gives an introduction to the applied technology, then the experimental work is presented and discussed and a short conclusion/outlook on the specific experiments is given. Chapter 6 contains the overall conclusion and outlook.

2

Near Infrared Spectroscopy and Imaging

2.1 Introduction

Although NIR radiation was discovered by Herschel as long ago as 1800 [2], and some more work considering this region was done at the end of the 19th and the beginning of the 20th century, NIR spectroscopy had a slow start. The many weak and overlapping peaks were too confusing, difficult to resolve and to interpret and the region was considered useless. It was only in the second half of the 20th century that the breakthrough in industrial applications of NIR occurred. Norris started to use NIR spectroscopy for the analysis of agricultural products in the 1950s and 1960s. Commercial instruments became available in the 1970s [3]. As modern NIR technology depends on computers, for example for data acquisition and analysis, the fast development of this area at the end of the 20th century promoted the development of NIR as well.

The NIR region spans the range from 800 nm to 2500 nm or 12500 cm^{-1} to 4000 cm^{-1} (figure 2.1). It contains absorption bands corresponding to

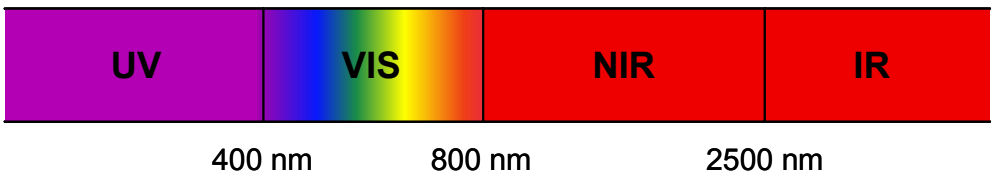

Figure 2.1 Part of the electromagnetic spectrum with the NIR region.

overtones and combinations of fundamental vibrations which occur in the mid infrared (IR). The bonds that contribute most are CH, OH, SH and NH bonds [4]. At room temperature, most molecules are at rest or at their ground energy

levels. The absorption of light energy leads to stretching and deformation of bonds between atoms, i.e. atom-to-atom bonds within molecules vibrate, and they are excited to higher energy levels [3]. At room temperature, these transitions occur from the ground state. Transitions between this ground state and the first energy level are called fundamental vibrations; they occur mainly in the mid infrared region. If the transition occurs between the ground state and energy level 2, 3, or higher, it is called overtone (figure 2.2). Transition between multiple states can also occur, these are the combinations. Among those

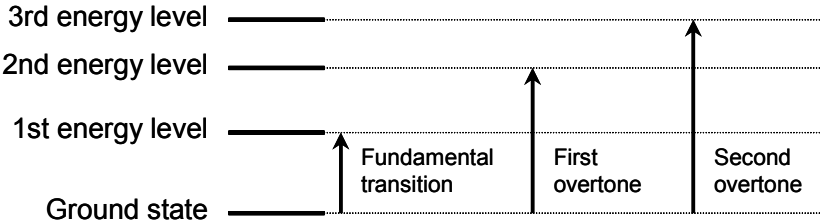

Figure 2.2 Energy level diagram with fundamental transition and overtones.

transitions, fundamental transitions need least energy. Basically, overtones and combinations are not allowed, but they appear due to anharmonicity or Fermi resonance [3]. The transition probabilities for overtones and combinations are lower than for fundamentals, and the intensities of absorption bands are 10 to 1000 times weaker than those of fundamental bands [4].

These low absorption coefficients are the reason that, when using NIR, a sample preparation is most often not necessary, unlike in mid infrared analysis, where a sample dilution is mostly needed. This is of course advantageous, but might bring problems when a low concentrated compound is present in an absorbing matrix. NIR spectra do not only contain chemical information, e.g. about the components that are present in a tablet, but also physical information, e.g. about the particle size in a powdered sample.

Common sampling modes in NIR spectroscopy are diffuse reflection, transmission and transflection (figure 2.3). In diffuse reflection, the source and the detector are on the same side of the sample. The light penetrates the sample to a certain depth, a part is absorbed and the rest is reflected. If a sample is inhomogeneous, this measurement mode might be problematic as

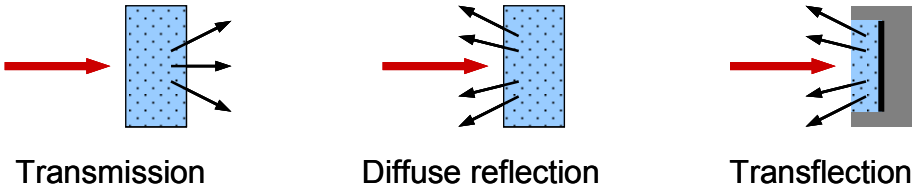

Figure 2.3 Different sampling modes; incident light beam in red, sample in blue.

only a part of the sample is analyzed. In transmission, source and detector are on opposite sides of the sample. The light has to cross through the sample completely before reaching the detector. The advantage is that a bigger part of the sample is analyzed than in reflection, but if the sample gets too thick, the light might not be able to pass through it and thus no light reaches the detector. In transflection, source and detector are placed on the same side of the sample. The light passes through the sample, is reflected by a mirror, and passes through the sample again before reaching the detector. This way, transmitted and diffusely reflected light are detected. The spectra which are recorded in raw reflectance or raw transmittance are normally converted to absorbance using the term $\log_{10}$ (1/reflectance) or $\log_{10}$ (1/transmittance), respectively.

A wide variety of instruments is available. Different criteria to distinguish between spectrometers exist, for example by scan rates (fast, medium and slow), detector types (e.g. multichannel diode array, broadband single channel) and ruggedness (e.g. dustproof, insensitive to vibrations). Mostly, spectrometers are differentiated by their optical configuration as they often correlate with the previously named criteria. There are instruments with interference filters, diffraction gratings, prisms, NIR emitting diodes, interferometers and acousto-optical tunable filters [3]. The choice has to be made according to the intended use; for example, in a laboratory environment Fourier transform (FT) spectrometers containing an interferometer are often used because of the high spectral resolution they provide, for on-line measurement the choice may be a robust and fast diode-array spectrometer. As glass is transparent for NIR radiation, the spectrometers may be used in

combination with fiber optics and fiber probes, increasing the flexibility for the use of the instruments and for example allowing remote sampling.

In NIR spectroscopy, only one spectrum per sample is obtained. This spectrum is normally the average of multiple spectra taken from the same spot of the sample in order to improve the signal-to-noise ratio. There is no spatial information in this spectrum; it contains the average information of the whole region that is analyzed. However, in some cases, it is useful or necessary to obtain spatial information. For example, the content of API in a tablet might be determined by NIR spectroscopy, but this technique is not able to provide information about the distribution of the active ingredient within the tablet. But a technique has been developed that also provides spatial information: hyperspectral NIR imaging. The basics of NIR imaging are the same as for NIR spectroscopy. But instead of acquiring one spectrum per sample, a data cube with several thousand spectra is obtained by one measurement. This is achieved by using, for example, a focal plane array (FPA) detector. Such a detector consists of multiple pixels, e.g. 256 x 320 pixels. Each pixel forms a small detector and during measurement, each pixel records a spectrum. In the above-named example, this results in 81920 spectra per measurement instead

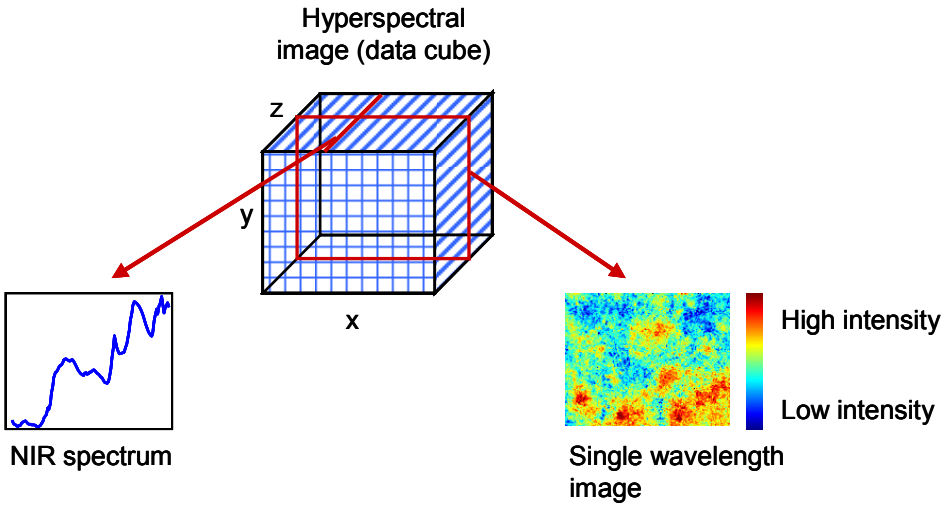

Figure 2.4 Diagram of hyperspectral NIR imaging; x- and y-axis provide spatial information and z-axis provides spectral data.

of one like in classical NIR spectroscopy. Thus, spatial and spectral information is obtained. The x-axis and the y-axis, i.e. the location of the pixels, provide spatial information and the z-axis contains the spectral data, i.e. the spectra (figure 2.4). Images are usually displayed as false-color images and a color scale determines which color goes with which intensity, i.e. absorbance value. Very common is the so-called jet color scale where red indicates the highest and blue indicates the lowest intensity (figure 2.4). The gray scale is also used; in this case white corresponds to the highest and black to the lowest intensity values. There are other possibilities in NIR imaging besides FPA detectors, such as push-broom-devices. In this case, the detector is only a single line of pixels that records one line of spectra after another, in a kind of scanning or "brooming" over the sample. However, instruments with FPA detectors are more established at the moment than the faster but younger push-broom-devices. Although transmission measurements are basically possible in NIR imaging, diffuse reflection is the sampling mode that is commonly used.

NIR spectroscopy and imaging offers advantages such as being fast and non-destructive, and normally no sample preparation is needed. Many applications in pharmaceuticals have been reported. For example, the quality control of solid pharmaceuticals plays an important role; here NIR has been used to determine drug dissolution [5-7], tablet hardness [8], tablet content [9-11] and identity [12]. It has also been used in packaging [13,14], coating [15,16] and for counterfeit drug detection [17,18]. Other examples for application of NIR in pharmaceuticals include blending [19-24], granulation [25-30], roller compaction [31], lyophilization [32] and development [33]. The number of applications is still growing.

The broad, overlapping bands in NIR spectra make it difficult to interpret the data directly. Therefore, multivariate data analysis is normally applied in NIR spectroscopy and imaging. Spectral pretreatments are used to filter or reduce secondary effects. For example, derivatives with smoothing factors such as Savitzky-Golay 2^{nd} derivative are used to show the peaks better and to reduce noise. Normalizations such as the standard normal variate (SNV) transformation suppress baseline shifts. There are many ways that can help in extracting the

wanted information out of the data. For example, principal component analysis (PCA) helps to better display the sought information in the spectra by reducing the multidimensional space and showing the biggest variances in the data; an operation that is very difficult or impossible to do by univariate analysis or “by the eye”. Partial least squares (PLS) is mostly used in quantitative analysis where, for example, a model of a set of known samples is built and then used to determine the content of unknown samples of the same kind. Partial least squares discriminant analysis (PLS-DA) can be used non-quantitatively, for example, in NIR imaging to determine the distribution of compounds in a sample. Here, not a quantitative model is built, but information about the components, i.e. reference spectra of the pure components, is “fed” to the algorithm to help it to find the wanted information in the data.

2.2 Applications of Near Infrared Spectroscopy in the Full-Scale Manufacturing of Pharmaceutical Solid Dosage Forms

2.2.1 Introduction

In many industries and work fields, such as food, paper, agriculture, oil, or dairy, near infrared spectroscopy is widely known and has been used for many years. In the pharmaceutical industry, the case is different: owing to a very strict regulatory environment, the introduction of or switch to new technologies is difficult. For example, new technologies have to be validated and compared with currently used techniques – a time and cost-involving procedure. Thus, NIR spectroscopy was adopted by pharmaceutical industry only some time after it had been well established in other fields and the starts of NIR in pharmaceutics were rather slow. However, regulations changed and were updated to meet more easily the possibilities that modern technologies offer. As explained in chapter 1, the PAT initiative encouraged the wider use of new technologies such as NIR spectroscopy [1]. Of course, PAT is not just the use of new technologies; they are only part of the strategy. However, they have their justification as tools that help process understanding and control.

Nowadays, NIR spectroscopy is well established in pharmaceutics. It can be used in many fields and steps in the manufacturing of pharmaceuticals. For example, Blanco and Serrano showed the ability of NIR spectroscopy for reaction monitoring: they were able to monitor and quantify the acid-catalyzed esterification of butan-1-ol by acetic acid by NIR spectroscopy [34]. A number of applications is reported for content determination and quantification. For example, Gottfries et al. used NIR spectroscopy to quantify metoprolol succinate in controlled-release tablets [9] and Chalus et al. determined the content of active pharmaceutical ingredient in low-dosage tablets by NIR spectroscopy [10]. Berntsson et al. used NIR spectroscopy for the quantification of binary powder mixtures [35] and Trafford et al. developed a rapid quantitative assay of paracetamol tablets by NIR spectroscopy [36]. As shown by Räsänen and Sandler, NIR spectroscopy is also a useful tool in the development of solid dosage forms [37]. That NIR spectroscopy is valuable for identification is shown

for example by Candolfi et al., who applied NIR spectroscopy to identify pharmaceutical excipients [38]. Applications of NIR spectroscopy also exist for process monitoring: Rantanen et al. measured the moisture content during fluidized bed granulation [27] and Berntsson et al. monitored the blending of powders quantitatively by NIR spectroscopy [22]. NIR spectroscopy can also be successfully applied in quality control, as shown for example by Petri et al. [39]. The number of applications is still growing, taking into account the recently developed NIR imaging as well. Owing to their fast and non-destructive nature NIR techniques enable a better process understanding and better process control, thereby ensuring more robust processes and speeding up the whole manufacturing process, e.g. by reduced analysis times.

This chapter gives an overview of the full-scale manufacturing process of oral solid dosage forms from incoming raw materials via steps like blending, granulating, drying to tabletting and the application of NIR spectroscopy during those manufacturing steps in ten solids manufacturing plants of leading pharmaceutical companies in Switzerland and Germany. Classical methods that are used for control in solids manufacturing such as power consumption monitoring during high-shear granulation or compaction force monitoring during tabletting are not considered here. The focus lies entirely on the applications of NIR spectroscopy in full-scale manufacturing of oral pharmaceutical solid dosage forms; areas like development are not considered.

Mainly on- and in-line applications are taken into account. As the terms “at-line”, “on-line” and “in-line” are used inconsistently, the terms employed in this text refer to the definitions that are given in the PAT – Guidance for Industry [1]. “At-line” refers to a “*measurement where the sample is removed, isolated from, and analyzed in close proximity to the process stream*”. An “on-line” measurement is a “*measurement where the sample is diverted from the manufacturing process, and may be returned to the process*”. “In-line” describes a “*measurement where the sample is not removed from the process stream and can be invasive or noninvasive*” (figure 2.5). The earliest developed, easiest to use and most common is the at-line analysis. The samples, e.g. tablets, are taken out of the process and analyzed by means of a closely related, mostly

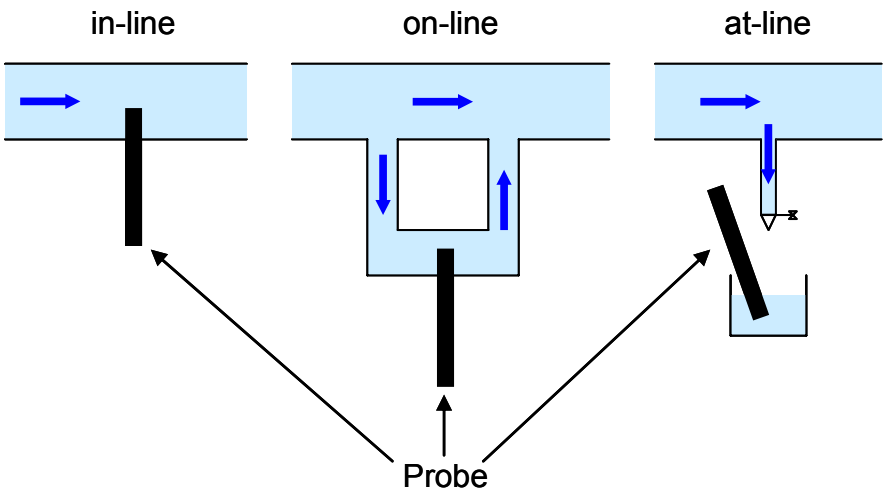

Figure 2.5 Schematic illustration of in-line, on-line and at-line measurements.

stand-alone NIR device. One of the reasons that this is the most widespread method is the fact that, normally, the sampling procedure is already established: it is the same as for classical controls and analyses. For example, tablets are sampled right after the press and brought to a close-by laboratory for classical in-process controls such as hardness or friability, or they are brought to the same lab and analyzed by NIR. Moreover, NIR spectroscopy was developed in research laboratories on stand-alone NIR devices, and of the named applications in manufacturing the at-line methods are the ones that are closest to analysis in a research laboratory. Thus, the implementation of such a method is relatively easy. More complex than this are on-line methods: the sample is diverted from the process stream, but not completely removed, and it may be returned to the process. Normally in this case the sampling is automated, meaning the implementation of autosampling devices, and the measurement is conducted very close to the process stream, e.g. in a by-stream. On the one hand, this method brings the possibility to analyze greater amounts of samples; on the other hand, this requires higher measurement speed. In-line measurements permit non-stop or 100% control of the processes and products. Tempting as this may sound, the measurements are very complex, sometimes the most complex of the three possibilities. The sampling, which sometimes causes problems, is no longer necessary, but this method normally requires the

highest speed, and the manufacturing equipment has to be designed to allow measurement directly in the process stream, e.g. via probes or windows. In the manufacturing of an established product, where the process has been designed and in use for several years, the rebuilding of the equipment with the involved cost and registration work is a factor that must not be underestimated. The benefits of NIR spectroscopy such as time and cost savings by creating more robust processes or reducing analysis time are worth implementation in certain cases. In other cases, however, the challenges and costs are too high and an implementation may not (yet) be possible. For example, a 100% in-line control of tablets requires a measurement speed that is very difficult to meet, considering the fact that modern tablet presses can work at speeds of more than 1 million tablets per hour.

One fact that has to be considered when talking about NIR spectroscopy is that the implementation, including the development and validation of the method, is very laborious and time-consuming. Once implemented, it is indeed fast and easy to use, but before the benefits are reaped, a lot of work has to be performed and finance has to be put in. To develop a NIR method, classical analytical methods are required for validation, which in some cases may be difficult, e.g. for sampling problems. And even though NIR spectroscopy has a great potential, for some problems it might be unable to provide the answer. However, for other problems, it may be the technique that offers the solution.

2.2.2 Solids Manufacturing

Solid dosage forms contain one or more API and most often several excipients. They include powders, granules, capsules, tablets and film-coated tablets. Manufacturing starts with the so-called raw materials, in this case powders. API and excipients are blended, this mixture can be directly compressed into tablets, filled into capsules or it is already the final dosage form. More often, the mixture is granulated to improve processability. The resulting granulate can again be filled into capsules, compressed into tablets or used as the dosage form. In case of wet granulation, a drying step is required, e.g. fluidized-bed drying. Intermediate blending steps may also be necessary.

Tablets and other forms, such as pellets, a special granulate form, can be coated in order to enable controlled release, ensure stability or for taste masking, for example.

A very common process flow starts with the raw materials (API and excipients) that are weighed and wet-granulated, then dried in a fluidized-bed dryer, mixed with some more excipients and then compressed into tablets (figure 2.6). In such a process, NIR spectroscopy can theoretically be applied to all steps: identification of incoming materials, blend monitoring and blending

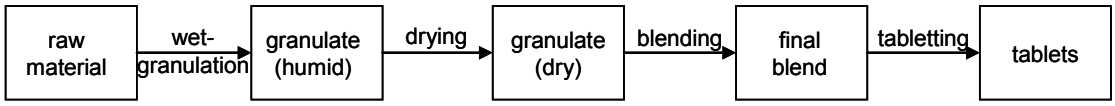

Figure 2.6 Common process flow in the manufacturing of solid dosage forms.

end-point determination, monitoring of the granulation, moisture determination during drying and drying end-point determination, monitoring of the tabletting and tablet control directly at the press. The present chapter focuses on the named process steps, not taking into account other possible steps like dry granulation or coating, as in the considered manufacturing plants mainly the named steps are addressed by NIR spectroscopy.

The decision to apply NIR spectroscopy in solids manufacturing can be made on the basis of different approaches. One approach would be to take the manufacturing process, look at the different steps, carry out a risk analysis to see where closer control or more process understanding is necessary, and choose analytical methods to monitor the steps where necessary. NIR spectroscopy may then be one of the possible methods that can be applied theoretically. In other cases, the approach is more historical, NIR spectroscopy having been already applied in laboratories in quality control, for example, and then “coming closer” to manufacturing. It is also possible to try NIR spectroscopy for one product in production at first and expand it to more products eventually. However, before aiming to implement NIR in production, experiments and tests with the spectrometer in a laboratory or up-scaling environment make sense, giving a better understanding if first NIR

spectroscopy and second the chosen spectrometer are suitable for the problem or not.

2.2.2.1 Raw-Materials Identification

Identity and quality of raw-materials have to be ensured [40]. Especially for identification of single substances, NIR spectroscopy is a fast and easy-to-use tool in the warehouse of the manufacturing plant. A library with the materials that have to be identified is normally developed in the laboratory, e.g. a quality control laboratory, enabling fast identification of the incoming materials. The identification can then be done in the warehouse and/or directly before weighing the powders by the workmen themselves. Most pharmaceutical companies use NIR spectroscopy in the warehouse for several reasons: it is fast and helps ensure quality by excluding wrong or bad-quality substances, and identification directly before further processing minimizes possible mix-up errors. Moreover, it is easy to use, which means that no specialized personnel are necessary, but that warehouse workers can use it. It was also one of the first applications of NIR spectroscopy in the pharmaceutical industry, which is one more reason that this is now a very common application.

Measurements can be performed in different ways. The classical method is to fill some of the powder into a vial or a similar small container and measure it by placing it on the spectrometer. Very common is the use of fiber optic probes. They are inserted directly into the powder or in some cases the measurement is done non-invasively through the plastic bag that contains the material. This is especially valuable when having highly potent material, avoiding open handling of the substances. However, when choosing to measure through the packaging material, this material has to be transparent for NIR radiation and the library has to be built up considering this material. It also requires that the supplier of the raw materials does not change the packaging material.

2.2.2.2 Granulation

The most often used granulation method is wet granulation. There, two different types are very common: granulation in the fluid bed and in high shear

mixers/granulators. Basically, NIR spectroscopy can be used to monitor different parameters, such as humidity/water content, particle size, homogeneity, etc. Measurement can be done through a window that is transparent to NIR radiation or via the insertion of a probe. A special problem in wet granulation is the sticking of the material to the window or the probe, thus making measurement difficult or impossible. This problem may be solved by windows that are cleaned during the process, e.g. by air flow, or probes that are periodically withdrawn to be cleaned (figure 2.7). The parameter that is easiest

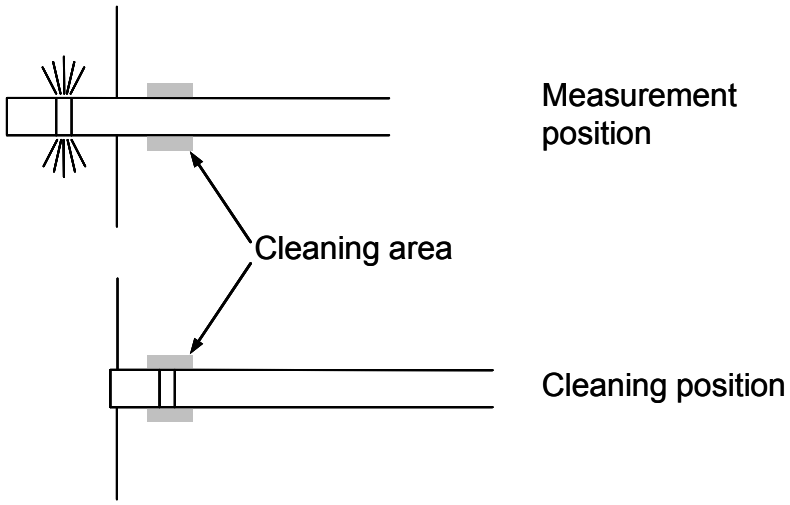

Figure 2.7 Schema of a probe that can be cleaned during the granulation/drying process e.g. by rinsing with water or cleaning liquid and drying by air without the need to open the chamber.

to monitor is probably the water content owing to the very dominant water absorption bands in NIR spectra. However, the question is if it really has to be monitored during granulation by such a sophisticated method as NIR spectroscopy when it can be easily calculated via the amount and flow rate of the granulation liquid. Thus, the monitoring of water content is more commonly applied in drying. Overall, granulation monitoring via NIR spectroscopy is not a very common application in the manufacturing of solid dosage forms.

2.2.2.3 Drying

Drying of granules in the manufacturing of solid dosage forms is mostly obtained by fluid bed drying. As mentioned above, the water content can be monitored with NIR spectroscopy through windows in the dryer or probes that

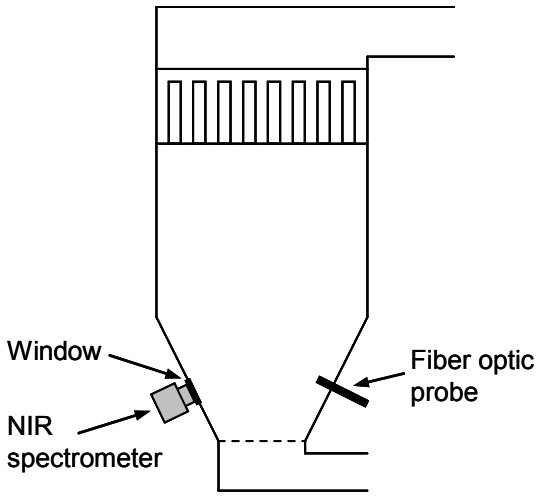

Figure 2.8 Schema of possible installations for in-line moisture monitoring in a fluid bed dryer by NIR spectroscopy.

are inserted in the chamber (figure 2.8). If sticking is a problem with the analyzed product, it may be avoided by different methods. One possibility is to place the probe in the upstream air flow. Another is the use of a probe that can be withdrawn during the process without opening the process chamber, cleaned while withdrawn and reinserted into the drying chamber (figure 2.7). In this case the measurement cannot be continuous but has to be stopped during the cleaning. Normally this does not pose a problem, as full-scale drying processes are not this fast. One solution can be to insert the probe only at a late stage of the drying process when the material is less wet and therefore less sticky. An advantage of using NIR spectroscopy is the speed of the humidity determination. Moreover, the chamber does not have to be opened to retain a sample for classical water content monitoring (e.g. loss on drying). This is of course an advantage when handling highly potent material. By determining the water content, the end-point of the drying can be defined and it may be possible to stop the drying process automatically. However, if open handling of material is not critical, samples can be taken and measured at-line by NIR spectroscopy. This is possibly still faster than determining the humidity by classical analysis like loss on drying. Both the in-line and at-line method are applied in solids manufacturing.

2.2.2.4 Blending

Bin blenders are commonly used for blending of powders or granules in the manufacturing of solid dosage forms. For in-line blend monitoring by NIR spectroscopy basically two installations are possible. If the blender has a window where the spectrometer or probe head can be placed, measurement can be performed through the window. The window material has to be transparent to NIR radiation; e.g. materials like sapphire glass are used. If there is no window in the blender, the lid of the blender can be modified to feature a window through which measurement can be carried out. The spectrometer can be mounted on the blender and turn with it during the mixing process. Owing to the turning of the blender, the use of cables for data transfer or power supply is not possible. Data can be transferred by wireless means or, less preferably, saved and read out after the process. The power supply to the spectrometer can be by batteries or slip rings. Measurement might be continuous or triggered, e.g. by time or gravity. If continuous, spectra are not only recorded when the window is covered by material but also when it is on the up-side and therefore not covered by material. In that case the bad spectra, i.e. those that are taken when the window is uncovered, have to be eliminated after the measurement. If triggered, the measurement only takes place when the window is on the down-side, meaning that it is covered by material. A goal is to ensure homogeneity of the blend, but also the monitoring of the mixing process provides valuable information. In a classical blending process, the mixing is performed over a certain time period that has been developed and validated and it is stopped after that certain time. If homogeneity can be determined in real time by NIR spectroscopy, the blending end-point can be determined and thus blending time can be saved, as in the classical method the mixing is conducted mainly too long to ensure homogeneity of the blend. However, as de-mixing may occur with excessively long blend times, this approach sometimes presents a risk. The monitoring of the process by NIR spectroscopy allows one not only to determine the end point but also to observe such de-mixing phenomena, thus ensuring better homogeneity and quality. In-line end-point determination may be applied to give feedback to the blender, enabling automatic stopping of the mixing process. Even if not applied in-line, at-line NIR spectroscopy can help

reduce time and work. If samples are taken from the blender, e.g. by a sample thief, homogeneity can be determined by a stand-alone spectrometer instead of by classical time-consuming wet-chemical methods. The direct in-line measurement has the advantage that it avoids sampling errors. Only if the material is very sticky, care has to be taken that it does not adhere to the window and tamper with the analysis. Applications of blend monitoring and end-point control exist in the manufacturing of solid pharmaceuticals, but they are maybe more appreciated as a valuable tool in the development and up-scaling of solid dosage forms.

2.2.2.5 Tabletting

Some tablet presses are enormously fast and produce more than 1 million tablets per hour. This is a speed where a 100% on-line control by NIR spectroscopy is not (yet) possible, at least not if only one or two spectrometers are used. Theoretically, it is possible to measure any amount of samples in a short time by using enough spectrometers, but this solution is too expensive to be considered seriously. At a lower speed, e.g. 200 000 or 300 000 tablets per hour, a 100% in-line control by one or two NIR spectrometers is possible but still very challenging. For example, if a double rotary press ejects 125 000 tablets per hour per side, by installing a spectrometer at each ejection side, 100% tablet control is possible with an overall press speed of 250 000 tablets per hour. Installation can be made by using a probe head connected via fiber optics to the spectrometer that is placed inside the tablet press directly before the tablet scraper. This type of probe enables reflection measurements. Parameters that can be determined theoretically are identity, inter-tablet homogeneity and content or content uniformity, which is however very challenging owing to the required speed not only of the spectrometer but of the calculations as well. Moreover, dust may be a big problem for anything installed on the press: dust overlying the measurement head may disturb analysis. A possible goal would be to identify “bad” tablets, i.e. tablets that do not conform with the specifications, and to remove them from the process. Even though 100% in-line control at the tablet press is possible, it is very challenging and not implemented very often yet, and the implementations have still to be developed further.

A more common application is the on-line or at-line control of tablets by NIR spectroscopy; measured parameters are mainly identity and content/content uniformity. For on-line control, a certain amount of tablets is automatically taken out of the process stream and analyzed by a spectrometer that is directly linked to the press. After measurement, it may be brought back to the process, though more often it is kept for further analysis. This method can be easily linked to classical automated in-process controls (IPC) such as tablet hardness, weight or thickness. After NIR measurement, the tablet can be transported automatically to a device that is checking the named tablet quality parameters. An automated feedback to the press is possible, e.g. so that, in the case of non-conforming tablets, the pressing parameters are adapted or the process is stopped. An at-line solution is in use as well: sampled tablets are brought manually to a small lab close to the tablet press room, e.g. an IPC lab where classical IPC like friability ore disintegration time are performed, and are analyzed there on the NIR spectrometer. Addressed parameters can be content or content uniformity, for example. Such a fast IPC on content is useful if the tablets have to be coated afterwards. Ensuring the correct content of the tablets prevents out-of-specification tablets from being processed further, thus saving money by preventing processing of a product that is out-of-specification and cannot be used afterwards. Such IPC can also be carried out by classical wet-chemical methods, but the NIR method is much faster and therefore time-saving. It also saves storage space that would be needed if the product were quarantined until the result of the classical analysis was obtained. Up to now, the risk of processing out-of-specification material is kept low by using validated robust processes.

An interesting application would be to monitor homogeneity of the powder or granulate in or directly above the feed shoe of the press. In the event of inhomogeneous material, the process could be stopped before the pressing were carried out, therefore preventing the production of bad quality. No such application is implemented at the moment to the knowledge of the author.

2.2.3 Instrumentation

For the applications mentioned above, mainly four different types of spectrometers are used: diode-array, acousto-optical tunable filter (AOTF), Fourier transform and grating spectrometers. Both diode-array and AOTF spectrometers belong to the fastest options in NIR measurements. FT and grating devices are slower, but have advantages such as wider spectral range, better resolution or better signal-to-noise ratio. Therefore, they are often used for at-line applications, for raw-material identification or in the laboratory where time is not such a critical factor. For applications where speed is crucial, such as 100% in-line control of tablets during tabletting, the diode-array technique is used. For blending and drying processes, diode-array devices are a good choice as well as AOTF spectrometers; but they are also used for other on-line and at-line applications. Overall, the devices have to be robust, as in a production environment the handling of the spectrometers may be harsher than in a laboratory. Devices with moving parts such as FT or grating spectrometers are more sensitive to vibrations than diode-array and AOTF spectrometers that feature no moving parts and are therefore very robust. Special care has to be taken with fiber optics: the fibers are easily stressed and likely to break when bent or handled carelessly. This can be a reason for a company to avoid using a fiber optic probe in raw-materials identification in the warehouse where operators, used to handle heavy bags and bins, may have difficulties with the delicate fibers. On the other hand, fiber optics enable the use of one spectrometer for several applications. A multiplexed spectrometer can be placed in one room, one fiber optic is connected to the incoming material identification and another one to the fluid bed dryer for example, this way saving the purchase of a second spectrometer. One more advantage is the fact that the spectrometer can be placed in the “black” zone, i.e. non-GMP (good manufacturing practice) zone, allowing it to be more easily accessible for maintenance or the like. Also, by placing the spectrometer outside the explosion protected zone and using fiber optics, the use of NIR in an explosion protected area is easily possible.

Basically, measurements can be performed in reflection or transmission, transflection playing only a small role in solids. Transmission is for example applied to analyze tablets. Overall, reflection is the most common method as it can be used for analyses such as blend monitoring through a window or humidity control by fiber optic probes, where transmission can hardly be applied or not applied at all.

2.2.4 Conclusion

NIR spectroscopy is nowadays a useful and well-established tool in the pharmaceutical industry. Being applied in all fields of the manufacturing of pharmaceutics, it is also used in full-scale manufacturing of solid dosage forms. For historical reasons, at-line applications are the most common, but it is being used more and more for on-line and in-line analyses as well. Basically, it can be applied to all manufacturing steps such as raw-material identification, granulation, drying, blend-monitoring and tabletting. For identification of incoming powders, NIR is already a standard method. In granulation, NIR spectroscopy is still quite irrelevant. Some companies apply in-line NIR spectroscopy for water content determination during drying or monitoring of blending processes. In tabletting, at-line and on-line methods are more common than a 100% in-line control, but the latter is already implemented, even though further development is still necessary in that case. Overall, NIR spectroscopy is being applied more and more in the manufacturing of solid dosage forms. It helps to understand processes better, e.g. by blend monitoring, enables faster analysis and gives enhanced assurance of product quality. In this way, it has its place in the context of PAT, and may also play a role if aiming for parametric or real-time release.

2.3 Near Infrared Imaging and Spectroscopy for Capsules Quality Determination

2.3.1 Introduction

Another solid dosage form beside tablets are hard-gelatin capsules. Hard-gelatin capsules can be filled with various ingredients like powders, granules, pellets, small tablets and even liquids [41]. Normally, the capsule shells are produced by a specialized manufacturer and purchased by the pharmaceutical company that fills them. The capsules which were analyzed in the described study contained granules. For the manufacturing of this hard-gelatin capsule product, the capsule filling machine slightly compresses the granules to form a kind of briquette, and fills this briquette into the empty lower part of the capsule shell which is then closed with its top part (figure 2.9). The briquette in the capsule either stays complete, breaks into smaller parts or disintegrates completely due to vibrations during handling, for example (figure 2.9).

For some products, the presence of the briquette or parts thereof is essential for correct dissolution of the capsule. Dissolution is an important quality parameter as it influences directly the bioavailability of the product. If correct dissolution depends on briquettes, the presence thereof has to be

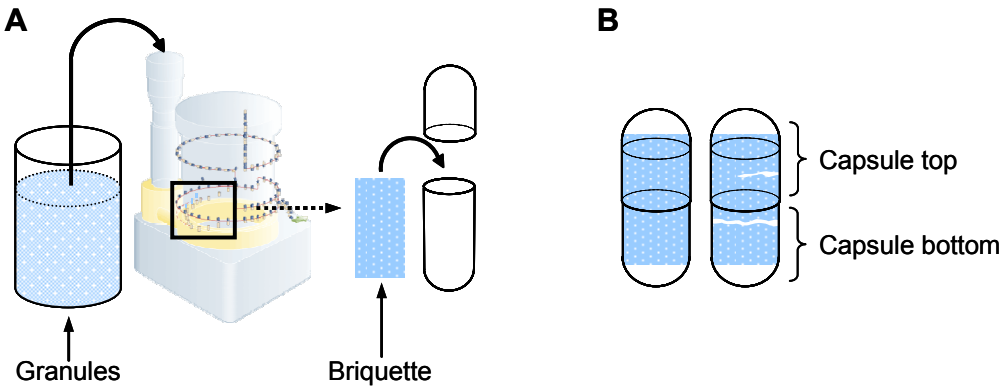

Figure 2.9 A: schema of capsules filling machine where granules are compressed into briquettes and filled into the capsule shells (schema of machine: www.ima.it). B: schema of capsules with briquette, right capsule displaying cracks in the briquette.

ensured. This can be done by opening the capsules, emptying them carefully and checking visually if they contained a briquette. This method has the clear disadvantage of being destructive, meaning that only a small number of capsules can be checked, as otherwise the losses would be too high.

The aim of the present study was to determine the presence of the briquette or parts thereof in a capsule product non-destructively by NIR imaging. Additionally, classical spectroscopy was tried to distinguish between capsules with and without briquette. It was not proved that the briquette was necessary for good dissolution of the analyzed product; nevertheless the dissolution of some capsules was tested after NIR analysis and a possible correlation between dissolution results and NIR analysis was looked at.

2.3.2 Materials and Methods

2.3.2.1 Samples

For filling of the capsules with granules, a Matic 120 (IMA, Italy) capsules filling machine was used (figure 2.9). The machine slightly compresses the granule material to form a briquette which is then filled into the capsule shells. The compressing strength can be chosen by adjusting how deep the pin that compresses the material goes. In this study, the highest compression level used is set as being 100%. Capsules with low compression levels do not contain briquettes but only uncompressed granules (figure 2.10). After the capsules are filled, they leave the machine and are transported through pipes to storage drums via vacuum.

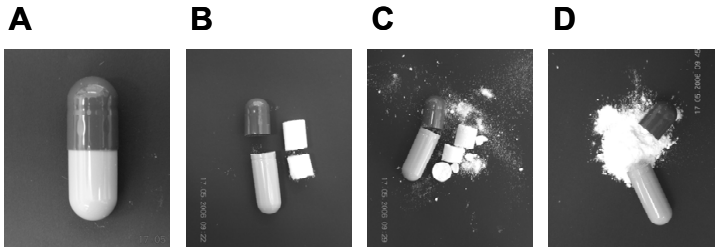

Figure 2.10 Pictures of capsule (A), emptied capsule with briquette/parts thereof (B,C) and emptied capsule with uncompressed granules (D).

The capsules were named product A. Table 2.1 gives an overview of the analyzed capsules. From several routinely produced batches, capsules were sampled for NIR analysis. First, two capsules each from the beginning, middle and end of the filling process of five different batches (batches a to e) were taken to be analyzed by NIR imaging. From three further batches (batches f to h), 12 samples were taken from the drums and 6 capsules were sampled directly at the machine. Additionally, from batches g and h, capsules produced with lower compression were analyzed by NIR imaging and spectroscopy. These samples were also used for dissolution testing. Of batch e, capsules with ten different compression levels (0, 11, 22, 33, 44, 56, 67, 78, 89 and 100%) were produced in order to have a ranking from briquettes to uncompressed granules and analyzed by NIR spectroscopy and imaging.

Product	Batch	Additional characteristics	Quantity
A	a	B, H, and E	2 each
A	b	B, H, and E	2 each
A	c	B, H, and E	2 each
A	d	B, H, and E	2 each
A	e	B, H, and E	2 each
A	e	x%	10
A	f	D	12
A	f	M	6
A	g	D	12
A	g	M	6
A	g	C	2
A	h	D	12
A	h	M	6
A	h	C	2

Table 2.1 Overview of samples of product A. Additional characteristics: B, H and E: sample from the beginning, middle and end of the capsules filling process; D: samples taken from the drum; M: samples taken directly at the filling machine; C: capsules produced with lower compression levels; x: different compression levels, x=0, 11, 22, 33, 44, 56, 67, 78, 89, 100%.

2.3.2.2 Near Infrared Imaging

The Sapphire with SapphireGo software (Malvern Instruments Ltd, Malvern, UK) was used for NIR imaging (figure 2.11). This device takes images

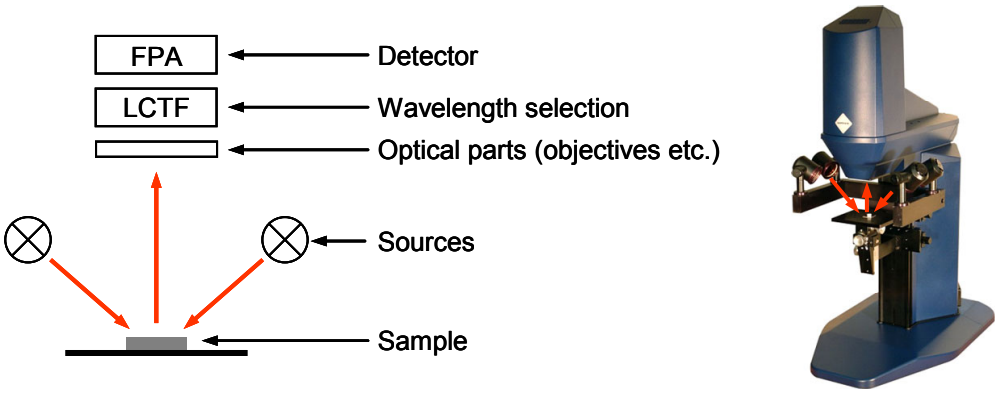

Figure 2.11 Schematic setup and picture of the Sapphire NIR imaging instrument, red arrows indicating NIR radiation (picture: Malvern Instruments Ltd, Malvern, UK).

in diffuse reflection mode. Halogen lamps provide NIR radiation, which is reflected by the sample to the focal plane array detector. This cooled indium antimonide (InSb) focal plane array with 256 x 320 pixels allows the simultaneous acquisition of 81920 spectra per measurement. A liquid crystal tunable filter (LCTF), located before the detector, is used for wavelength selection. The spectral range covered 1100 nm to 2450 nm with a spectral sampling interval of 10 nm, thus the spectra contained 136 data points each. Each image was collected as 16 coadds. Measurement time per image was below 5 minutes. For measurements, samples were placed on a metallic mirror which completely reflected the NIR radiation and made it easier to remove the background later on. Before conducting a measurement over the whole spectral range, a so-called live image of the sample was taken. This is a single channel image at 1930 nm, giving a first impression of the sample and displaying high contrast as the detector signal is at its maximum there.

For data treatment, the ISys software (Malvern Instruments Ltd, Malvern, UK) was used. Basic data treatment consisted in removing the bad pixels from all images by applying a 3 x 3 median filter and converting the spectra to

absorbance units. Then, the background area around the capsules was removed by masking.

First, images of two capsules of batch e were taken at different magnification levels, i.e. pixel sizes of 128 µm x 128 µm, 79 µm x 79 µm, 39 µm x 39 µm, 20 µm x 20 µm and 9 µm x 9 µm, respectively. One of the two capsules was produced at 100% compression level and contained a briquette with a crack, the other one was produced at 0% compression level and thus contained uncompressed granules. With one exception, all further measurements were conducted with a pixel size of 79 µm x 79 µm.

To see if the heating of the samples during the measurement due to NIR radiation would cause problems, a kind of stability test was conducted. Two capsules of batch e, one with highest and one with lowest compression, were imaged ten times in intervals of 10 minutes, starting with the initial measurement at 0 minutes. The capsules stayed on the measurement area, thus they were exposed to the radiation for more than 90 minutes. Images of all measurements were concatenated for comparison; a concatenated image of the first eight measurements was used for principal component analysis. Owing to computational power limits, a PCA of the concatenated image of all measurements was not possible. The concatenated images were also compared after a SNV transformation.

NIR images of all capsules of all batches (see table 2.1) were taken with a pixel size of 79 µm x 79 µm. Images of one capsule each of the ten different compression levels of batch e were concatenated to form a bigger image that allowed direct comparison of the capsules. The images of capsules of batches a to e from the beginning, middle and end of the process were also concatenated batch-wise. Additionally, one image with one capsule of each different compression level of batch e was taken with a pixel size of 128 µm x 128 µm. In order to find differences in the capsules and to see if a briquette was existent or not, different methods were tried. Live images were studied, images were looked at at different wavelengths, SNV was performed as well as Savitzky-Golay 2nd derivative and PCA. Additionally, with some images edge and line

detection algorithms were applied under Matlab software (The MathWork Inc, Natick, USA).

2.3.2.3 Near Infrared Spectroscopy

Two different FT-NIR spectrometers were used. For transmission measurements, the Bruker MPA (Bruker Optics, Ettlingen, Germany) spectrometer was used. Spectra were collected between 12500 cm^{-1} and 5800 cm^{-1} (800 nm – 1724 nm) with a resolution of 8 cm^{-1}; each spectrum was the average of 32 scans. Ten samples of each compression level of batch e were measured; spectra were collected from the top and the bottom of each capsule.

The Nirvis (Büchi Labortechnik AG, Flawil, Switzerland) spectrometer was used for reflection measurements. Spectra were recorded from 10000 cm^{-1} to 4000 cm^{-1} (1000 nm – 2500 nm) and contained 500 data points; each spectrum was the average of ten scans. Ten capsules of batch e with 100% compression level and 0% compression level were analyzed. All the capsules from batches f, g and h that were analyzed by NIR imaging and tested for dissolution were also analyzed. From each capsule, six spectra were recorded: the top and bottom of the samples were measured three times each, and between measurements capsules were rotated around the longitudinal axis by around 120°.

For data treatment, the Unscrambler (Camo Software AS, Oslo, Norway) was used. Both transmittance and reflectance data were converted to absorbance units. For the data generated with the samples of batch e, PCA was conducted with raw or pretreated spectra. Pretreatments consisted of SNV, Savitzky-Golay 2^{nd} derivative, cutting the edges of the spectra in order to use only a part of the data, and a combination of the different pretreatments. For the data of the samples of batches f, g and h, PCA was applied on the raw spectra.

2.3.2.4 Dissolution Testing

The dissolution was tested according to pharmacopoeial requirements with the basket stirring method and high performance liquid chromatography (HPLC). A dissolution value after a certain time was considered; a specific value was set as a minimum limit. If the result of the dissolution test was above this

limit value, dissolution was considered to be good, if it was below it was considered to be bad.

2.3.3 Results and Discussion

2.3.3.1 Near Infrared Imaging

Comparison of the images with different magnification levels showed that a pixel size of 79 µm x 79 µm was the most advantageous for this study (figure 2.12). On one hand, this magnification is high enough to display details like

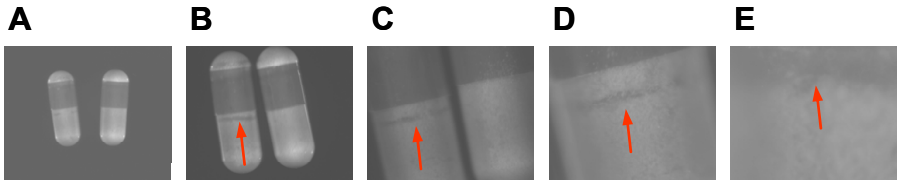

Figure 2.12 Comparison of different magnification levels, live images are shown. Pixel sizes: A: 128 µm x 128 µm; B: 79 µm x 79 µm; C: 39 µm x 39 µm; D: 20 µm x 20 µm; and E: 9 µm x 9 µm. A crack in the briquette of the left capsule is visible (indicated by red arrows).

cracks in the briquettes, on the other it allows the acquisition of images that contain one or two complete capsules, not only parts of it. One image is then of the size 20.2 mm x 25.3 mm.

The stability test showed no substantial changes in the capsules during heating time except a light drying (figure 2.13). This is for example visible at the fifth principal component of the concatenated image of the first eight recorded images. The scores image shows a higher intensity at the first two capsules, i.e. the first measurement; in the loadings it can be seen that this is due to the peak at 1930 nm which corresponds to the water absorption band at 1930 nm in NIR spectra. When the concatenated image is pretreated with a SNV transformation, the drying influence is already visible at a single wavelength image at 1930 nm as a SNV suppresses physical influence and enhances chemical information in the spectra. However, the drying influence during measurement was not strong and no other changes seemed to take place, thus it was concluded that the heat during measurement was not problematic.

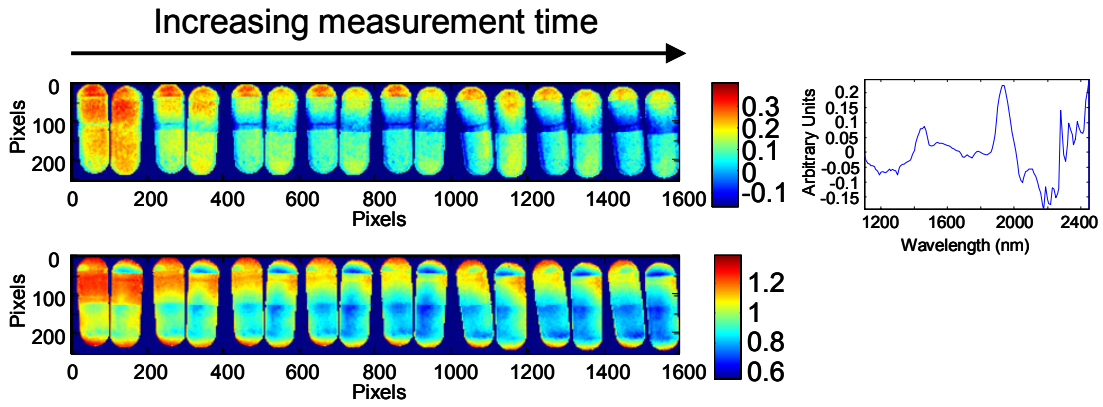

Figure 2.13 Concatenated image of the first eight measurements of the stability test. Top: 5th principal component scores and loadings image of non-pretreated image; bottom: SNV transformed image at 1930 nm. Drying effect is visible by intensity decrease over measurement time.

The concatenated image of the capsules with different compression levels was first studied visually at different wavelengths. In the capsules with higher compression levels, the briquettes or cracks therein are visible at certain wavelengths (figure 2.14). As cracks are not existent in uncompressed granules, they indicate the existence of a briquette or parts thereof. Then, PCA was applied to the concatenated image. The image was used without further pretreatment or with SNV transformation or Savitzky-Golay 2nd derivative prior to PCA. Although the cracks that made the existence of briquettes visible could still be seen in the PCA scores images, the PCA was not able to differentiate between capsules with different compression levels, neither with the pretreatments nor without (figure 2.14). The situation was analogous to the bigger image where ten capsules with different compression levels were imaged simultaneously; and the same applied to the other images of batches a to h.

Although a differentiation was not possible by PCA, single wavelength images and also the live images allowed briquettes and cracks to be detected non-destructively by visual study. This is advantageous insofar as analysis at a single wavelength is much faster than recording the full spectrum and less computational power is needed than for multivariate data analysis like PCA. On the other hand, it is not possible to quantify the results or sort the capsules by hard criteria. Some capsules show very distinct cracks or briquettes, in others

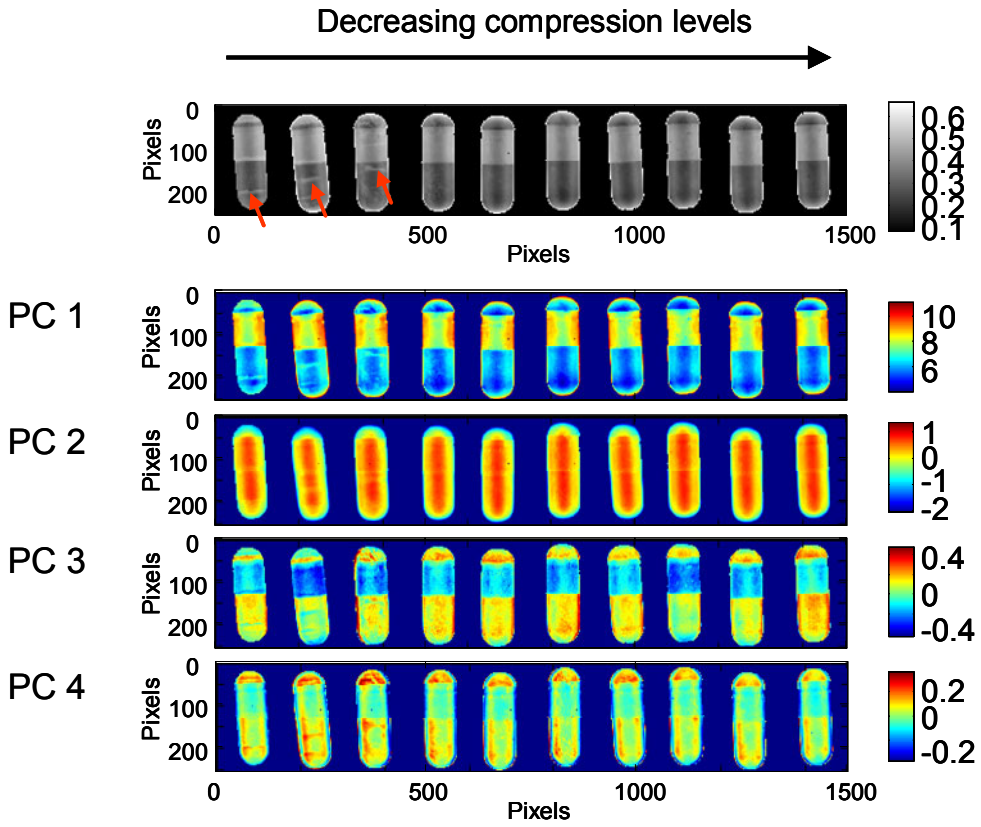

Figure 2.14 Top: grayscale image of concatenated image of capsules with different compression levels at 1870 nm, cracks in the briquettes of capsules with high compression levels are visible (indicated by red arrows). Bottom: scores images of principal components 1 to 4; it can be seen that PCA does not differentiate between capsules with different compression levels.

only little structures are visible, making it difficult to decide whether a real briquette or parts thereof are present or not. This explains that a correlation of "presence of a briquette" with dissolution results is not possible.

However, attempts were made to show a possible way to automate detection of the briquette by applying edge and line detection algorithms to single wavelength images. If a briquette is present in the capsule shell, it is visible by either cracks or, if it is unbroken, by its contour itself, leaving air in the tips of the capsule shell (see figure 2.9 B). Edge detection algorithms allow areas of sharp contrast in images to be found automatically, for example the edges or contours of capsule shells, but also of cracks. A line detection algorithm can then be used for filtering and displaying the straight lines found by the edge detection. Figure 2.15 shows the single wavelength image of two

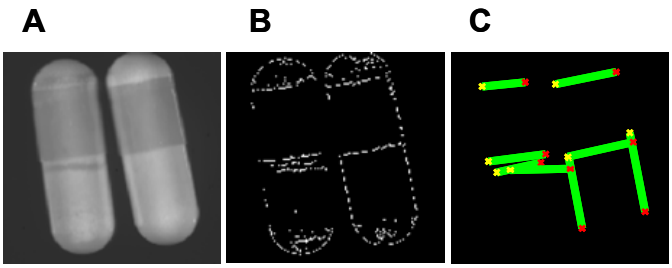

Figure 2.15 A: image of capsules at 1870 nm, left capsule has a briquette with a crack, right capsule contains uncompressed granules. B: Sobel edge detection of image A, contours and crack of the capsules are detected. C: Hough line detection of image B, some of the contours are detected as well as the crack.

capsules, one produced with the highest compression level and featuring a briquette and the other being produced at lowest compression level, thus without briquette. A crack in the briquette is clearly visible. Sobel edge detection finds the contrasts in the capsules, also detecting the crack and thus the briquette [42]. Hough line detection, following the edge detection, shows the straight contours and the crack more clearly [42].

2.3.3.2 Near Infrared Spectroscopy

Spectra collected by the transmission measurements were very noisy. This was most likely due to the fact that the layer thickness of the capsules was too high: a big part of the radiation was absorbed and only a small part of the NIR light reached the detector. Though it was possible to distinguish between the capsules' top and bottom side by applying PCA, further differentiation was not possible, neither with raw nor with pretreated spectra.

The spectra from the reflection measurements were less noisy than the ones from transmission measurements. PCA was applied to raw and pretreated spectra of the reflection measurements of capsules with 100% and 0% compression level of batch e. Differentiation between capsules' top and bottom was easily possible. To distinguish between capsules with high and low compression level, raw spectra of the bottom side were best. Figure 2.16 shows the spectra and the PCA scores plot of those spectra. It can be seen that a differentiation is possible, however, the two clusters are close to each other and

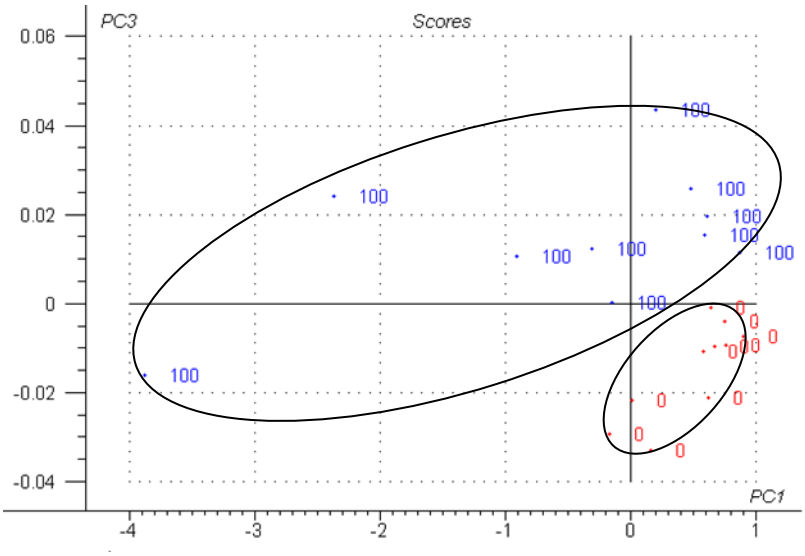

Figure 2.16 PCA scores plot of spectra of capsules bottom with 100% and 0% compression level.

especially the cluster corresponding to the high compression level data is widespread. Pretreated spectra, for example with SNV or Savitzky-Golay 2nd derivative, resulted in overlapping clusters in the PCA, thus they did not improve the differentiation. PCA was also applied to the spectra of the capsules of

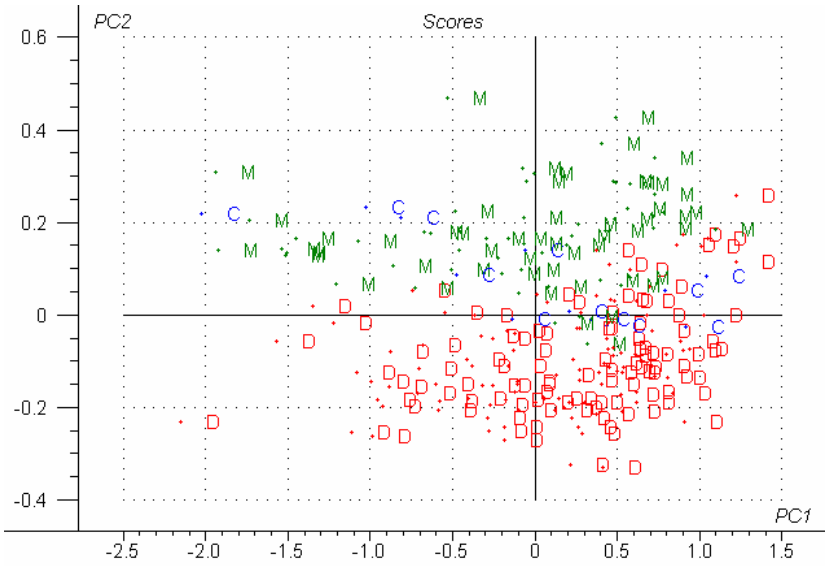

Figure 2.17 PCA scores plot of spectra of capsules bottom from batches f, g and h. D: correspond to capsules sampled at the drums; M: correspond to capsules sampled at the machine; C: correspond to capsules with low compression level.

batches f, g and h. Raw spectra were used in accordance with the fact that for batch e the differentiation with raw spectra was the best. Again, the differentiation between top and bottom sides of the capsules was possible. Figure 2.17 shows the PCA scores of the bottom side spectra. Although scores from spectra recorded from capsules sampled at the drums on the one hand and at the machine on the other hand tend to form two groups, the clusters are overlapping; and the scores from the spectra of the capsules with lower compression cannot be differentiated from the two other scores clusters. Thus, a differentiation between capsules with and without briquette was not possible. Note that in both cases, i.e. capsules from batch e and from batches f to h, the scores plots that differentiate best between the searched characteristics of the capsules are shown.

2.3.3.3 Dissolution Testing

Dissolution values of all capsules were around the same range. It was observed that the dissolution values of the capsules of batches g and h that were produced with low compression and had no briquette were in the same range. By applying the t-test on the dissolution results, it was found that all the values belonged to the same population, thus a statistical differentiation between “good” and “bad” dissolution values was not possible. Considering this, it is clear that a correlation with NIR data would not make sense and was therefore given up.

2.3.4 Conclusion and Outlook

The study shows that it is possible to determine the presence or absence of a briquette in capsules non-destructively by NIR imaging. Although the multivariate analysis method PCA did not help in distinguishing between capsules produced with different compression levels, thus displaying briquettes or loose granules, a differentiation was possible nevertheless. As the capsule shell was virtually transparent to NIR radiation, it was possible to “look through” it and see the content of the capsule without opening it. It was then possible to see if a briquette or parts thereof were present or not. This fact would allow for a

fast and non-destructive control by using, for example, a single-wavelength NIR camera and analyzing the images visually.

For the studied product, the briquette did not seem to be necessary for a correct dissolution. However, there are other hard-gelatin capsule products where the presence of a briquette or parts thereof is essential for a good dissolution. In this case, the capsules are opened and carefully emptied by the workers on the production line to check the presence or absence of a briquette visually as an in-process control. This is of course destructive. A NIR camera, which could be installed in the production area, could be used for non-destructive in-process controls, this way replacing the so far used destructive visual in-process control. The workers could then decide on the basis of the single-wavelength image if a briquette is present or not. This in-process control is more difficult than other classical in-process controls like for example weight or tablet hardness as no upper and lower limits are given; the “presence of briquette” cannot be quantified. However, this should not be a problem as it is no more difficult than the so far applied destructive control, and workers that are trained to carry out the destructive visual control would not have problems to decide on the presence of a briquette when seeing the NIR single-wavelength images. Moreover, automation with such a camera might be possible; the application of edge and line detection algorithms could be a step in that direction. Overall, it would be advantageous to replace the destructive in-process control by a non-destructive one if a high amount of samples should be analyzed. It could also be advantageous, for example, in cases where product is classified as highly potent and exposure has to be avoided.

As no images, but only spectra, are obtained in NIR spectroscopy, one has to rely more on multivariate data analysis than on visible analysis of the data. The detection of briquettes with transmission measurements was not possible. Reflection measurements partly allowed a differentiation between capsules with high and low compression levels, but no real determination of a briquette could be made. Thus, NIR imaging is to be favored in this case.

Correlation with dissolution results was not possible, partly because a quantification of presence or absence of the briquette was not possible and

partly because a statistical differentiation in “good” and “bad” dissolution values was not possible.

2.4 Near Infrared Imaging to Study the Distribution of the Active Pharmaceutical Ingredient in Low-Dosage Tablets

2.4.1 Introduction

Tablets are widely-used solid dosage forms; they normally consist of one or more API and several excipients. Besides other quality parameters like hardness, weight, friability, or dissolution time, the content of tablets is very important. According to pharmacopoeial requirements [40,43], the quality parameters have to be tested. The content is often tested by classical wet-chemical methods such as HPLC. This is a destructive, time- and solvent-consuming method that gives only an average value per sample. If the tablet is breakable, not only the overall content is important but also the content in each piece, i.e. the distribution of the API in the whole tablet, in order to ensure that the patient gets the right amount of drug. This means that classical wet-chemical methods have to be carried out to determine the content in each piece, resulting in even lengthier measurements. It would be advantageous to be able to study the distribution and the content of the API in the whole tablet non-destructively with one measurement. A possible tool for this is NIR imaging: the spectral information obtained can give information about the chemical identity, and the spatial information can give information about the distribution of the chemical substances in a matrix.

In this study it was investigated if NIR imaging can determine the distribution of API in a specific breakable low-dosage tablet product. As explained in the introduction to chapter 2, NIR spectroscopy/imaging is based on low-intensity absorptions. This is on the one hand advantageous, as normally a sample dilution is not necessary. On the other hand, the determination of low concentrations can be problematic; higher concentrated compounds tend to obscure the spectra of the low concentrated components. Therefore, the determination of API in low-dosage tablets is challenging. This is even more the case if NIR imaging is applied instead of NIR spectroscopy: first, in spectroscopy, the information about a bigger area is averaged; second, the combination of lamp and detector used in NIR spectrometers results in higher

sensitivity. One more problem exists: normally, one would try to determine the content of a tablet in transmission mode as a bigger part of it is investigated in that case. In NIR imaging, however, measurements are conducted in reflection (see chapter 2.1). This means that, depending on the penetration depth of the radiation, only part of the sample, i.e. a layer of a certain depth, is analyzed. Basically, NIR imaging measurements are non-destructive, and normally no sample preparation is necessary. However, in this study some of the samples were mill-cut in order to analyze not only the surface of the sample, but also inner layers. Different images of one tablet and from individual tablets were compared. The aim was to show the distribution of the API at the surface and on inner layers of the tablets, and the penetration depth of the radiation at a certain wavelength was estimated.

2.4.2 Materials and Methods

2.4.2.1 Samples and Sample Preparation

The analyzed tablets of product B were round with a breaking notch. They consisted of one API and several excipients. The API content was below 3% (w/w). Besides minor excipients, there were two major excipients, excipients 1 and 2. Excipient 1 accounted for more than 30% (w/w) and excipient 2 accounted for more than 60% (w/w) of the tablet weight. Granules were manufactured via a wet granulation step and then tablets were compressed by a rotary press. Tablets from three different batches – batches a, b and c – were analyzed (table 2.2). They were either imaged without further sample

Product	Batch	Tablet	Magnification	Analysis
B	a	1-6	FOV 3	Surface quarters
B	a	7, 8	FOV 3	Mill-cut layers
B	a	9	FOV 12	Penetration depth
B	b	10-15	FOV 3	Mill-cut layers
B	b	16-21	FOV 12	Mill-cut surface
B	c	22-27	FOV 12	Mill-cut surface

Table 2.2 Overview of samples of product B.

preparation or mill-cut. The mill-cutting was done in order to remove the breaking notch and achieve a planar surface, and to allow images to be taken from “inner layers”. Mill-cutting was performed by the Leica EM Trim microtome (Leica Microsystems, Wetzlar, Germany) or by using commercially available sandpaper. Cutting with the microtome had the advantage of providing smoother surfaces and it was used for most samples. Sandpaper allowed the removal of thinner layers compared with the microtome and it was used to prepare the samples for the penetration depth analyses. The thickness of mill-cut samples was measured using a Mitutoyo Digimatic Caliper (Mitutoyo Corporation, Kawasaki, Japan). Pure API and excipients in powdered form were used as references. For determination of the penetration depth of the radiation, silicone (Silastic, Dow Corning Corporation, Midland, USA), which has characteristic, sharp peaks in its NIR spectrum, was used as background material.

2.4.2.2 Near Infrared Imaging

The Sapphire with SapphireGo software (Malvern Instruments Ltd, Malvern, UK) was used for NIR imaging analogously to the NIR imaging measurements in chapter 2.3.2.2. A detailed description of the instrument and the method is given there (see also figure 2.11). Images were acquired with a spectral range from 1100 nm to 2450 nm and a spectral sampling interval of 10 nm, and they were taken as 16 coadds. Per image, 81920 spectra were collected simultaneously. Measurement time per image was below 5 minutes. For normal analyses, the samples were placed on a metallic mirror; for penetration depth measurements the samples were placed on a silicone layer. Live-images at 1930 nm were also acquired.

Images of a tablet were taken at two different magnification levels. Pixel sizes for the lower magnification were 39 µm x 39 µm, also called field of view (FOV) 12; and 9 µm x 9 µm, also called FOV 3, for the higher magnifications. The images were then of a size 10.0 mm by 12.5 mm for FOV 12 and 2.3 mm by 2.9 mm for FOV 3. Tablet surfaces were mainly imaged with FOV 3. Here, four images per tablet were acquired, one for each quarter, and the quarters were numbered 1 to 4. As the heating of the tablets due to NIR radiation

resulted in a slight drying during those measurements which could have disturbed the analyses, tablets were kept on the measurement area for 15 minutes before the measurements were started. However, on some samples an image of quarter 1 was acquired prior to and after this 15-minute “heating phase” to allow a comparison. The FOV 3 magnification level was also used to acquire images of different tablet layers after mill-cutting. For these measurements, the surface was mill-cut in order to remove the break notch and obtain a flat surface first. From the surface of this layer, an image was taken and then three more trimming steps followed, each removing a layer between 60 and 320 µm. From each of those intermediate layer surfaces, a hyperspectral image was acquired. Layers were named 1 to 4. The FOV 12 was used to acquire images of tablets where the surfaces were made planar by mill-cutting and for the determination of the penetration depth. For penetration depth analyses, a silicone layer was used as background instead of a metallic mirror like for normal measurements. One tablet was mill-cut several times and an image was acquired after each trimming step. Images of powdered pure API and excipients as well as pure silicone were taken for reference spectra.

For data treatment, the ISys software (Malvern Instruments Ltd, Malvern, UK) was used. As a basic data treatment, first the bad pixels in the images were removed by applying a 3 x 3 median filter. Then, the spectra were converted to absorbance units and SNV normalization was performed in order to reduce the influence of physical variation in the data. On the images that were taken at FOV 12 magnification level, the background area around the tablets was removed by masking. Images with the higher magnification, i.e. FOV 3, that were taken at the surface of the tablet quarters were cut at the edges. This was necessary to remove the artifacts resulting from non-focus problems at the breaking notch and at the tablet edge. The resulting images were of the size 150 pixels by 200 pixels, i.e. 1.4 mm by 1.80 mm. Images were then concatenated, i.e. put together, to allow direct comparison. Figure 2.18

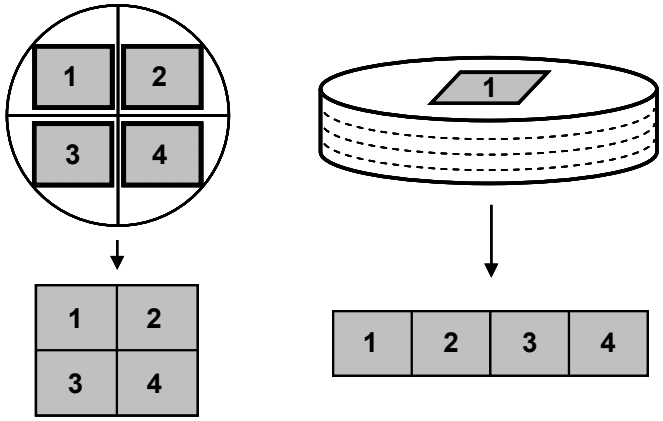

Figure 2.18 Concatenation of the images taken at FOV 3: left, concatenation of surface images; right, concatenation of images from the mill-cut layers.

illustrates the concatenation of the images of the higher magnification from the tablet surface and the mill-cut layers.

Images were studied at different wavelengths that were characteristic for the API; and PCA was performed as well as PLS-DA. The latter was tried with different reference libraries, one containing spectra of pure API and all excipients as reference, the other one containing pure API and excipient spectra except the spectrum of the excipient with the lowest concentration. PLS-DA was performed with spectra of the full spectral range or with just a part of it. It was also applied to images without further pretreatments or with Savitzky-Golay 1st derivative or Savitzky-Golay 2nd derivative. On PLS-DA scores images, also called distribution maps, API- or excipient-related areas were encircled by an intensity-based threshold method. The percentage of the encircled areas in relation to the whole area was then calculated. The mean classification scores values of the PLS-DA scores images were also calculated.

For determination of the penetration depth, the images of the six measurements where the tablets' thicknesses were lowest were concatenated and looked at at single wavelengths, and PCA was performed as well as PLS-DA. Mean spectra of the tablet and of silicone were used as reference in the library.

2.4.2.3 Classical Content Determination

As the analyzed tablets were destroyed owing to the mill cutting, tablets of the same batches were used. The content and content uniformity were determined by HPLC according to pharmacopoeial requirements.

2.4.3 Results and Discussion

Figure 2.19 shows the live image of one tablet at FOV 12 and for comparison the area that is imaged at FOV 3. Images at FOV 12 provide the possibility to image a complete tablet at once whereas FOV 3 has a resolution

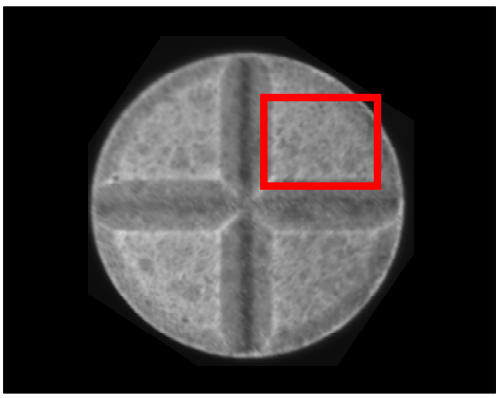

Figure 2.19 Live image of a tablet of product B taken at FOV 12; size of the original image is 10.0 mm by 12.5 mm. Red frame illustrates size of an image taken at FOV 3, image size is then 2.3 mm by 2.9 mm.

that is around four times higher. At FOV 12, imaging analysis is disturbed owing to non-focus problems at the breaking notch. Therefore, when acquiring images with FOV 12, tablets were mill-cut prior to analysis in order to make a planar surface.

As NIR radiation was heating the samples, a slight drying of the tablets occurred during longer measurement times. This was not problematic for the tablets that were imaged only once at FOV 12 or if images of different layers were acquired after mill-cutting steps. However, when images of the surface quarters were acquired, it meant that the tablet was on the measurement area for around 20 minutes. This resulted in tablets getting dryer during the measurements, especially at the beginning. This is illustrated in figure 2.20 where images of tablet B1 are shown at 1940 nm, a wavelength that is

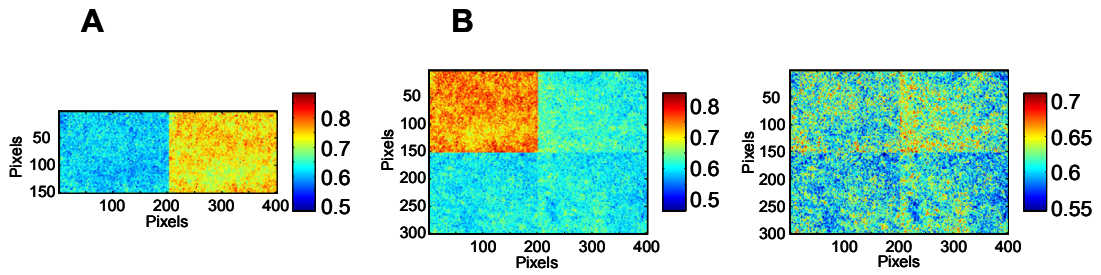

Figure 2.20 A: image of quarter 1 of tablet B1 at 1940 nm before (right) and after (left) a 15 minutes "heating" phase at the measurement area. B: concatenated image of quarters 1 to 4 at 1940 nm; left image: quarter 1 was not "heated", right image: quarter 1 was "heated" for 15 minutes.

characteristic for water. An image of the same quarter before and after a "heating" phase of 15 minutes shows a clear difference. The same applies if all four quarters are measured. One initial measurement of quarter 1 was followed by 15 minutes' resting on the measurement area. Then, quarter 1 was imaged once more and images of the other quarters were acquired without time delay. If the images of the quarters are concatenated – once using the "unheated" image of quarter 1 and once using the "heated" one – at 1940 nm, one can see that the "unheated" quarter 1 is different. The "heated" quarter shows no more difference, indicating that 15 minutes' "heating" time is sufficient. For further surface measurements, tablets were therefore kept on the measurement area for 15 minutes prior to analysis. This prevented differences in the quarters due to drying.

Figure 2.21 shows the mean spectra of pure API, the two major excipients and one tablet. The API has characteristic peaks at 1140, 1670, 2170, 2220 and 2270 nm. However, those peaks are not clearly showing up in the spectrum of the tablet as the API concentration is low and the spectra of the two major excipients dominate the spectrum of the tablet. Due to this interaction it is difficult to extract information about the spatial distribution of the active by only choosing a specific wavelength. This is illustrated in figure 2.21 where two different single wavelength images of tablet B1 at 1670 and 2220 nm – wavelengths that are characteristic for the API – are shown. Both images

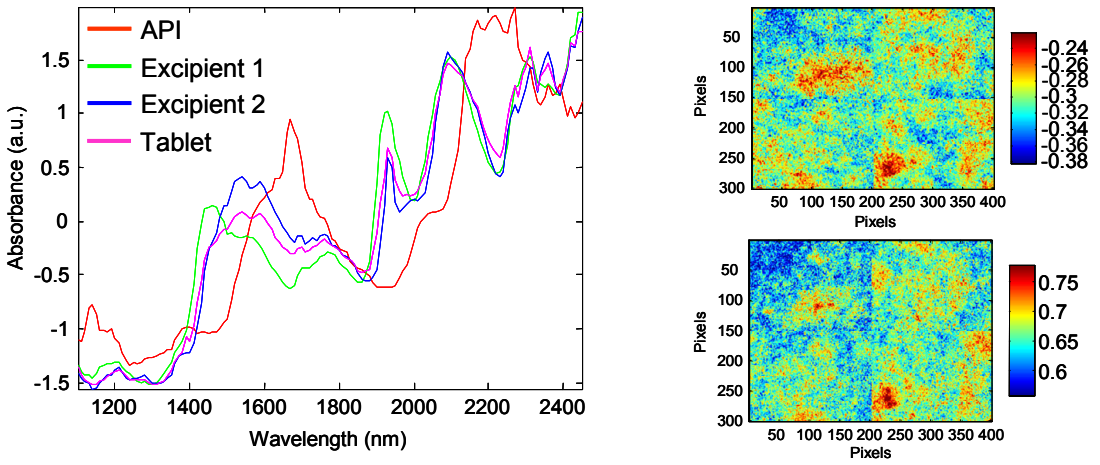

Figure 2.21 Left: mean spectra of API, excipient 1, excipient 2 and one tablet of product B, displaying characteristic peaks of the API at 1140, 1670, 2170, 2220 and 2270 nm. Right: single wavelength images of tablet B1 at two wavelengths that are characteristic for the API: 1670 nm (top) and 2220 nm (bottom).

display peaks with high intensity of API in the same regions, but the differences are nevertheless clearly visible.

In order to obtain more information, PCA was applied to the data. Figure 2.22 shows as an example the scores of factors 2 and 3 of the PCA and the corresponding loadings of the concatenated hyperspectral image from the surface quarters of tablet B1. The loadings of factor 2 have negative peaks and the ones of factor 3 positive peaks in the wavelength region around 2170 – 2270 nm where the API has characteristic peak maxima in its spectrum. Thus API related areas appear partly blue in the scores image of factor 2 and partly red in the scores image of factor 3. But the separation is not clear and thus it is not possible to extract the information about spatial distribution of the API by PCA.

As single wavelength images and PCA did not yield satisfying results, PLS-DA was performed on the hyperspectral images with the spectra of pure API and pure excipients as reference. If the spectrum of the lowest concentrated excipient was included in the library with the reference spectra, the distribution map of this excipient contained only noise. Therefore, it was not

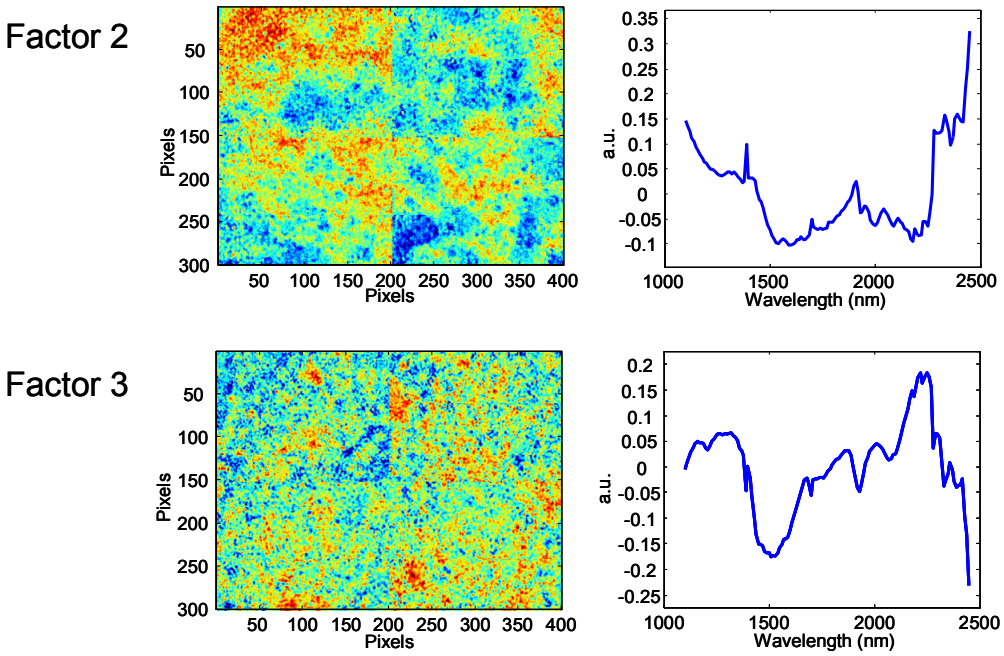

Figure 2.22 Scores images (left) and loadings (right) of factors 2 and 3 of PCA of the concatenated image of tablet B1.

useful to include this excipient in the library and, further on, a library without this excipient was used for PLS-DA.

As an example, the distribution maps of API and the two major excipients of the surface of tablet B1 and of the layers of tablet B11 are shown in figure 2.23; those analyses were carried out with FOV 3. The mill-cut surfaces of tablets B16 to B21 are shown in figure 2.24; those analyses were carried out at FOV 12. Comparison of the API distribution map of tablet B1 surface obtained by PLS-DA and the single wavelength images of API of the same tablet in figure 2.21 shows that the PLS-DA is extracting the correct information as it shows pixels with high API concentration at the same regions as in the single wavelength images. The distribution maps of excipient 1 and 2 in the FOV 3 images are quite complementary. This is the same at the FOV 12 images, only it is less distinct there due to effects at the edges of the tablets.

However, it is difficult to judge the images just by visual inspection. Therefore, two different methods were tried in order to get a better idea about the distribution of the API. One method was to encircle the pixels that were related to high API intensity on the distribution map by an intensity-based

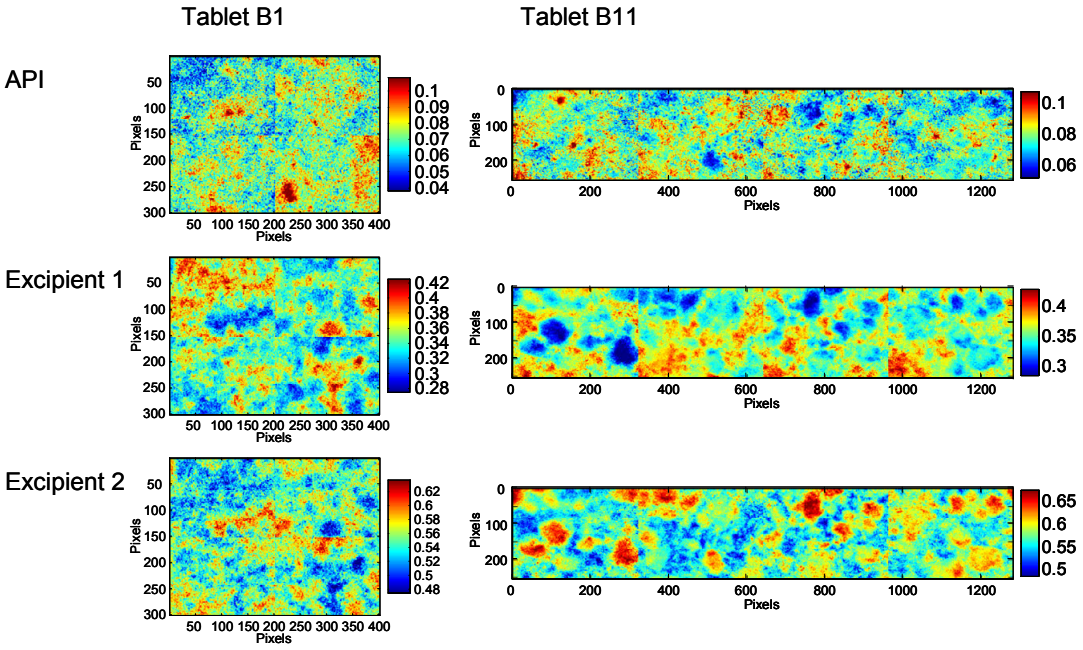

Figure 2.23 PLS-DA distribution maps of the API and the two major excipients from the surface of tablet B1 and the layers of tablet B11.

threshold method. The threshold was chosen manually. Then, binary images were created where all the pixels that were selected before form API-related areas and the percentage of those areas in relation to the whole area was

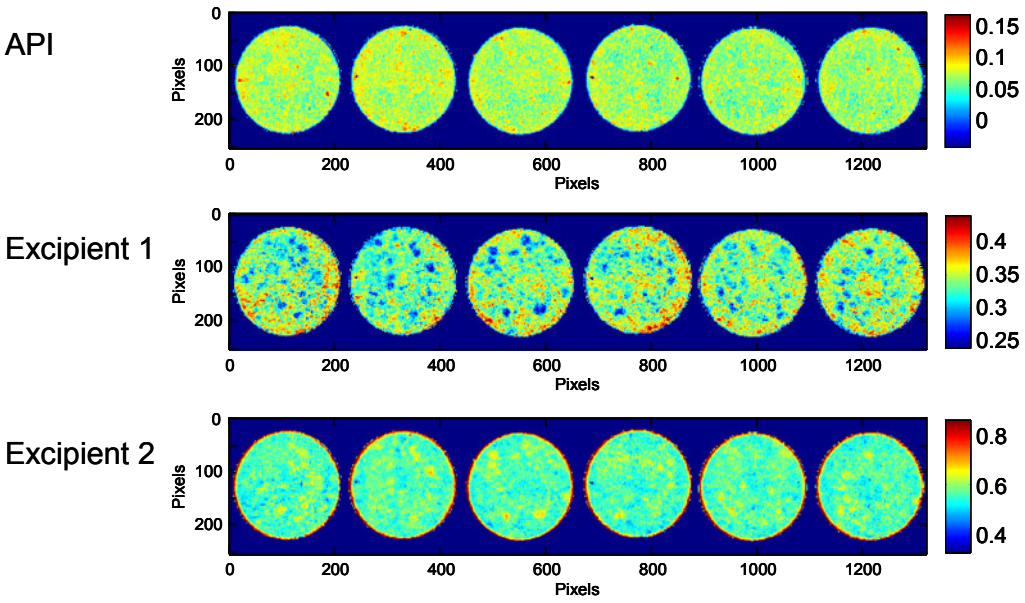

Figure 2.24 PLS-DA distribution maps of the API and the two major excipients from the mill-cut surfaces of tablets B16 (left) to B21 (right).

calculated. This method is illustrated in figure 2.25. The idea was to be able to compare the images taken of one tablet – either surface quarters or layers – for the FOV 3 images and the images of several tablets taken at FOV 12. However, the values obtained fluctuate very much; and the values of the images taken at

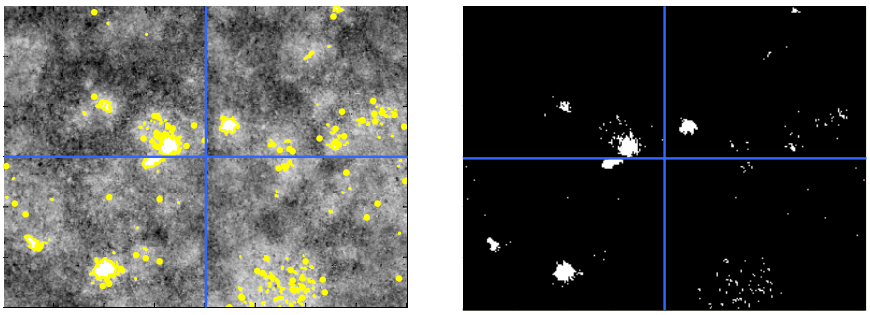

Figure 2.25 API-related pixels on the API distribution map are encircled in yellow by an intensity based threshold method (left), then a binary image is created where the before encircled pixels form areas that are displayed in white (right).

the higher magnification level fluctuate more strongly than the ones acquired at lower magnification level. The latter might be explained by the fact that at FOV 12, a bigger area is analyzed and one pixel covers more than four times the area than is the case at FOV 3. Thus, at FOV 12 the information is more averaged. Also, at FOV 3 not even the complete surface quarter is measured but only a part of it. Overall, the measurement mode is reflection, thus only a certain layer under the imaged area is analyzed, depending on the penetration depth. The fact that the threshold has to be set manually is very critical because there is no real systematic criterion on how to chose the threshold. The different pretreatments that were tried did not improve the results; and using just a part of the spectral range did not help either. However, the results are unlikely to be true, as classical wet-chemical analysis of tablets of the same batches proved that the content and the content uniformity were good, indicating that this method is not suitable for analyzing the data.

Therefore, a second method that uses the “concentration values” of the scores images was tried. Normally, PLS is applied in order to predict concentrations. Reference spectra of samples of different concentration levels are used to form the library that is utilized by the PLS. In the case of PLS-DA,

the principle is the same, but instead of using spectra of different concentration levels as references, only spectra of the different components are given. Thus, the resulting scores images are distribution maps, but concentration values are not obtained. However, the pixels in the scores images of PLS-DA refer to certain values that are called classification scores. From these values, a histogram can be created, that is to say a plot showing how many pixels there are per classification score. An example is shown in figure 2.26. In order to

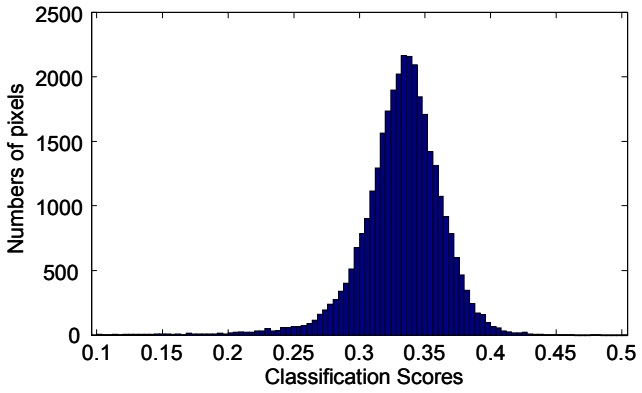

Figure 2.26 Example of a classification scores histogram: the number of pixels is plotted against the classification scores.

compare the different images acquired of one tablet at FOV 3 or of several tablets at FOV 12, the mean values of those classification scores of the PLS-DA scores images were calculated. The values were then compared. The important point was not a quantitative value but the fact that by comparing the values of the surface quarters, layers, or mill-cut surfaces of the tablets it was possible to compare the concatenated images objectively. Figure 2.27 and figure 2.28 plot

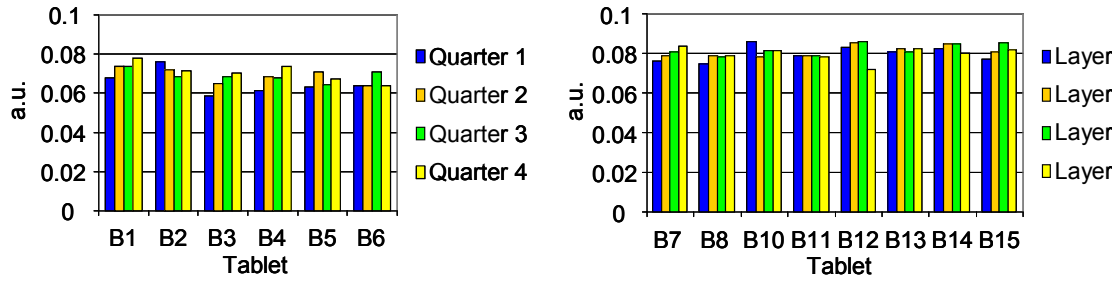

Figure 2.27 Mean classification scores values from the PLS-DA API distribution map. A comparison of the surface quarters and layers of individual tablets it possible.

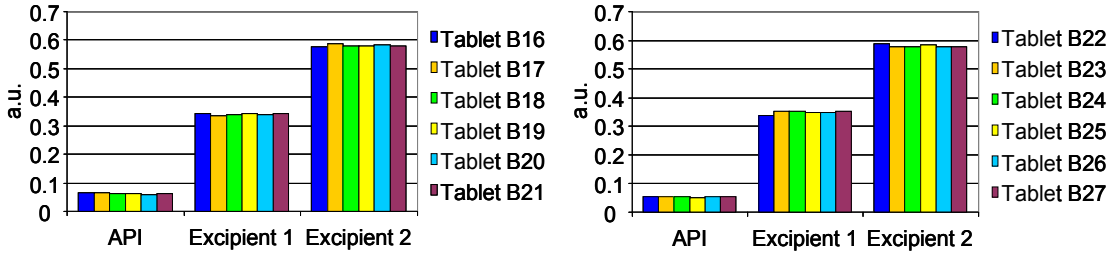

Figure 2.28 Mean classification scores values from the PLS-DA distribution maps. The different tablets can be compared.

the obtained data. The values of the FOV 3 images fluctuate more than the ones of FOV 12. This can be explained by the fact that with the lower magnification, a bigger overall area is considered and one pixel covers a bigger area than at FOV 3, thus information from a bigger area is averaged in one pixel, making the measurement somewhat more robust. Overall, the values do not vary much, meaning that the distribution of the API (and the excipients as well, as shown in figure 2.28) is quite uniform in the analyzed area. The results of this method are more in accordance with the wet-chemical content determination than the threshold-based method. What has to be considered with this method is that when using the mean classification scores, the information from a certain area, for example a surface quarter image, is averaged. Thus, spatial information gets lost. However, different areas can be compared when several images of the different areas are acquired. It might be also possible to image a whole tablet with FOV 12 and divide it into areas of a specified size afterwards, for example into equal quarters. For this, a routine would be necessary to ensure that really equal areas are considered.

As explained above, the measurements are performed in reflection, thus only a part of the sample is analyzed, i.e. the surface and a certain layer under it. This means that information is only obtained about that part, but not about the whole sample. Therefore, the calculations explained above provide information about the API distribution of a certain layer only. In order to get an idea of how much of the sample was analyzed, i.e. how “thick” the layer was, the penetration depth of the NIR radiation was estimated. For this analysis, one tablet was mill-cut several times. Table 2.3 shows the thicknesses of tablet B9

Tablet thickness	Thickness at breaking notch
1.84	1.28
1.73	1.17
1.60	1.04
1.50	0.94
1.42	0.86
1.30	0.74
1.14	0.58
1.03	0.47
0.90	not applicable
0.80	not applicable

Table 2.3 Thickness of tablet B9 at the different mill-cutting steps. All values in mm.

after each mill-cutting step. As the tablet got thinner, it was less stable and finally broke in halves and then in quarters. Therefore at the last two thicknesses, there was no more breaking notch. After each trimming step an image was taken with silicone as background. Unlike the tablets, silicone has sharp peaks at 1700 nm and 1740 nm in the NIR spectrum (figure 2.29). When

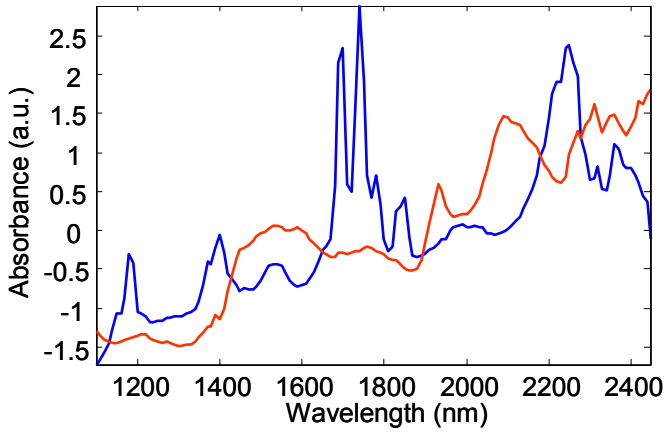

Figure 2.29 Mean spectra of tablet of B9 (red) and silicone (blue); characteristic, sharp peaks of silicone at 1700 nm and 1740 nm.

silicone is used as a background, those peaks will appear in the mean spectrum of the tablet as soon as the sample is thin enough to allow the light to pass it completely. Then the reflected light contains information about the background as well. Figure 2.30 shows the concatenated image at 1700 nm, at 1740 nm,

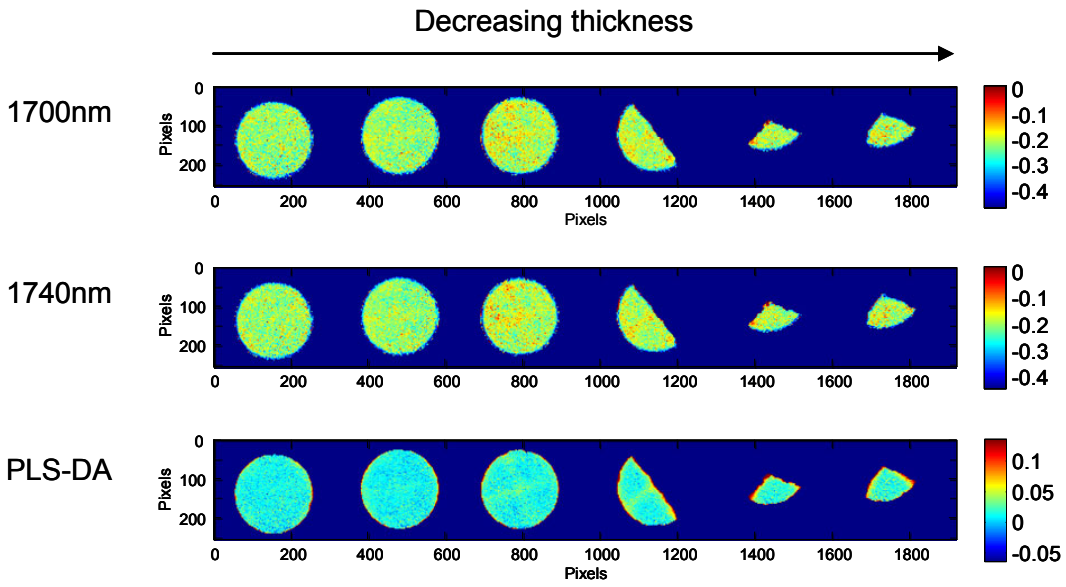

Figure 2.30 Concatenated image of the mill-cut tablet with 1.42, 1.30, 1.14, 1.03, 0.90 and 0.80 mm thickness at single wavelengths and PLS-DA silicone distribution map. The influence of the silicone is visible at the break notch of the third and fourth tablet from the left.

the two wavelengths that are characteristic for silicone, and the PLS-DA distribution map corresponding to silicone. PLS-DA was done for the spectral region from 1640 nm to 1880 nm. At the fourth tablet from the left, the intensity at the breaking notch is higher than at the rest of the tablet. This can be seen also at the third tablet from the left, but is less intense there. The higher intensity is due to the fact that the tablet is so thin at the breaking notch that the radiation penetrates it completely and also interacts with the silicone behind, thus the spectra also contain information about silicone. At the breaking notch, the tablets have a thickness of about 0.47 mm to 0.58 mm. This means that the radiation penetrates to this depth in this product. However, the penetration depth is wavelength-dependent. As in this case, the two characteristic wavelengths are 1700 nm and 1740 nm, the estimated penetration depth is valid only for this spectral region. It will be higher at shorter wavelengths and lower at longer wavelengths. Therefore, it is difficult to obtain quantitative concentration values of components in tablets by NIR imaging: depending on the wavelength, the penetration depth and thus the information depth are different. Components whose spectra have strong peaks at shorter wavelengths

will influence the analysis more, as a bigger part of the sample is analyzed at short wavelengths.

2.4.4 Conclusion and Outlook

In this study, it was investigated if NIR imaging is able to give information about the API distribution in a specific low-dosage tablet product. Different methods were tried to compare images that were acquired from tablet surfaces or “inner” layers. With PLS-DA, distribution maps of the different components were obtained. From those images, mean classification scores were calculated. Although no quantitative values were obtained, the classification scores allowed comparison of images from the surface or layers of one tablet and of individual tablets. The results did not vary much and thus were in accordance with classical HPLC content determination. However, by this method a certain amount of spatial information got lost as the images were averaged. Moreover, as measurements were in reflection mode, only a part of the sample was analyzed. The penetration depth of NIR radiation at a certain wavelength range was estimated in order to get information on how big the part that is analyzed actually was at that wavelength range.

It was hoped that NIR imaging would give additional information compared with wet-chemical analyses and that it would allow faster measurements. While this study shows that NIR imaging has a certain potential in analyzing low-dosage tablets, it also shows that quantitative analyses are not yet possible. One problem that would have to be resolved is the fact that only a small part of the sample is analyzed. This may be overcome by building a model where this fact is “built-in” in some form. Another problem is the fact that each pixel contains information about a bigger area than it actually covers. In diffuse reflection, the light travels through the sample and interacts with it before going to the detector. This means that, normally, each pixel averages information not only from the area that is “under” it in the sample but also from the neighboring area. Thus, too high a magnification does not really result in a higher resolution, and only if API particles are very big or if agglomerates are present, will pixels contain pure spectra. Such agglomerates can be seen in NIR

images. But, normally, one pixel contains information about more than one component and it is difficult to extract the individual information. In this study, it was necessary to average the information about certain areas of the tablets in order to be able to compare them. Then there is the question of whether a sophisticated method like NIR imaging needs to be applied or if classical NIR spectroscopy could not solve the problem as well. For example, by using special sample holders where only a certain area, for example a quarter of a tablet, is illuminated, NIR spectroscopy could be applied for a kind of API distribution determination; only, in that case, the resolution would be very bad. However, NIR imaging has potential there. For quantitative routine analysis it might not be so well suited, partly because it is much more expensive than, for example, classical NIR spectroscopy, but for trouble shooting or in the development of tablet products it can be very helpful. It nevertheless gives spatial information, and would be able, for example, to detect API or excipient agglomerates.

3

Terahertz Pulsed Spectroscopy and Imaging

3.1 Introduction

The terahertz, also called far-infrared, region is located between the mid-infrared and microwave region of the electromagnetic spectrum. It covers the range from 30 µm to 3000 µm, or 3.3 cm^{-1} to 333.3 cm^{-1}, or 100 GHz to 10 THz (figure 3.1). Owing to difficult generation and detection of terahertz radiation, it was hardly used and stayed an "unknown gap" in the electromagnetic

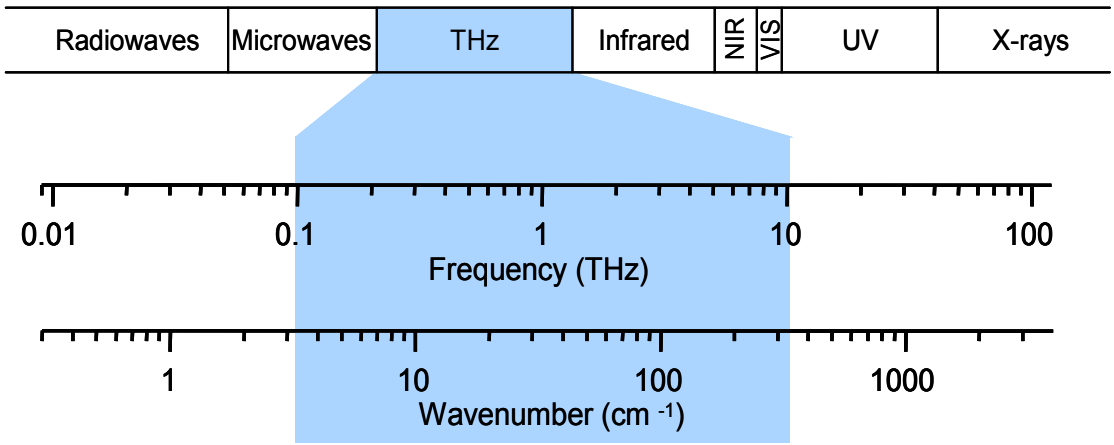

Figure 3.1 Diagram of the electromagnetic spectrum with the terahertz spectral range (adapted from TeraView Ltd).

spectrum for a long time. It was at the end of the 1980s and beginning of the 1990s that the basis was founded for terahertz pulsed spectroscopy as it is used nowadays [44-46].

Terahertz radiation can induce intermolecular bond vibrations, large-mass intramolecular oscillations and phonon lattice dynamics. All those

interactions are strongly distinct in crystalline materials but not in amorphous materials. As many materials used in pharmaceutics e.g. lots of excipients and most tablet coating materials are amorphous, they have low terahertz absorptivity and are semitransparent in the terahertz region. This allows a deep probing of the sample. Owing to the low energy nature of the terahertz radiation, there is no danger of heating the material or inducing photochemical reactions, thus the technique is non-destructive and non-invasive. As macroscopic structures of pharmaceutical tablets are normally smaller than the wavelengths in the THz region, scattering does not pose a problem. Because of the coherent nature of the signal, the technique has a very high signal-to-noise ratio, and it can be applied at room temperature.

In TPS, the terahertz pulse is generated by an ultrashort laser pulse with a duration of less than 90 fs that is focused on a so-called terahertz emitter. This is a semiconductor where the laser pulse generates electron-hole pairs. Those pairs are accelerated by an electric field that is applied across the emitter. This results in the emission of short pulses of coherent THz radiation (figure 3.2). The terahertz pulses then interact with the sample and are detected by the so-called terahertz receiver. This receiver works analogously to the emitter: it is

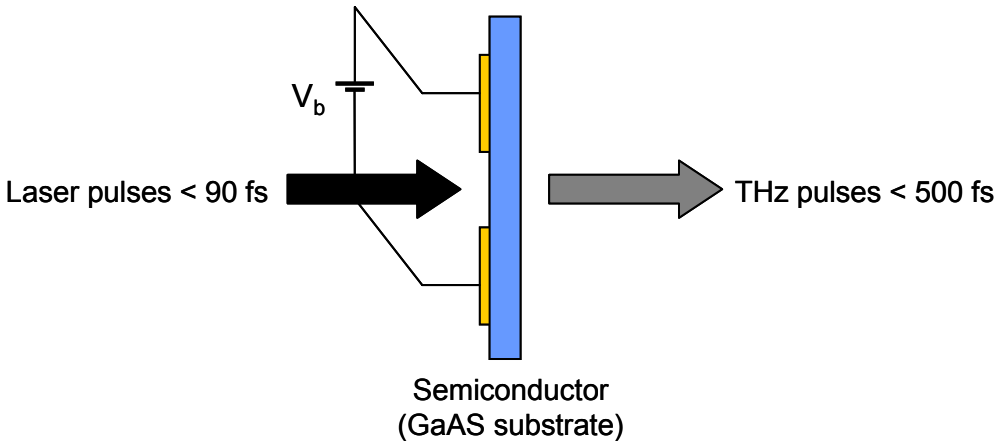

Figure 3.2 Schema of the terahertz emitter (laser gated photoconductive semiconductor; adapted from TeraView Ltd).

a semiconductor where a small part of the initial laser pulse, that was used to generate the terahertz radiation on the emitter, generates electron-hole pairs. Unlike the emitter, there is no electric field applied across the receiver. The

arriving terahertz beam provides the electric field, thus inducing a photocurrent that is measured. The technique is time-resolved: by varying the path length that the part of the laser pulse that is sent to the terahertz receiver has to go before reaching the receiver, the time the THz pulse needs can be measured.

There are two measurement modes: transmission and reflection. Analogously to other spectroscopic techniques such as NIR spectroscopy, in transmission the THz pulse passes through the sample which is placed between terahertz emitter and receiver. The transmission mode is used in TPS to obtain chemical information or information about polymorphism and crystallinity. In reflection mode, the pulse interacts with the sample and is reflected back to the receiver at each interface. Reflection is mainly used in terahertz pulsed imaging, for example to scan the whole surface of a sample or to obtain information about the internal structure of a sample.

The resulting spectrum is in the time domain and there are two possibilities to analyze it. It can be fast Fourier transformed to frequency domain spectra. This is done in TPS transmission measurements where for example chemical or crystallinity information is wanted. It can also be applied in TPI reflection measurements if, for example, the distribution of one component is studied. But also without Fourier transformation, the time domain spectrum directly provides information about the internal structure of a sample. This is due to the fact that the coherent terahertz pulse is reflected by internal layers of the sample, e.g. different coating layers in a tablet. Wherever there is sufficient change in the refractive index, a part of the pulse is reflected from this interface (figure 3.3). The time delay of the reflected pulses depends on the refractive index of the material and the depth of the feature, therefore the thickness of a coating or the depth of the feature can be calculated by the time delay and the refractive index.

As mentioned above, TPS mainly provides information about the chemical composition of samples or polymorphism and crystallinity. The sample is analyzed in transmission and the frequency domain spectra that are obtained by fast Fourier transform of the time domain spectra are used. In a pharmaceutical context, TPS has been used to study the crystallinity of pure

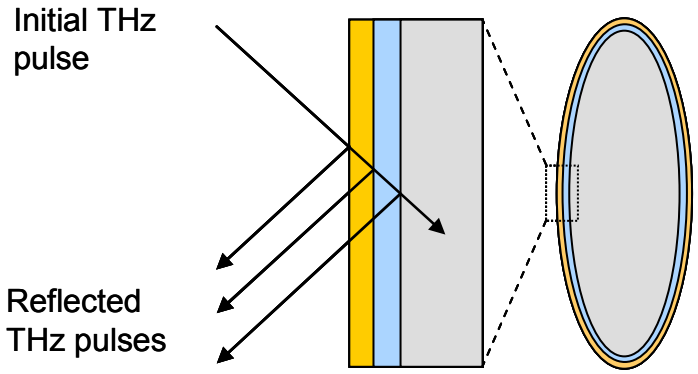

Figure 3.3 Schema of the reflection of the THz pulse at interfaces: example of a tablet with two different coating layers. At each interface, a part of the pulse is reflected and the other part goes further into the sample.

pharmaceutical compounds and polymorphs in tablets [47,48]. It has also been used for the quantification of different levels of polymorphism [49]. Temperature-dependent terahertz pulsed spectroscopy allowed the study of solid-state reactions [50]; and TPS was able to quantify different levels of API in tablets [51].

In TPI, unlike TPS, the measurement is done in reflection and not only one spectrum per sample is obtained, but several thousand. Many point measurements are mapped over the whole surface of a sample, and at each point, or pixel, a terahertz time-domain signal is obtained. In this way, information over the whole surface is obtained. The lateral resolution is limited by the wavelength and usually lies at 200 µm by 200 µm for one pixel. The depth resolution is limited by the pulse duration. By using the directly obtained time domain spectrum, information about internal structures or layers can be obtained, for example the coating thickness at each point can be calculated by the time delay of the signal. When the time domain spectra are Fourier transformed, they provide chemical or crystallinity information as described above. Thus TPI provides three-dimensional information: the x- and y-axis describe vertical and horizontal dimensions of the sample and the z-axis represents the time domain or frequency domain. In pharmaceutics, terahertz pulsed imaging has been used to investigate tablet film-coats and internal structures of oral solid dosage forms [52-54]. It has also been applied for component distribution and quantitative analysis of tablets [55-57].

3.2 Terahertz Pulsed Spectroscopy and Imaging to Study the Distribution of the Active Pharmaceutical Ingredient in Low-Dosage Tablets

3.2.1 Introduction

Tablets are the most common pharmaceutical dosage forms. They are composed of one or more API and excipients. Important quality parameters are for example hardness, friability, disintegration time, dissolution time, content and content uniformity. Some tablets feature break notches and can be split into halves or smaller parts by the patient. In this case, not only the content of the whole tablet is important, but also the uniform distribution of the API in the tablet. It has to be ensured that after breaking, each part contains the same amount of API. This is especially critical in so-called low-dosage tablets, where only a small amount of a potent drug substance is present.

Normally the content is determined by classical wet-chemical methods such as HPLC. These are time- and solvent-consuming and laborious. Therefore, non-destructive analysis by spectroscopy, for example TPS or TPI, would be advantageous. Terahertz pulsed imaging offers the possibility to obtain information from all over the tablet by recording spectra at thousands of points. Therefore this method would be very advantageous if the distribution of one or more components has to be investigated. However, measurements are performed in reflection mode and the radiation penetrates only to a certain depth. There, transmission has the advantage of gathering information from the whole sample as the radiation passes the sample completely. It is also assumed that as in transmission the radiation interacts with a big part of the sample, it might be able to detect lower concentrations. Nevertheless, the detection of low concentrations of substances in the presence of other absorbing materials, as it is the case for tablets, is very challenging.

In this study, two different low-dosage tablet products were analyzed. The aim was to determine the distribution of API. Owing to the low content of API and the resulting assumption that detection would be difficult, the focus lay

on terahertz pulsed spectroscopy where the measurement mode is transmission. With one product, terahertz pulsed imaging was tried in addition.

3.2.2 Material and Methods

3.2.2.1 Samples

Tablets of product B were uncoated; the shape was round and biplanar, and they featured a breaking notch. The active pharmaceutical ingredient was called “substance B” in the study. Tablets of product C were uncoated cores that were oval and biconvex and had a break mark. The API for that product was named “substance C”. The API contents of both products were below 3% (w/w), and in both products lactose was a major excipient, accounting for more than 60% (w/w) of the tablet weight. The tablets were analyzed directly without sample preparation. For reference measurement, pure API was diluted with pure polyethylene powder. API and polyethylene were mixed and compressed into solid pellets in a pellet die under two tons of pressure. For reference of product B, one pellet of 5% (w/w), 10% (w/w) and 19% (w/w) substance B each were prepared. For reference of product C, three pellets of 10% (w/w) substance C were compressed. In order to show the peaks in the terahertz spectra that are characteristic for substances B and C better, the concentrations in the pellets were chosen higher than in the original tablets.

3.2.2.2 Terahertz Pulsed Spectroscopy and Imaging

All terahertz measurements were conducted at TeraView Ltd (Cambridge, UK) by their specialists. Spectra of tablets and references of both products were collected by TPS. The measurements were made in transmission using a TPS spectra 1000 spectrometer with TPI Spectra software (TeraView Ltd, Cambridge, UK). Figure 3.4 shows the schematic setup as well as a picture of the instrument. The sample compartment was purged with dry nitrogen during the measurements to minimize influence of atmospheric water vapor. Spectra were collected from 1 cm^{-1} to 120 cm^{-1} (30 GHz to 3.2 THz) at a resolution of 1.0 cm^{-1} for product B and 1.2 cm^{-1} for product C. Each spectrum was the average of 1800 co-added scans and took one minute to record. Time domain spectra were Fourier transformed to frequency domain spectra. Tablets of

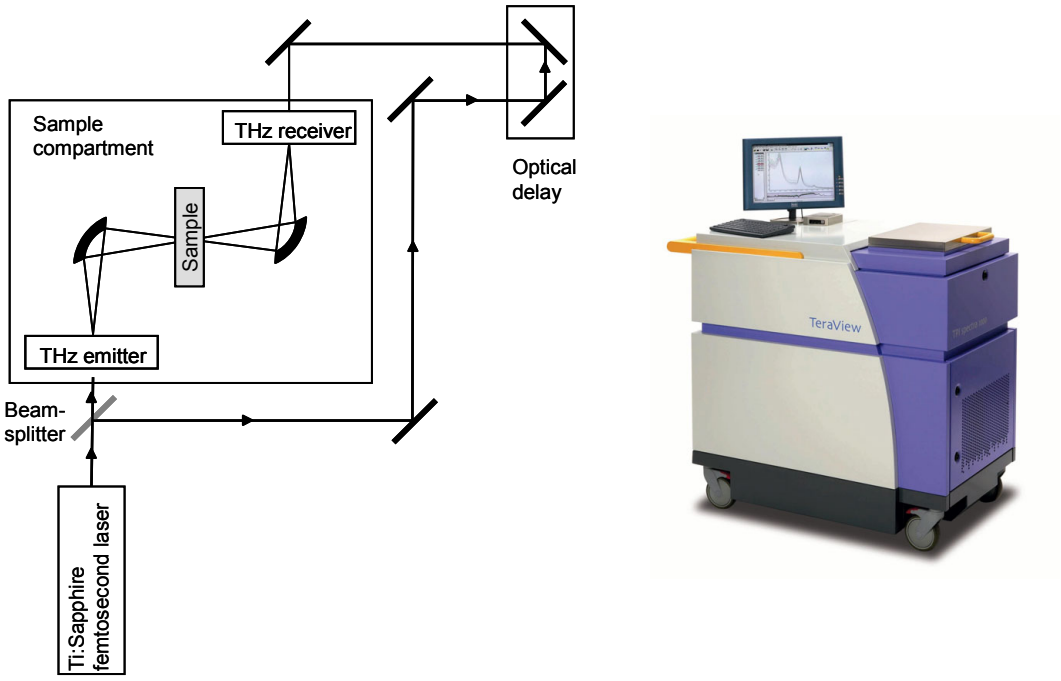

Figure 3.4 Schematic setup and picture of the TPI spectra 1000 system (picture: TeraView Ltd, Cambridge, UK).

product B were also analyzed by TPI with a TPI 2000 imaga instrument (TeraView Ltd, Cambridge, UK). Approximately 2000 point measurements were recorded in reflection over one face of each tablet. Reference measurements were made on a metallic mirror. To obtain chemical information, the directly obtained time domain spectra were Fourier transformed to reflectance spectra in the frequency domain. Details of the instrument and the method are given in chapter 3.3.

3.2.3 Results and Discussion

3.2.3.1 Product B

Figure 3.5 shows the terahertz absorbance spectra of the pellet samples prepared with 5% (w/w), 10% (w/w) and 19% (w/w) substance B obtained by TPS measurements. Especially in the spectrum obtained from the pellet with the highest drug concentration, several characteristic peaks can be seen. Apart from the peaks at wavenumbers over 80 cm^{-1}, characteristic peaks at 37 cm^{-1} and 63 cm^{-1} and a shoulder at 60 cm^{-1} are visible. The signal for the pellet with the lowest amount of API is much weaker so that mainly a band at 60 cm^{-1} to 63

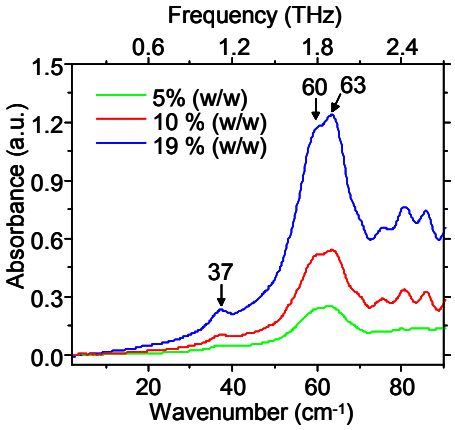

Figure 3.5 Terahertz absorbance spectra of reference pellets of product B obtained by TPS measurements. Pellets prepared with 5% (w/w), 10% (w/w) and 19% (w/w) substance B.

cm^{-1} is visible. Figure 3.6 shows the absorbance spectrum, obtained by TPS, of one tablet of product B as well as the spectrum of pure lactose as reference. Although in the spectra of the reference pellets substance B showed a unique terahertz spectral signature, those peaks at 37 cm^{-1}, 60 cm^{-1} and 63 cm^{-1} are

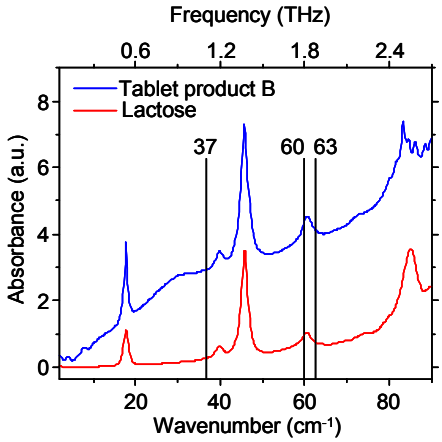

Figure 3.6 Terahertz absorbance spectrum of one tablet of product B obtained by TPS transmission measurement. Spectrum of pure lactose shown as reference.

not shown in the spectra of the whole tablet. The reason for this is clear when comparing the spectrum of the tablet with the spectrum of lactose. The tablet spectrum shows mainly peaks at the wavenumbers where lactose has its principal absorption features. As lactose is a major excipient, it dominates the tablet spectrum, obscuring the influence of the other components of the tablet

on the spectrum. Therefore the detection of the API is not possible in this case. But also the fact that the lowest concentrated reference pellet, the one with 5% (w/w) substance B, has only a weak signal in the THz spectrum shows that it is difficult to detect low concentrations of this API even when there are no other absorbing substances present.

Determination of the API in the tablet was also tried by TPI. Figure 3.7 shows the reflectance spectrum of one point on the tablet. Although the

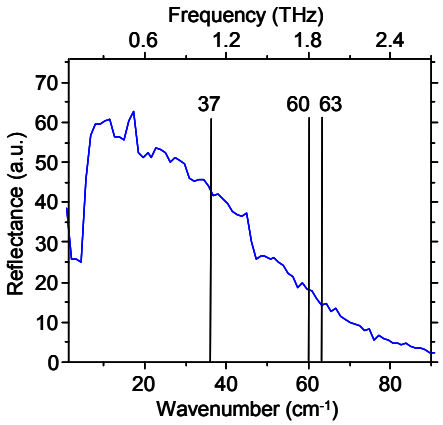

Figure 3.7 Terahertz reflectance spectrum of one point on one tablet of product B measured by TPI.

measurement was conducted in reflection, the characteristic peaks of the API would be at the same positions. No such peaks can be observed, indicating that the level of API is below the detection limit. Therefore detection of the API was not possible with TPI. As determination of the API in the tablet was already not possible with TPS, this result must have been expected.

3.2.3.2 Product C

Figure 3.8 shows the absorption spectra of the three 10% (w/w) pellets obtained by TPS transmission measurements. There are no sharp peaks but a broad band centered at about 53 cm^{-1}. In figure 3.9, terahertz absorbance spectra of five tablets of product C are shown. The small differences in the five spectra are caused by the non-specific background. Two spectral bands can be observed: one at 17 cm^{-1} and the other at 41 cm^{-1}. They result from lactose which is a major excipient and dominates the tablet spectrum. Above 42 cm^{-1} the measurement is saturated, meaning that no radiation reaches the detector,

therefore no information can be obtained from that region. As the spectral feature of substance C is at 53 cm^{-1}, detection of the API of product C in the tablets was not possible.

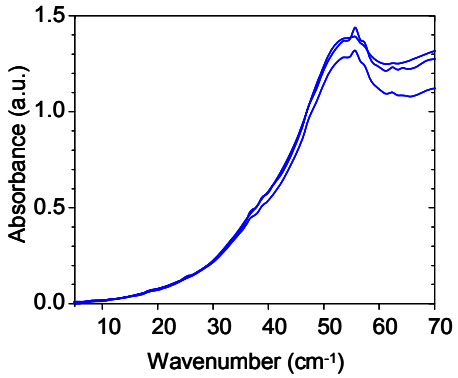

Figure 3.8 Terahertz absorption spectra of the three 10% (w/w) pellets of substance C obtained by TPS.

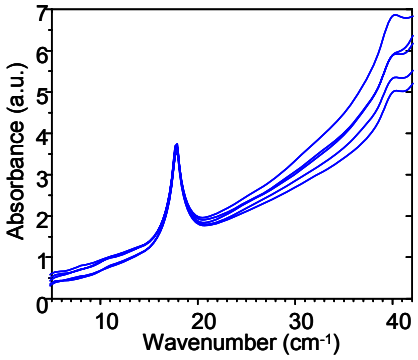

Figure 3.9 Terahertz absorbance spectra of five tablets of product C obtained by TPS.

3.2.4 Conclusion and Outlook

In this study, two different products were analyzed by TPS and one by TPI in order to determine the distribution of the API in the tablets. For both products, the analysis of the API in the tablet was not possible. In the case of product B, lactose dominated the spectrum and overlaid the characteristic API peaks. Detection was not possible with TPS or TPI; the API was under the limit of detection. For product C, lactose dominated the spectrum as well. At the spectral region where the API has its characteristic band, the measurement was

saturated and no information could be obtained about that region. Thus, determination was not possible with TPS.

In the spectra of both products, it can be seen that lactose has a strong influence, dominating the spectra of the tablets and masking the information about the other components. To a certain degree this can be expected as lactose is a major ingredient in both products. Moreover it seems that lactose itself absorbs the terahertz radiation relative strongly. Therefore, detection of other substances in the presence of lactose is difficult. If the level of other components is as low as in the case of the API level in the low-dosage tablets used, it is definitely below the detection limit of the technique. Comparison of the spectra of a verum and a placebo tablet would not allow detection either as the influence of the lactose is too strong.

The study showed that at the moment, determination of the API in low-dosage tablets is very difficult with TPS and TPI. In the case of the two chosen products, it was impossible. However, it might be possible for other products, where for example the API has other or stronger characteristic spectral features, and where for example less or no lactose is present. The detection limit might also decrease in the future owing to improvements in the technique or mathematical analysis of the data.

3.3 Terahertz Pulsed Imaging for the Monitoring of the Coating Process of Film-Coated Tablets

3.3.1 Introduction

Pharmaceutical tablets are often film-coated. This is done for various reasons. A coat can for example improve the shelf-life of the product by protecting the tablet core against moisture or light, thus preventing the degradation of the active pharmaceutical ingredient. A coat can also serve to determine the appearance of the product, making it easier for the patient to recognize a tablet by a specific color. It can mask an unpleasant taste or odor and make the tablet easier to swallow. As a coat acts as a barrier between a core that contains highly potent API and the environment, it allows the manufacturer to handle the coated product like a normal product without special precautions that are necessary for highly potent products. Important fields are coatings that modify or control the drug dissolution rate. For example, coatings that show pH-dependent behavior allow the disintegration of the tablet only in the small intestine but not in the stomach; or they control the release of the API by a limited diffusion of the API through the coating layer. The coating thickness and uniformity are important, as they are closely related to its functionality. A wrong coating thickness may have unwanted effects: for example, if it is too thick, the dissolution may be too slow, if it is too thin, it might not protect the core sufficiently against humidity. But not only the average coating thickness is important, but also the uniformity: the coat can only be as good as its weakest point, for example its thinnest spot. From this it is clear that the quality of the film-coat has to be controlled.

It is difficult to determine the quality of the film-coat non-destructively over a whole sample. TPI is so far the only method that has the ability to determine the coating thickness over a whole tablet non-destructively and provide direct thickness data. Other methods to monitor the coating process or control the quality of the film are available, but they are mainly indirect, localized, or destructive. An overview of such other methods is given in chapter 4. In the present study, TPI was used to determine the coating thickness and uniformity

of film-coated tablets of three different products as well as to monitor the coating process of one of the products.

3.3.2 Material and Methods

3.3.2.1 Samples

Three different products – products D, E and F, respectively – were analyzed. For each tablet, the upper face (face a), lower face (face b) and the center-band were mapped. All products were coated in pan coaters on a medium or large scale. 16 tablets of product D were used for a first evaluation of the technique. The round, biconvex tablets were coated with Opadry White and only tablets with finished coating were analyzed. On the first part, batch a, the coating weight was 3% of the core weight. Those samples were named Da1, Da2, etc. On the second part, batch b, the coating weighed 5% of the core weight; samples were named Db1, Db2, etc. Product E was coated with Opadry Pink and the oval, biconvex tablets were embossed on both faces. Tablets were taken out of the coating pan during the coating process at different time points in order to monitor the coating process and to demonstrate the correlation between signal and coating thickness. 20 samples were analyzed, they were named E1 – E20, E1 having been sampled at the beginning of the process with nearly no coating, and E20 at the end, thus having the thickest coating. Table 3.1 shows the coating time in percent of maximum coating time of tablets E1 –

Sample	Coating time (% of max. coating time)
E1	9
E2, E3	43
E4, E5	51
E6, E7, E8	60
E9, E10, E11	77
E12, E13, E14	85
E15, E16, E17	94
E18, E19, E20	100

Table 3.1 Coating time of tablets E1 – E20 in percent of maximum coating time.

E20. Product F, also oval and biconvex and featuring an embossing, was coated with Opadry Yellow. A sample was stressed during storage to develop cracks in the coating. The sample was named F and used for an evaluation of the ability of the technique to detect fine structures and defects in the coat.

3.3.2.2 Terahertz Pulsed Imaging

For analysis of the coating thickness and uniformity of all three products, a TPI imaga 2000 with data acquisition and analysis software TPIScan and TPIView (all TeraView Ltd, Cambridge, UK) was used. The measurements were conducted at TeraView Ltd (Cambridge, UK) by their specialists. Figure 3.10 shows the schematic setup and a picture of the instrument. A Ti:Sapphire

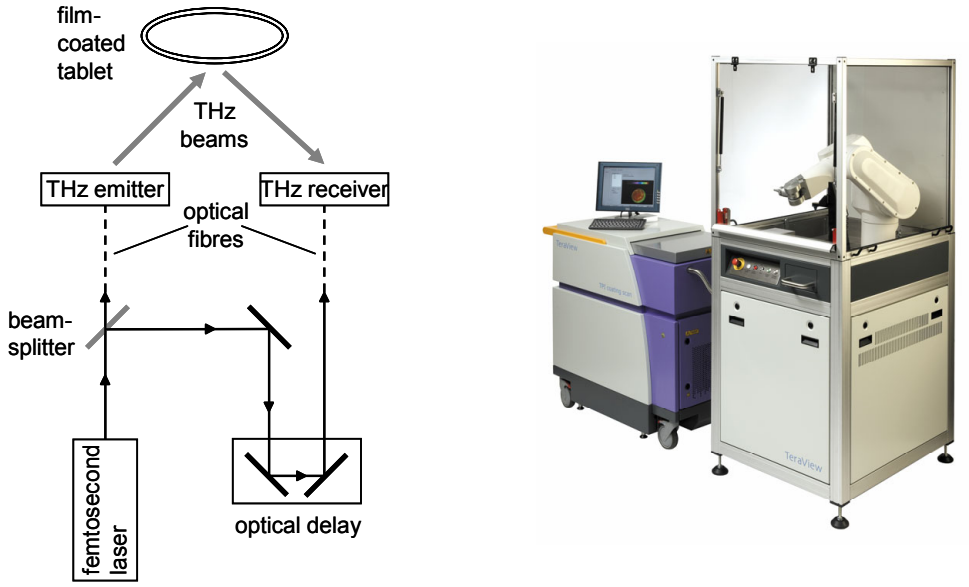

Figure 3.10 Schematic setup and picture of the TPI imaga 2000 system (picture: TeraView Ltd, Cambridge, UK).

femtosecond laser at 800 nm and THz emitter and receiver are used for generation and detection of terahertz pulses. The sample is held by a suction cup on a robotic arm (figure 3.11). This robotic arm moves the tablet in front of the static emitter/receiver probe head and thus allows scanning of the sample surface. On multiple points of the sample surface, measurements are made, resulting in a mapping of the sample surface and thus providing coating thickness information. Each point, or pixel, has the size 200 µm x 200 µm.

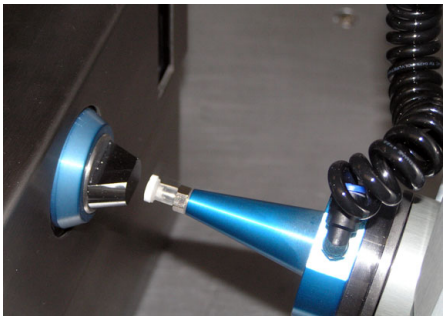

Figure 3.11 Close-up of tablet on robot arm during terahertz analysis with TPI imaga 2000 system (picture: TeraView Ltd, Cambridge, UK).

Depending on the size of the sample, more or fewer point scans were recorded. For product D, 2000 point measurements were recorded over both faces of each tablet as well as over the center-band. For product E, 3200 point scans were recorded over each face and 2800 points were measured on the center-band. The number of point scans for product F was 5300. The refractive index of the coating was taken from a library and was 1.5 for all products. Reference measurements were made on a metallic mirror.

Figure 3.12 shows a typical terahertz time domain waveform of one point measurement. Whenever a reflection of the pulse at an interface occurs, the

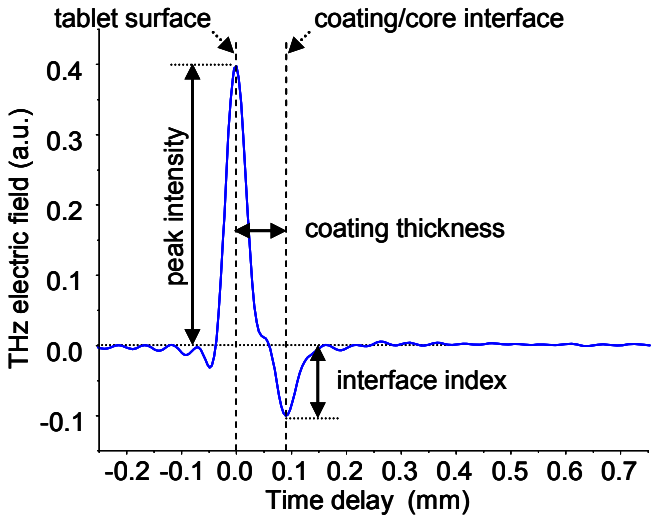

Figure 3.12 Typical terahertz time domain waveform. Reflection from the tablet surface (i.e. air/coating interface) and from the coating/core interface are indicated by dashed lines; drawn through arrows indicate how TPI parameters (peak intensity, interface index, layer thickness) are related to the waveform.

waveform shows a peak. A change from a lower to a higher refractive index results in a positive peak; if the refractive index gets smaller, a negative peak occurs. In figure 3.12, the high, positive peak indicates the reflection of the pulse at the tablet surface, i.e. air/coating interface. The second peak, which is smaller and negative, results from the reflection at the coating/core interface. Several items of information can be extracted from this waveform. From the time delay between the maximum of the first peak and the minimum of the second peak, the thickness of the coating can be calculated. As the peak intensity of the air/tablet surface depends on the refractive index of the tablet surface and as it can be affected, for example, by the roughness of the surface, it can provide information about the smoothness of the surface. The interface index, which is the peak height ratio of the reflection from the coating/core interface and the reflection from a metallic mirror (the reference measurement), provides information about the coating/core interaction. As such a waveform is obtained at each measured point, providing the named information at each point, maps displaying the different characteristics can be built up, for example coating thickness maps. A coating thickness map shows the coating thickness at each point of the surface of the sample, thus also providing information about coating uniformity and integrity.

The measurements resulted in coating thickness maps and histograms for all products, providing information about the thickness as well as uniformity of the coating. For product F, a peak intensity map and an interface index map were also built up to detect small defects in the coating layer.

3.3.3 Results and Discussion

3.3.3.1 Product D

Measurements gave an average coating thickness of 56.5 µm for tablets of batch a and 76.5 µm for tablets of batch b; the minimum was 53.0 µm and the maximum was 92.5 µm. TPI clearly detected the inter-batch differences that could be expected from the fact that more coating mass was applied on batch b. Intra-batch differences and differences on individual tablets were also detected. Figure 3.13 shows the coating thickness maps and histograms of tablets Da1

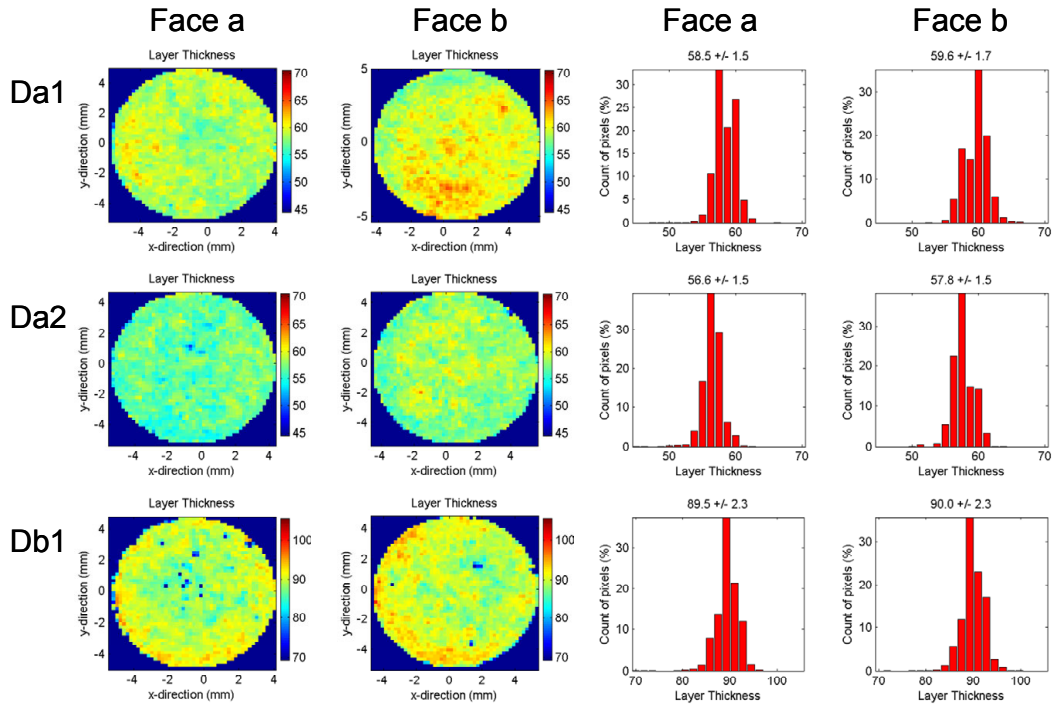

Figure 3.13 Coating thickness maps and histograms of tablets Da1, Da2 and Db1. Note that the color scale for tablet Db1 is different from the ones of tablets Da1 and Da2. Differences between the two batches, tablets, tablet faces and within individual faces can be observed.

and Da2, and Db1. Both sides (face a and face b) are shown. Intra-batch differences can be seen by comparing the images and histograms of tablets Da1 and Da2; tablet Da1 has a slightly thicker coating. Differences of coating thickness on individual faces can also be observed, e.g. on face a of tablet Db1, where the coating in the center seems to be slightly thinner than at the edge. As can be seen on the images of tablet Da2, differences of coating thickness can also occur between the two faces of one tablet. Face a has a thinner coating layer than face b. However, the differences are small and the tablets showed sufficient coating thickness. None of the tablets displayed real defects in the coating.

3.3.3.2 Product E

On tablet E20, a precision study was undertaken. Ten repeat measurements were recorded over 4 days (three measurements on each of the first three days and one measurement on day 4) to determine the coating

thickness on both faces and the center-band. The mean thickness over the ten repeats was 58.25 µm with a standard deviation of 0.21 µm for face a, 52.21 µm with a standard deviation of 0.19 µm for face b, and 44.8 µm with a standard deviation of 1.03 µm for the center-band, thus demonstrating very good repeatability. The difference in coating thickness between face a and b might be explained by the different embossing on faces a and b, respectively. The higher standard deviation at the center-band compared with faces a and b is due to the instrument scanning close to and around the edges of the center-band.

The coating thickness of tablet E1 could not be determined by TPI because the thickness was below the detection limit. This can be seen in figure 3.14, where the visible image, coating thickness map and histogram of face a are shown. The start of a coating layer can be seen in the photograph as little

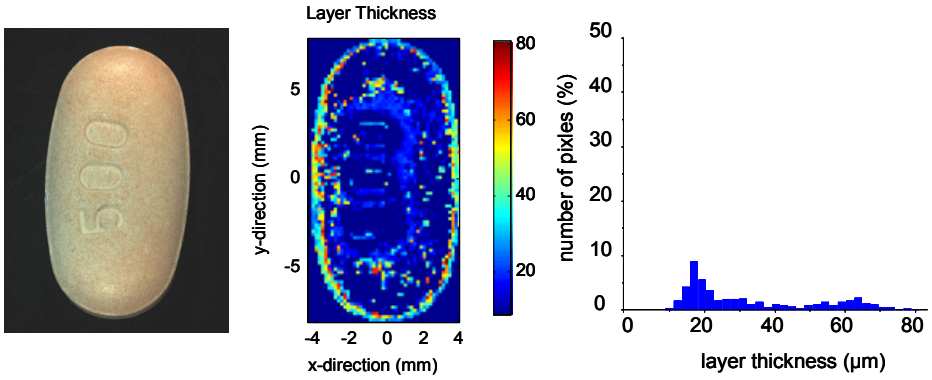

Figure 3.14 Photograph, coating thickness map and histogram of tablet E1. Sample taken at the beginning of the coating process. Photograph shows the beginning of the coating layer, histogram indicates that layer thickness is below the detection limit of the instrument.

reddish dots on the tablet, but as the coating is very thin the core is still clearly visible, which was expected owing to the fact that the sample was taken at the beginning of the coating process. The very broad distribution in the histogram indicates that a coating thickness measurement by TPI is not possible. However, this does not pose a problem, as coating layers on tablets from a later stage of the process and on finished products are much thicker and normally do not lie under the detection limit of the instrument.

Table 3.2 shows the average coating thickness of tablets E2 – E20 for both sides and center-band, including the standard deviations. Figure 3.15 plots

Sample	Average coating thickness of face a	Standard deviation (of average coating thickness of face a)	Average coating thickness of face b	Standard deviation (of average coating thickness of face b)	Average coating thickness of center-band	Standard deviation (of av. coating thickness of center-band)
E2	24.0	7.8	23.0	6.1	23.8	5.8
E3	22.5	4.9	24.2	6.3	22.6	7.1
E4	27.4	7.0	25.8	5.5	23.3	7.0
E5	27.7	3.8	25.2	5.0	24.5	6.8
E6	32.4	4.7	38.3	5.4	29.7	6.0
E7	25.0	5.1	24.3	6.2	23.1	4.7
E8	26.7	5.1	26.7	5.5	25.4	4.7
E9	29.9	5.1	32.1	5.1	26.0	3.9
E10	40.7	5.8	34.7	5.4	29.9	4.6
E11	30.2	5.3	29.1	5.5	26.5	5.9
E12	29.7	5.1	27.4	6.2	25.9	4.9
E13	32.9	6.0	40.2	5.3	30.1	3.5
E14	28.8	5.5	29.2	5.8	26.5	3.9
E15	51.9	4.8	52.5	4.9	39.9	4.3
E16	45.9	4.7	49.2	4.6	38.9	4.0
E17	43.1	4.7	39.5	4.6	32.2	4.1
E18	41.7	5.0	39.3	5.2	35.0	3.7
E19	42.3	4.6	43.1	5.0	38.9	4.0
E20	58.5	4.6	52.1	4.7	44.2	3.8

Table 3.2 Average coating thickness with absolute standard deviations of tablets E2 – E20. All values in µm.

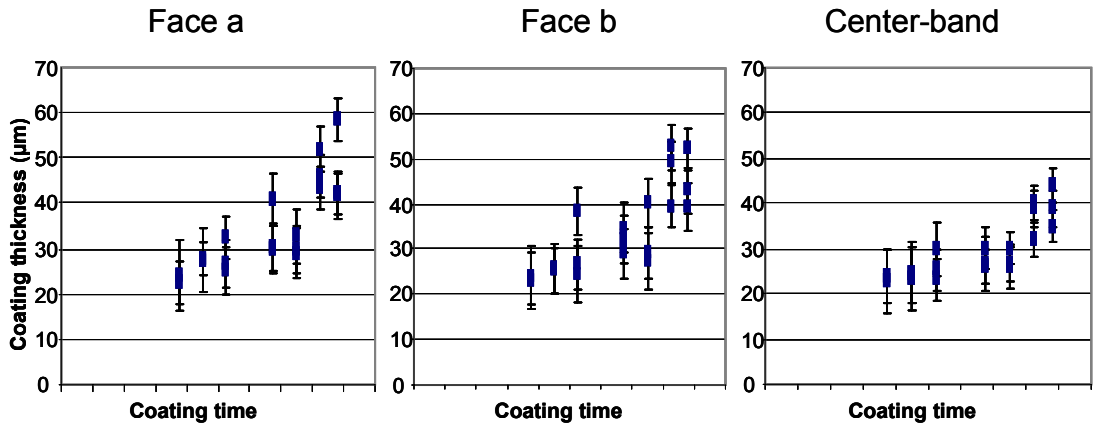

Figure 3.15 Plot of the data from Table 3.1, showing the growth of the coating thickness against time. Error bars display the standard deviation for each measurement.

the data from table 3.2, showing the growth of the coating thickness against time. The coating on the center-bands tends to be thinner than on the top and bottom faces. This can be explained by the fact that in a pan coater, the top and bottom sides of a tablet have a higher probability of facing the spray nozzles

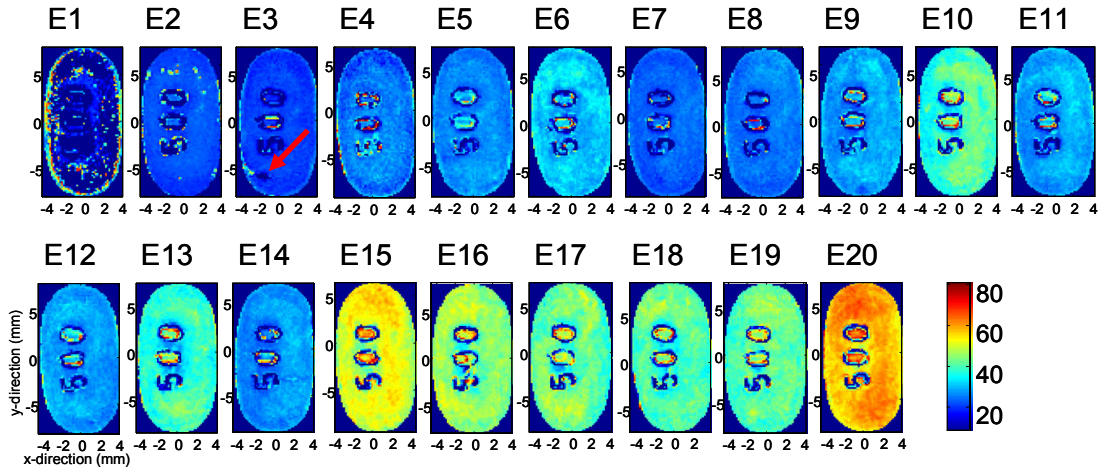

Figure 3.16 Coating thickness maps of face a of tablets E1 – E20. Color scale is in µm and the same for all images. Growth of coating thickness can be seen. Tablet E3 shows a defect in the coating (indicated by arrow).

than the center-band. Figure 3.16 shows the coating thickness maps of face a of all 20 tablets. All images are scaled to the same color scale, thus visualizing the growth of the coating. Defects in the coating can also be observed: for example, tablet E3 shows a defect close to the “5” of the embossing on face a. This is a scratch that occurred during sample handling and which removed the coating layer on that area.

It can also be observed that on all tablets, the coating on the embossing seems to be thinner than on the rest of the tablet. This is unlikely, as the coating on the embossing tends rather to be thicker than thinner compared with the coating on the rest of the tablet. It is assumed that this is an artifact of the measurement. The spatial resolution is 200 µm x 200 µm, but the width of the embossing fonts of product E is slightly smaller. Therefore, on the embossing, the focus of the THz pulse that is crucial for correct measurement cannot be guaranteed, probably resulting in wrong thickness indications.

3.3.3.3 Product F

Owing to the fact that determination of the coating thickness on the embossing of product E seemed to be problematic, the question arose of whether fine structures such as thin cracks can be detected by the instrument or not. As can be seen on the photograph in figure 3.17, tablet F has fine cracks in

the coating in the region of the embossing. The picture was taken under a microscope with approximately 6x magnification. In the coating thickness map, also shown in figure 3.17, these cracks cannot be seen. However, on the peak intensity map and especially on the interface index map (see also figure 3.17), features corresponding to the cracks on the visible image can be seen.

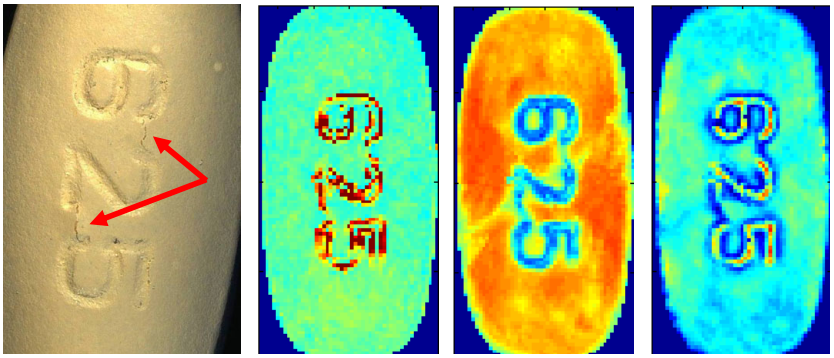

Figure 3.17 Tablet F: a) Photograph with 6x magnification, cracks in the coating indicated by arrows; b) coating thickness map; c) peak intensity map; d) interface index map. Cracks are not visible in the coating thickness map but can be seen in the peak intensity map and the interface index map.

Although the cracks are not shown on the coating thickness map, the instrument detected a failure in the area of the cracks and displayed it on the peak intensity map and on the interface index map. This shows that fine features are a problem with coating thickness maps, although, by considering the other information that the waveform provides, it might be possible to detect small defects nevertheless. However, the cracks in the coating were still easily visible on a photograph with approximately 6x magnification. A coating might have even finer cracks, so-called hairline cracks. Surely those small defects will not be detected by building up a coating thickness map, and it is questionable whether defects of such a small size can be detected by peak intensity or interface index maps.

3.3.4 Conclusion and Outlook

In this study, terahertz pulsed imaging was used to analyze the coating thickness and uniformity of film-coated tablets of three different products D, E and F non-destructively and to monitor the coating process of one of the

products. The first product served for a first evaluation of the technique. Inter- and intra-batch differences of the coating thickness were determined as well as differences on individual tablets. For the second product, the focus lay on the monitoring of the coating process. Tablets sampled during the coating process were analyzed by TPI and the increase of the coating thickness was shown. The sample from the beginning of the process had a coating thickness that was below the detection limit of the TPI instrument. The detection of the coating thickness on the embossing of this product seemed to be problematic, which can be explained by the fact that the width of the embossing is slightly smaller than the spatial resolution of the device. On the third product, the ability of the technique to detect small defects was examined. For this test, one tablet of the product was stressed during storage to develop fine cracks in the coating. Although the cracks were visible under a microscope with a low magnification, the coating thickness maps did not reveal them. However, by building the peak intensity map and the interface index map the defects could be detected.

The study shows the ability of terahertz pulsed imaging to determine coating layers of different thickness on different products and to provide direct thickness values for the layers without destroying the samples. However, the technique has some limits: if a coating or layer is too thin, it is below the detection limit of the instrument. In this case, the limit was below 22 µm, but as it depends not only on the thickness of the layer but also on the refractive index of the material, this value will be different for other products. Fine cracks can also pose a problem.

Overall, TPI proved to be a valuable technique to determine coating thickness and uniformity of film-coated tablets non-destructively and with a good repeatability. In this way, it also provided the possibility of monitoring the coating process of film-coated tablets.

4

Comparison of Near Infrared Imaging and Terahertz Pulsed Imaging for Coating Analysis

4.1 Introduction

As explained in chapter 3, tablets are often film-coated and the coat can serve various purposes. It can, for example, mask a taste or an odor, improve stability or modify release of the active pharmaceutical ingredient. Coating thickness and uniformity are important quality parameters as they can influence, for example, stability or disintegration and dissolution time and hence can have an impact on bioavailability. Different methods for quality control of the coating of tablets can be applied, but most of them have disadvantages, like being indirect or destructive measurements. One possibility for determining the amount of coating is to analyze the amount of one compound in the coating on the finished film-coated tablet by HPLC. The disadvantages are that this is a very laborious method and that it gives only the overall amount of applied coating mass, but no information about the distribution or uniformity of the film coat. Moreover, it is destructive. Fast and easy methods are to weigh the vessel from which the coating solution is taken during the coating process continuously and calculate the amount of applied coating mass, or to calculate it from the flow- or spray-rate of the coating liquid. Both methods are indirect and give only average information. A classical method to monitor the coating process and to determine its end-point is to take samples during the process, weigh a known sample size and compare the weight of the samples with coat with the weight of the same amount of uncoated samples. This allows determination of the theoretical amount of applied coating mass. Again, this method is indirect and does not give information about coating uniformity. Another problem with this

method is that the mass loss of core material during the process due to friability is not taken into account. A fast and simple method is the use of a tablet thickness tester, comparing the thickness of uncoated and coated tablets; but again, it is an indirect method and only provides average data and approximate values. A better evaluation of the film coat thickness and uniformity might be obtained through functionality testing by disintegration or dissolution studies, but they are destructive, indirect, time-consuming and laborious measurements. Another destructive, but direct, method is optical microscopy, providing direct thickness data. For coating uniformity determination it is nevertheless only partly suited as the coating thickness is measured only at a few points and not over the whole tablet surface. Scanning electron microscopy can be applied to evaluate microheterogeneities visually, but the method is lengthy and also destructive. An interesting tool is attenuated total reflection – infrared imaging, which was used for the chemical visualization of microheterogeneities and film coat thickness [58]. For imaging film-core interface and surface defects of film-coated tablets, confocal laser scanning microscopy has been applied [59]. As an autofluorescent agent in the coating layer is needed, this method is more a tool for laboratory studies than for routine production. Another tool for the determination of coating thickness and uniformity is laser induced breakdown spectroscopy [60]. An advantage of this method is its speed which allows the measurement of a large amount of samples in a short time, but as it is destructive it is not really applicable for analyzing big sample volumes. Recently, Raman spectroscopy has been applied as a non-destructive and indirect method for the determination of coating thickness and uniformity of film coated-tablets [61-64]. Another fast and non-destructive, but also indirect, spectroscopic method that has been used for the determination of coating thickness and the monitoring of the film-coating process is near infrared spectroscopy [15,16,65,66]. With NIR spectroscopy it has also been possible to predict the coating time and to detect small changes in the coating formulation [67].

Even if the results of the studies have been promising, one problem exists with both spectroscopic methods: the fact that the spectrum obtained is the average spectrum of part of the sample, depending on the spot size. This

problem can be avoided by applying hyperspectral chemical imaging, for example NIR imaging. In that case, three-dimensional data, i.e. spectral and spatial information, are obtained. The spectra provide, for example, information about the chemical identity and the spatial data provide information about the distribution. A detailed introduction to NIR imaging is given in chapter 2. Several applications of NIR imaging in pharmaceuticals have been reported. It has been used, for example, to determine powder blend homogeneity [21] and blend uniformity in final dosage products [68]. It has also served to identify tablets in blister packs [12] and to extract process related information from tablets and pre-tabletting blends [69]. It has also been applied to examine the internal structure of time-release granules [70], but coating analysis by NIR imaging is not widespread.

Another imaging method that provides detailed information about a big area of a sample is terahertz pulsed imaging. As demonstrated in chapter 3, TPI allows the fast, direct and non-destructive determination of coating thickness on multiple points on a sample surface. In this way, information about coating uniformity is obtained as well. Monitoring of the coating process is also possible by TPI, as was described in chapter 3.

NIR imaging analysis was conducted on the same samples that were used for the monitoring of the coating process in chapter 3. In the study described below, the results of the TPI and NIR imaging analysis are compared and advantages and disadvantages of the two methods are discussed.

4.2 Material and Methods

4.2.1 Samples

Samples E1 – E20 of product E, that were described in chapter 3, were analyzed by TPI and NIR imaging. The biconvex oblong tablets with embossing on both faces were coated with Opadry Pink in a large-scale pan coater. E1 was taken from the beginning of the coating process and had hardly any coating; E20 was from the end of the process and had the thickest coating layer. An additional sample, sample E0, was analyzed by NIR imaging. It was an uncoated core of product E. Upper face (face a), lower face (face b) and center-

band were analyzed. Pure Opadry Pink was measured by NIR imaging for reference.

4.2.2 Terahertz Pulsed Imaging

Coating thickness and uniformity were measured by a TPI imaga 2000 with acquisition software TPIScan and data treatment software TPIView (all TeraView Ltd, Cambridge, UK) as described in chapter 3. Measurement time was 20 to 30 minutes per tablet.

4.2.3 Near Infrared Imaging

For acquisition of NIR images, the Sapphire with SapphireGo software (Malvern Instruments Ltd, Malvern, UK) was used. The instrument is equipped with a focal plane array detector with a size of 256 x 320 pixels, which allows the acquisition of 81920 spectra simultaneously. Spectral range covered 1100 – 2450 nm with a spectral resolution of 10 nm; each image was collected as 16 coadds. Each pixel was 80 µm x 80 µm. Both faces of each tablet were imaged as well as the two flat sides of the center-band. Owing to the strong curvature of the round parts of the center-band and resulting focus problems, imaging was not possible in those parts. Measurement time was below 5 minutes for each image, thus below 20 minutes for the 4 images obtained per sample. An image of Opadry Pink powder was taken for reference. Data were treated using ISys software (Malvern instruments Ltd, Malvern, UK). From all images, bad pixels were removed by applying a 3 x 3 median filter and spectra were converted to absorbance units. The areas on the images that were around the tablets were removed by masking. SNV transformation was performed. Mean spectra of tablet 0, tablet 20 and Opadry Pink were computed for comparison. The images were then used as this or a Savitzky-Golay 2^{nd} derivative was applied. Images were either analyzed individually or several images were concatenated to form a bigger image which was then analyzed. On the images of the tablets, different methods were tried. The images were examined at single wavelengths that were characteristic for the core or coating. PCA was performed as well as PLS-DA. For PLS-DA, mean spectra of the core and of the longest coated tablet were used as reference.

4.3 Results and Discussion

4.3.1 Near Infrared Imaging

Figure 4.1 shows the mean near infrared spectra of Opadry Pink, tablet core and the longest coated tablet. At first glance, the spectra of the core and the coated tablet look similar, but upon closer inspection there are peaks in the core spectrum that are not visible or much weaker in the coated tablet spectrum

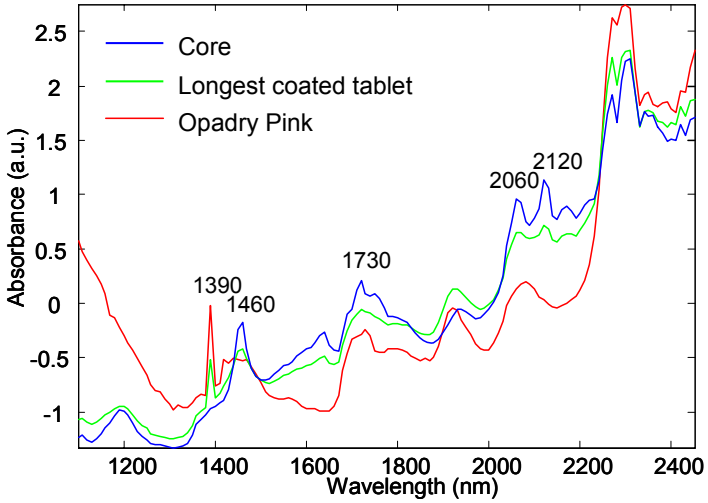

Figure 4.1 Mean NIR spectra of tablet core, longest coated tablet and Opadry Pink, displaying characteristic peaks. Differences between the core and the coated tablet due to Opadry Pink are visible owing to different absorbance values for example at 1390 nm, 1460 nm, 1730 nm, 2060 nm and 2120 nm.

and vice versa. Comparison with the Opadry Pink spectrum explains that those differences are due to the coating material. For example, a characteristic peak of Opadry Pink lies at 1390 nm. A peak at that wavelength is also visible in the coated tablet spectrum, but not in the core spectrum, indicating that a differentiation between coated and uncoated tablets should be possible at this wavelength. In the core spectrum, peaks are for example distinctive at 1460 nm, 1730 nm, 2060 nm and 2120 nm. They are also present in the coated tablet spectrum, but less strong, thus providing the possibility to differentiate between coated and uncoated tablets at those wavelengths. Images of face a of tablets E0, E1, E2, E6, E9 and E18 were concatenated and looked at at the different wavelengths that showed to be characteristic for core and coated tablet,

respectively. Only six tablets were concatenated, as the resulting data cube was otherwise getting too big and computations were no longer possible. Comparing the images, it proved that the best wavelengths for differentiating between coated and uncoated tablets as well as for visualization of the growth of the coating during the process were 1390 nm and 2120 nm. Figure 4.2 shows those two images as well as the mean spectra of the six tablets in the region of the two specific wavelengths. The absorbance at 1390 nm increases from the uncoated sample on the left to the most coated tablet on the right, visualizing the growth of the coating in the image by showing higher intensity values on the right. This could be expected, as 1390 nm is a characteristic wavelength for Opadry Pink, the coating material. The coating thickness growth results in an increase in absorbance. At 2120 nm, this is exactly the other way round. As the wavelength is characteristic for the core, the absorbance decreases with thicker

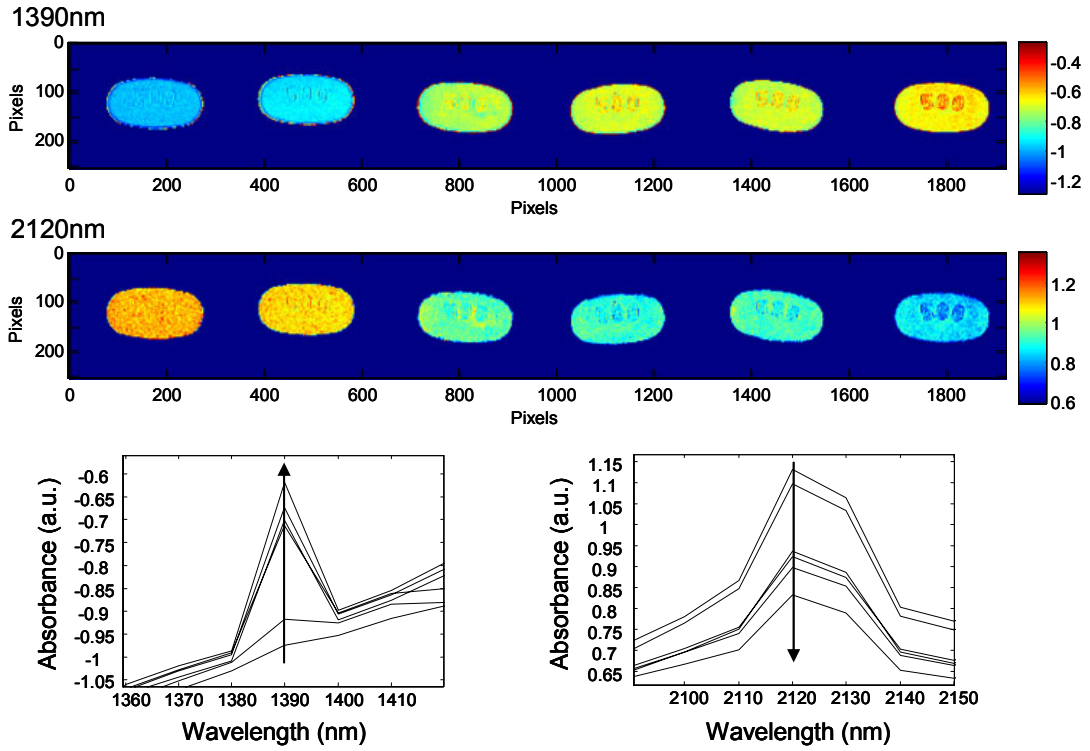

Figure 4.2 Top: Concatenated NIR image of tablets E0, E1, E2, E6, E9, E18 (from left to right) at 1390 nm and 2120 nm, showing the growth of the coating layer by change in absorbance. Color scale indicates absorbance values, with red being the highest and blue being the lowest absorbance, respectively. Bottom: Parts of the mean NIR spectra of tablets shown in the concatenated image, arrow indicating the growth of the coating layer.

coating, thus showing lower intensity on the right side of the image. With the same image, PCA and PLS-DA were performed. On the fourth principal component, the growth of the coating could be seen; PLS-DA was also able to visualize the different coating thickness. However, the results were analogous and PCA and PLS-DA did not provide additional information in that case. As PCA and PLS-DA required higher computational power, and displaying the images at a single wavelength was faster and easier, single-wavelength images were preferred in this case. The same applied to the Savitzky-Golay 2nd derivative. It provided similar results, but as no additional information could be obtained, it was not necessary to use this pretreatment.

In the concatenated image, a good and easy comparison between the different tablets is possible as all images are scaled to the same intensity color scale. However, owing to computational power limits, it was not possible to concatenate the images of all tablets. Therefore, single images were used in order to analyze all tablets. Images at 1390 nm of face a of tablets 1 to 20 are shown in figure 4.3. The increase of the coating thickness from uncoated to fully coated tablets is not as easily visible as in the concatenated image. As each image has its own color scale, an inter-tablet comparison is more difficult. But the intra-tablet differences are better seen in the single images. However, a comparison between the tablets is also possible by considering the different color scales. Absorbance values, indicated by the intensity color scale, increase from the image of tablet E1 to the image of tablet E20. This can be seen in figure 4.4, where the mean values of the single images of tablets E0 to E20 are plotted against the coating time. The absorbance of the samples over the coating process increases, thus indicating the growth of the coating.

Results from face b are equivalent. The situation at the center-band is more difficult. Not the whole of the center-band could be imaged owing to focus problems at the very round ends of the tablets. Imaging of the flat side of the center-band was possible, but the masking – i.e. the cutting away of the unwanted parts of the image, in this case the small part of the faces that could be seen but that are not part of the center-band – is difficult and it is not always possible to display just the center-band on the image without side effects.

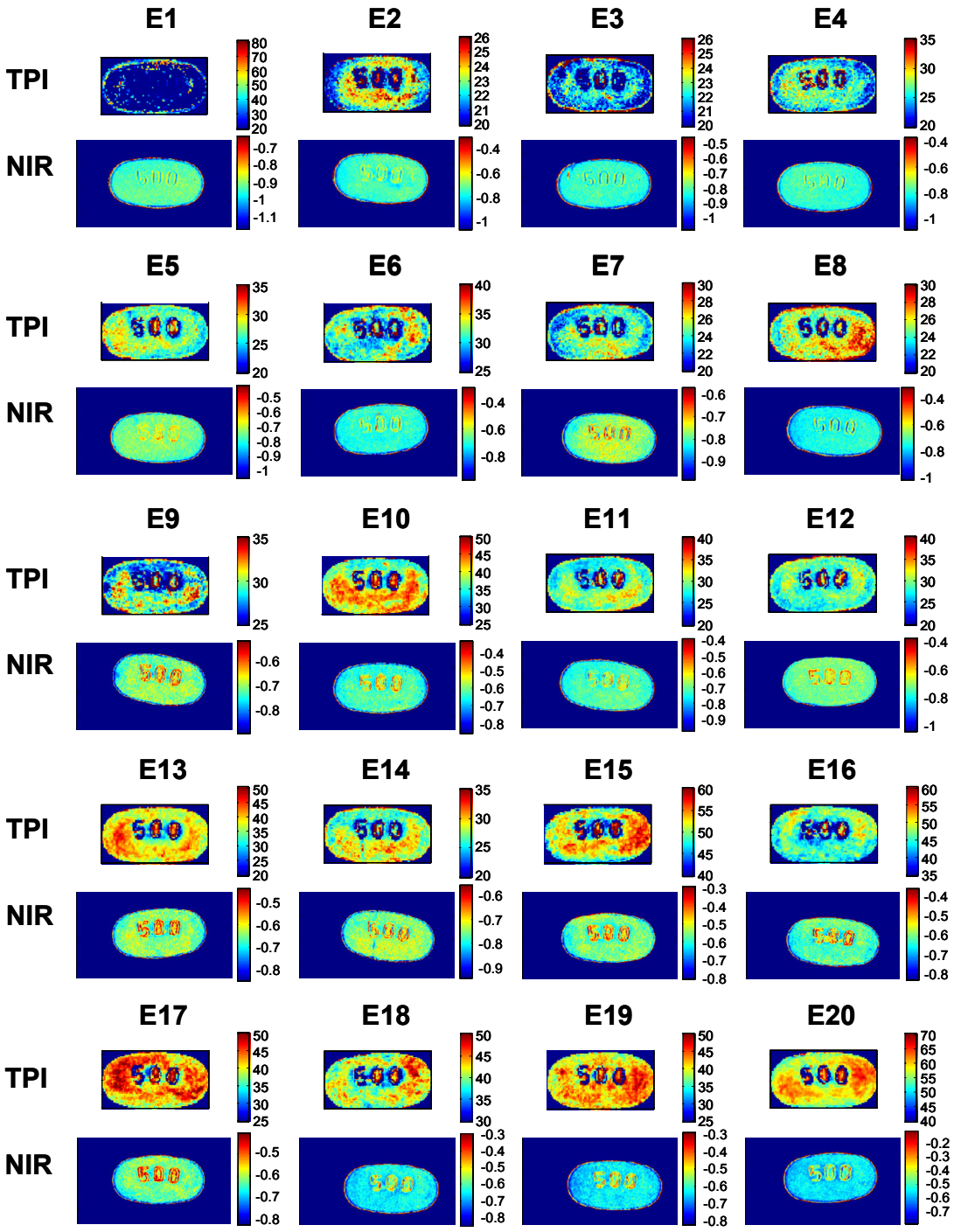

Figure 4.3 TPI coating thickness maps and NIR images at 1390 nm of face a of tablets E1 – E20. Color scales of the coating thickness maps indicate thickness in µm; color scales of NIR images give absorbance values. TPI and NIR images show the same pattern of coating layer distribution.

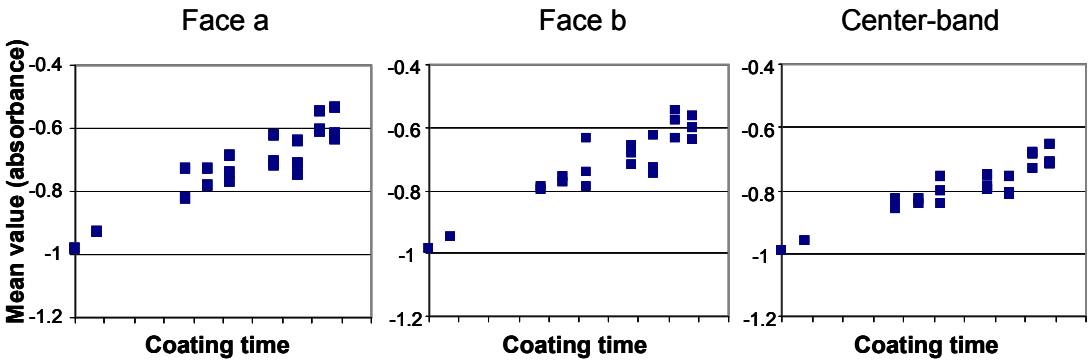

Figure 4.4 Mean near infrared values of absorbance at 1390 nm of tablets E0 – E20 plotted against coating time. Increasing absorbance values indicate growth of the coating layer during the process.

However, similar calculations to those on faces a and b, respectively, were possible and resulted in similar data, but it must be kept in mind that not all the center-band is looked at. Overall, the absorbance values at the center band were lower than at the faces, indicating a thinner coating layer at the center-band.

4.3.2 Terahertz Pulsed Imaging

Results of the TPI coating thickness and uniformity analysis of tablets E1 to E20 have already been discussed in detail in the chapter 3. Average coating thickness ranged between 22.5 µm and 58.5 µm and the growth of the coating thickness in relation to time was shown. The coating thickness of tablet E1 could not be determined by TPI as it was below the detection limit of the instrument. Small defects in the coating could be detected. Owing to the spatial resolution of the technique, coating thickness determination on the embossing was a problem. In chapter 3 the coating thickness maps of face a of all tablets were shown; the color scale was the same for all samples in order to visualize the growth of the coating better. In figure 4.3, coating thickness maps of face a of tablets E1 to E20 are shown. This time, the color scale is optimized for each image, therefore visualizing the intra-tablet differences better than the inter-tablet differences, as is the case if the color scale is the same for all coating thickness maps.

4.3.3 Comparison of Terahertz Pulsed Imaging and Near Infrared Imaging

Figure 4.3 shows the coating thickness maps of face a of tablets E1 to E20 and the near infrared images of face a of the same tablets at 1390 nm. Each image has its own color scale, i.e. the lowest value in the image is the lowest value of the color scale and the highest value is the highest, respectively. This accentuates the intra-tablet differences. Comparing the TPI image and the NIR image of the same tablet, it can be seen that they both have the same pattern. Where the TPI coating thickness map indicates a thicker coating layer, the absorbance in the NIR image is higher as well. Defects in the coat are also visible in images of both techniques. For example, the coating layer of tablet E14 was removed at the level of the “5” of the embossing by accidental scratching during sample handling. This scratch is detected in the TPI map as well as in the NIR image (see also magnification in figure 4.5).

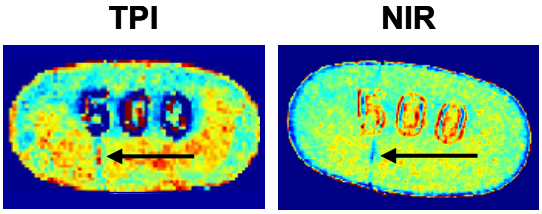

Figure 4.5 TPI coating thickness map and NIR image at 1390 nm of face a of tablet E14. Coating defect due to accidental scratching during sample handling (indicated by arrows) can be determined.

The biggest difference between each pair of images lies on the embossing. The NIR images show higher absorbance on the embossing, thus indicating a thicker coating layer, whereas the TPI coating thickness maps show a lower coating thickness in those parts. As discussed in chapter 3, the determination of coating thickness on the embossing of this product by TPI is problematic as the spatial resolution is slightly over the width of the embossing. Thus, the coating thickness values on the embossing on the TPI maps are considered as an artifact of the measurement. The NIR images have a higher spatial resolution than the TPI maps and therefore allow a more accurate analysis in problematic regions like the embossing.

Another difference is the fact that in the NIR images, the coating at the edge of the tablet seems to be thicker than on the rest of the face. This is not visible in TPI coating thickness maps. As in TPI the surface is mapped point by point, such edge effects can be avoided for example by not considering the outermost ring of point measurements. In NIR imaging with a FPA, where the whole sample is imaged at once, edge effects can be a problem. In this case, it might be due to the fact that the center-band is located “below” the edge of the face, thus imitating a thicker coating layer. But as it is the same for each tablet, the influence when comparing them should not be too big.

An advantage of NIR imaging is the lower detection limit. With TPI in this study, the coating thickness of tablet E1 could not be determined because it was below the detection limit of the instrument. With NIR imaging, detection is possible; a clear difference between tablet E1 and the uncoated tablet E0 can be seen (figure 4.6). On the other hand, it can be expected that when the coating gets very thick, TPI will still be able to determine the layer thickness

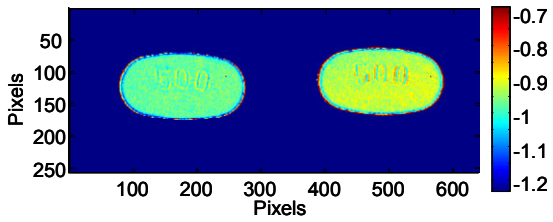

Figure 4.6 Concatenated NIR image of tablets E0 (left) and E1 (right) at 1390 nm; difference between the uncoated core E0 and the slightly coated tablet E1 can be seen.

whereas with NIR imaging this might not be possible. When the coating has reached a certain thickness, NIR radiation will not reach the core any more, therefore only information about the coating will be contained in the spectra. Then, it does not matter if the coating gets even thicker as differentiation is not possible any more.

Another advantage of TPI is the fact that the whole center-band can be analyzed. In NIR imaging, this was not possible owing to the very strong curvature of the ends of the tablet. From a measurement time point of view, the differences are not too high if the full spectrum is used in NIR imaging. If only a

few wavelengths are looked at, acquisition time decreases considerably and NIR imaging becomes much faster.

The biggest advantage of TPI is surely that it is a direct measurement and coating thickness values are obtained directly. NIR imaging is an indirect method; not the thickness is measured, but the change in absorption at a certain wavelength. This allows good intra- and inter-tablet comparison but in order to know how thick the coating layer actually is, other methods like TPI have to be applied and a calibration has to be made. It has also to be considered that in NIR imaging, as changes in absorption values are used, the spectra of coated and uncoated tablets have to be different enough to extract the wanted information. In this study, it was easily possible at a single wavelength, but it might be more difficult with other products. One other advantage of TPI is the low-energy nature of the THz radiation used, so there is no heating of the sample. Depending on the measurement time and the temperature sensitivity of the samples, heating might be a problem in NIR imaging where the radiation is much more energetic.

The two methods have in common that they are non-destructive; a sure advantage over other methods such as LIBS or optical microscopy where the sample has to be sectioned. When comparing the average thickness values given by TPI (shown in chapter 3) with the mean absorbance values of the NIR images (figure 4.3), both methods show the growth of the coating layer during the process. Both methods do also detect a thinner coating layer at the center-band compared with the faces of the tablets. This is due to the fact that the tablets in the pan coater have a higher probability of facing the spray nozzles with the relatively flat sides rather than with the center-band.

4.4 Conclusion and Outlook

TPI and NIR imaging were used to analyze the coating of film-coated tablets that were taken out of the coating pan during the coating process. Both fast, non-destructive methods were able to visualize the growth of the coating layer. TPI measurements provided direct coating thickness values over the whole sample surface, thus also showing inter- and intra-tablet differences. NIR

imaging also gave information about inter- and intra-tablet coating layer differences, but as an indirect method, real layer thickness values were not obtained. The pattern of the coating thickness distribution as shown by TPI coating thickness maps and NIR images is the same. The spatial resolution of NIR is better than that of TPI, and NIR imaging allows the visualization and comparison of layers that are below the detection limit of the terahertz pulsed imaging instrument. On the other hand, it is expected that TPI will be more suitable for very thick layers.

As both methods are valuable tools for monitoring the coating process, they may prove useful in a PAT context. They both have potential for rapid at-line analysis and process control. A very advantageous possibility could be the combination of both methods. TPI could be used for initial coating analysis of the complete surface of the tablet, supported by NIR imaging where, for example, a higher spatial resolution is necessary. If a calibration of NIR imaging results at a specific wavelength with TPI results is successful, fast NIR measurements could be possible; this could lead to on-line control of the coating process.

However, a combination would be quite expensive. At the moment, a TPI imaga 2000 costs approximately 684,000 Swiss francs, and a SyNIRgi (successor of the Sapphire) costs approximately 344,000 Swiss francs. Thus, the purchase of both devices needs to be thoroughly considered. If the coated products have a high financial volume, or if more sophisticated multilayered coating films are used, it might be worth buying a TPI instrument. It should not be forgotten that a TPI device can be used for other analytical problems like buried layers in tablets or interfaces in laminated tablets, for example. A TPI instrument could then be used in a central analytical unit for such questions and also for coating analysis for example during development. When developing or up-scaling the coating of a tablet product, TPI can help to decide when enough coating is applied, thus reducing coating cycle times later on in routine production. Even though TPI, from a technical point of view, is suitable for at-line analysis in a production environment, it might be used rather in a central analytical unit from a financial point of view. There, it can not only serve for at-

line or in-process controls, like in a production environment, but it can be used for other areas, like development and multiple analytical questions. It could then be also used to calibrate NIR imaging results to coating thickness values. Calibration could be possible by writing a little program that overlays the images first and then defines which NIR absorbance value goes with which TPI coating thickness value. After building such a calibration model in a laboratory environment, a NIR imaging device like the Sapphire could be used in production for fast at-line analysis. But basically, as a calibration would be done with only one or several wavelengths, a NIR camera that uses only those few wavelengths instead of being able to scan the full range could be used. This would be considerably cheaper and it would allow such a NIR coating analysis to be used in several production units while the TPI and NIR devices that are used for building the calibration are standing in a central analytical unit. Still, it has to be considered if absolute thickness values are necessary. If not, a NIR device alone might be sufficient. Although such an instrument still has its price and cannot be called cheap, it can be used for many applications other than just coating analysis. As NIR imaging is older and more widely used than TPI, the benefit of a NIR imaging instrument is probably higher at the moment. However, for some problems, TPI might be the analytical technique that provides the answer to a problem rather than NIR imaging. Then it has to be considered whether it is not profitable to buy a THz imaging device despite the high price. Overall, a TPI instrument would bring more benefit in a central unit than at production sites where its full potential would not be used. Basically, the same applies to NIR imaging, at least to full-spectral-range instruments like the Sapphire; while NIR cameras that cover just several chosen wavelengths provide a possibility for at-line analyses in a production environment that is financially realistic.

5

Laser Induced Breakdown Spectroscopy

5.1 Introduction

Laser induced breakdown spectroscopy is a technique based on atomic emission spectroscopy. In LIBS, the pulse of a high energy pulsed laser is focused on a sample surface. There it ablates a small amount of material, and the constituents of the ablated material are vaporized in a plasma. The elements in that plasma are excited, that is to say atoms dissociate, and they are ionized or electrons in the atoms are brought to excited states. This is followed by a relaxation to ground states by emission of radiation. The radiation is at defined wavelengths characteristic for the contained elements and can be detected. This allows the elemental composition of the sample to be determined. Thus, in this technique, elements are analyzed and, normally, molecular information about the components of the sample is lost. Sometimes, however, aromatic carbon structures give a signal as well and can be detected.

In order to determine a substance in a certain matrix, it has to be different from the matrix from an elemental point of view. If, for example, a sample like a tablet has to be analyzed, elements like C, O and H are contained in the matrix as most excipients are organic. Therefore, those elements form a background in the emission spectra. It would then be difficult or impossible to detect a substance composed of C, O and H only. On the other hand, metals and hetero-atoms like sodium, potassium, magnesium, calcium, chlorine, fluorine, bromine, phosphorus or sulfur have unique spectral emission lines and can be distinguished from the spectral signal of the matrix. Aromatic carbon structures have a spectral signal different from that of carbon and can sometimes be distinguished from the background matrix signal as well. If the

API in a tablet is to be determined, it must therefore contain an element that is absent in the matrix, or an aromatic carbon structure. As most active ingredients contain hetero-atoms or metals in their molecule or in their used salt form, it is possible to analyze them in the excipients matrix. Analysis under a helium atmosphere might improve the signal-to-noise ratio and therefore increase the sensitivity of the analysis [71].

A disadvantage of LIBS is that it is a destructive technique. Advantages are that it is rapid and that no or only minimal sample preparation is necessary. As explained before, it can be applied on a wide range of target analytes, and fiber optics can be used. Moreover, the craters that result from the ablation of the material by the laser pulse are not too big. For example, on tablets, the craters have diameters of several hundred micrometers up to one millimeter [60,71]. Thus, by focusing the laser on different spots, spatial information is obtained. A depth profile is received if several consecutive laser pulses are shot on the same site. As each pulse ablates some material, a hole is drilled in the sample and each time spectral information from a deeper layer is obtained. Normally, the penetration depth of one laser shot is known to be around 10 µm in the coating and 100 µm in the core of a tablet, but it might be different depending on the material [60].

LIBS analyses are possible on solid, liquid and gaseous samples and the technique has been applied in many fields such as metallurgy, environmental monitoring, geological analysis, space exploration, diagnostics of archaeological objects, remote material analysis in nuclear power stations, and hazardous materials [72-74]. In a pharmaceutical context, LIBS has been used mainly to analyze solids like powders and tablets. It has been applied to quantitatively analyze API and lubricant in tablets and powders [71,75,76]. The effects on different physical parameters during the manufacturing of tablets on LIBS analyses were also investigated [77]. LIBS has also been applied to analyze the film coat of tablets [60,78].

In this study, LIBS was applied for coating analysis of one product and for determination of the API and lubricant distribution in tablets of two different products. It was intended as a feasibility study and served mainly as a

comparison with NIR imaging and TPS/TPI. For the coating analyses, samples of product D were used, and LIBS results on coating thickness and uniformity were compared with TPI results for the same product. For determination of API distribution, samples of product B and D were used. The results of product B were compared with NIR and TPS/TPI results. Advantages and disadvantages of the different techniques are discussed.

5.2 Material and Methods

5.2.1 Samples

Tablets of product B were uncoated, round, and had a breaking notch. The API content was below 3% (w/w). Five tablets each of two different batches of product B were used. Tablets of product D were round, biconvex and coated with 3% (w/w) of Opadry White. This coating contained titanium (Ti) dioxide. The API accounted for more than a third of the tablet weight in product D. 10 tablets from each of two different batches of this product were analyzed. Both products contained a lubricant with magnesium (Mg) ions, in both cases the amount of this lubricant was below 2% (w/w). The API molecules of both products did not contain hetero-atoms as named above, but they had aromatic carbon structures.

For API and lubricant determination, 10 tablets of product B were analyzed without sample preparation. Also, 10 tablets – five from each batch – of product D were analyzed; in this case, the coating from the tablets of product D was removed by a knife in order to prevent interferences due to the coating. For coating analysis, five tablets from each of the two batches of product D were used and those tablets were measured without sample preparation.

5.2.2 Laser Induced Breakdown Spectroscopy

The samples were analyzed on the PharmaLIBS 250 instrument with dedicated software (ProSense B.V., Oosterhout, The Netherlands/Munich, Germany). Analyses were carried out by specialists at ProSense B.V. (Oosterhout, The Netherlands). A schematic illustration and a picture of the device are shown in figure 5.1. The device is equipped with a neodymium

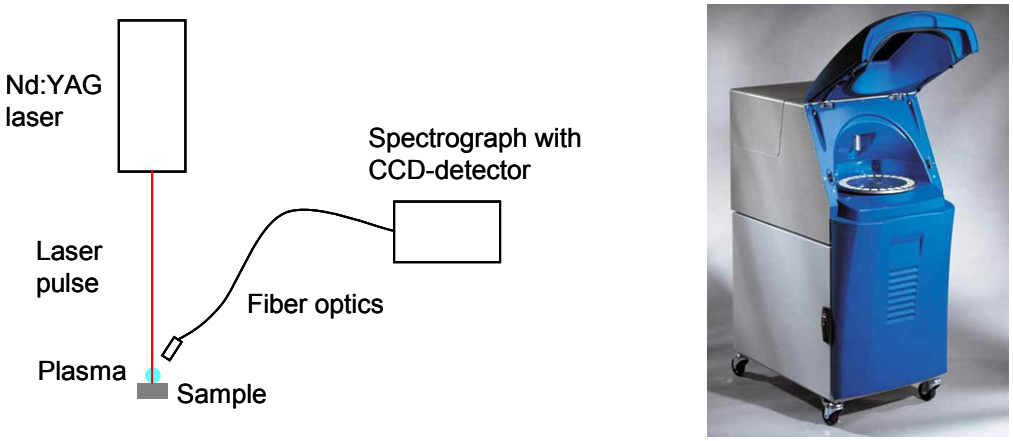

Figure 5.1 Schematic illustration (left) and picture (right) of the PharmaLIBS 250 instrument (picture: ProSense, Munich, Germany).

doped yttrium aluminum garnet (Nd:YAG) laser operating at 1064 nm. The energy was set at 150 mJ. The emitted light is transmitted via fiber optics to the spectrograph of Czerny-Turner configuration which contains a grating. The light is then detected by a charge-coupled device (CCD) camera. The signal of the specific element that was chosen for analysis at a specific wavelength is detected and an intensity value is obtained. As each shot drills deeper into the sample, a depth profile is obtained when plotting the shot numbers against the intensity values.

Seven sites of one side of each tablet were analyzed, as shown schematically in figure 5.2. 16 shots were done per site for the API and lubricant determination; and 26 shots per site were done for the coating analysis. The first shot was discarded as it generally contains too much information about surface contamination and was therefore regarded useless for the analysis. The analysis time was 1.5 minutes per sample for the samples with 16 shots and

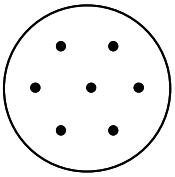

Figure 5.2 Illustration of the arrangement of the seven shot sites on a tablet.

2.5 minutes per sample for the samples with 26 shots. The depth of each shot was assumed to be 100 µm for the core and 10 µm for the coating.

For determination of API in products B and D, the signal of the aromatic carbon structure, which is also called C2, was used. For lubricant analysis in both products, the signal of Mg was used. The C2 and Mg signals were detected simultaneously and a depth profile was created. Analyses were carried out in a normal atmosphere. Attempts were made to improve the sensitivity of the measurement of tablets of product B by analyzing them also under a helium atmosphere. In order to determine the coating thickness of tablets of product D, the Ti signal resulting from the titanium dioxide in the coating was chosen as well as the Mg signal from the lubricant in the tablet core. A depth profile was constructed.

5.3 Results and Discussion

Figure 5.3 shows the emission spectra of a tablets of product B and

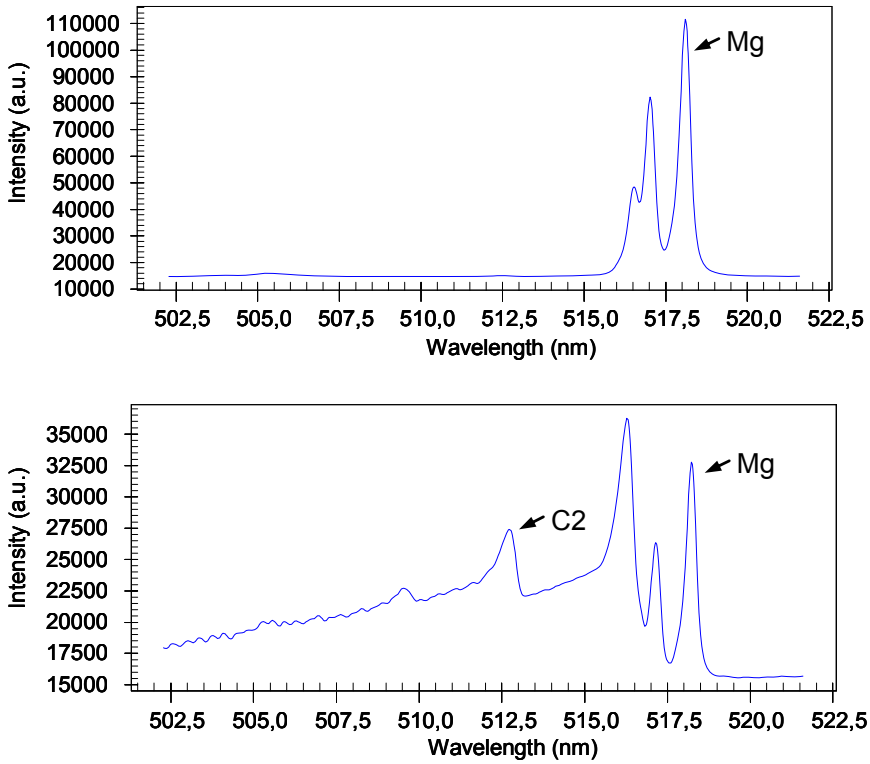

Figure 5.3 Emission spectra of a tablet of product B (top) and of a tablet of product D (bottom). The Mg peak is at 518 nm and the C2 peak at 513 nm.

product D, respectively. The Mg peak lies around 518 nm and is clearly visible. The C2 peak at approximately 513 nm is only present in the spectra of product D. This is due to the fact that this signal is less strong and more difficult to detect. Only in the case of product D, where the API accounts for more than one third of the tablet weight, thus being rather highly concentrated, it is visible. The API concentration of product B is more than ten times lower. This concentration is too low to allow the C2 signal of the API to be detected. Thus, for product B, it was only possible to obtain information about the distribution of the lubricant, but not of the API. Purging with helium did not improve the analysis; it was not possible to detect the C2 signal of tablets of product B under a helium atmosphere.

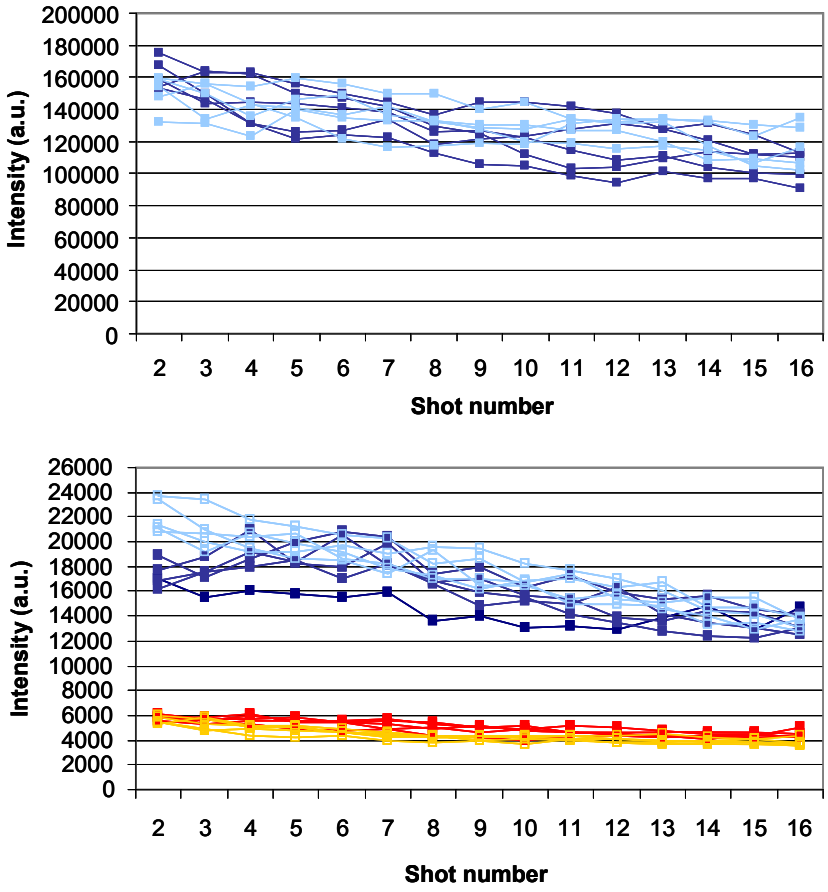

Figure 5.4 Depth profiles for tablets of product B (top) and D (bottom). Mean intensity values of the seven sites per tablet are shown. Top: Mg signal of the two batches in dark blue and light blue; bottom: Mg signal of the two batches in dark blue and light blue and C2 signal of the two batches in red and orange.

In figure 5.4 the depth profiles for the tablets of products B and D are shown. The intensity values of the seven sites of one tablet are averaged. It is important to keep in mind that the values do not give real concentration values of the component in the matrix, but only intensity values of the peak of the element in the spectrum. They allow only comparison of individual tablets or sites and shots on one tablet. The values of the Mg signal fluctuate more than the C2 values, which can be explained by the fact that its concentration is much lower than that of the API of product D. Overall, the values for the individual tablets of either product B or D are in the same region. For none of the products were strong inter-batch differences detected. It is noticeable that the intensity values of the Mg signal decrease with higher shot numbers. The same applies to the C2 signal but less strongly. This is probably due to the fact that with increasing shot numbers, the depth of the hole increases and less light reaches the detector. In order to estimate the differences between the different sites, the standard deviations of the intensities per site and shot were calculated. As an example, the mean intensity values of the Mg signal and the standard deviations of one tablet of product B are shown in figure 5.5. The standard deviations are relatively high, which can be explained by the low site number. However, they are all in the same dimension, which indicates that they do not refer to an inhomogeneous distribution of the component but rather to normal measurement variation.

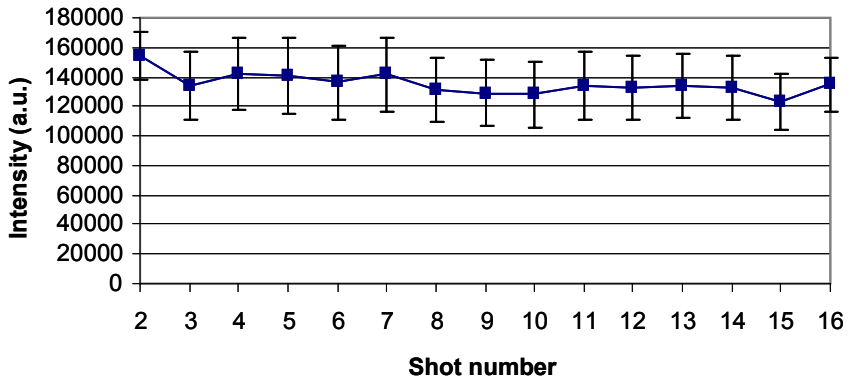

Figure 5.5 Mean intensity values of the Mg signal and the standard deviations of one tablet of product B.

Distribution of lubricant and of API of product D was not analyzed by NIR imaging or TPS/TPI. However, the distribution of the API of product B was investigated by the named techniques. With TPS and TPI the situation was similar to the LIBS analysis: the content of the API was below the detection limit and it was therefore not possible to obtain information about its distribution by those techniques (see chapter 3.2). However, NIR was able to provide information about the distribution of the API in those low-dosage tablets (see chapter 2.4).

For coating analysis, the Ti and Mg signals were detected simultaneously. Figure 5.6 shows the emission spectrum of one tablet of product D. The Ti peak

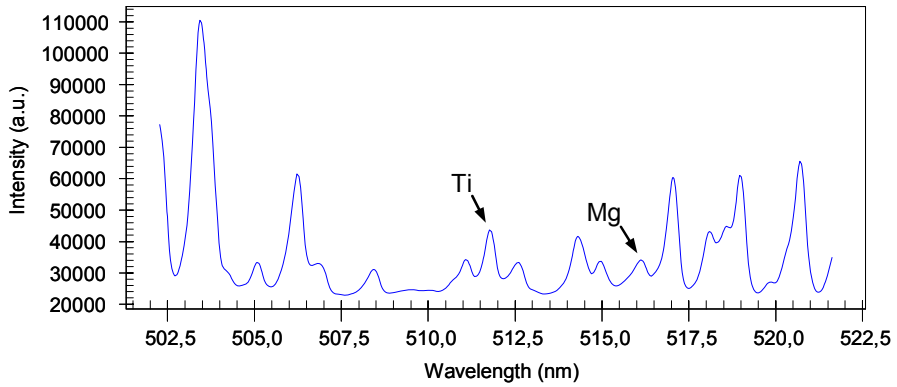

Figure 5.6 Emission spectra of the coating of a tablet of product D. The Mg peak is at 516 nm and the Ti peak is at 512 nm.

is just below 512 nm and the Mg peak, which has shifted compared with the analysis above, lies at approximately 516 nm. Titanium is contained in the coating as titanium dioxide and Mg is contained in the lubricant in the core. Thus, at the beginning of the analysis, i.e. at the first few shots, only Ti will be detected as only the coating is ablated. After a few shots, the coating will be removed completely on the site where the laser pulse is focused. Then, the Ti signal should vanish and only elements that are present in the core, like Mg, should be detected. In figure 5.7, the depth profiles of the coated tablets of product D are shown. As before, the values of the sites of one tablet are averaged. Strong inter-batch differences are not visible. As expected, only Ti is detected at the beginning and, after a few shots, the Mg appears. However, the Ti signal does not vanish completely. This is due to the Ti in the coating at the

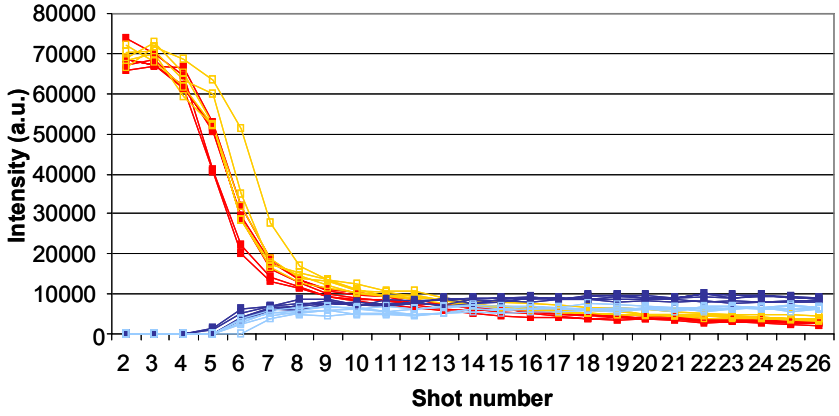

Figure 5.7 Depth profiles for coated tablets of product D. Mean intensity values of the seven sites per tablet are shown. The Mg signal of the two batches is in dark blue and light blue and the Ti signal of the two batches is in red and orange.

side of the hole which disturbs the measurement. When assuming that each laser pulse penetrates 10 µm in the coating layer, the coating would be around 60 µm thick as Mg starts to appear at the sixth shot. This is consistent with the TPI measurements where the average coating thickness was 56.5 µm for the tablets with 3% (w/w) of coating (see chapter 3.3). However, the LIBS analysis is very imprecise. The depth resolution, which is determined by the depth the laser ablates with each shot, is 10 µm in this coating and thus high compared with TPI. LIBS is therefore more a fast method for a first estimation of the coating thickness than a very precise technique, especially when considering that the penetration depth per pulse depends on the material. Therefore, it can be different for other coating materials and would have to be verified for example by profilometry measurements. Also, the spatial resolution is not outstanding. In this case, only seven sites per tablet were analyzed. By comparing the sites of one tablet and calculating the standard deviation, a certain spatial resolution is obtained. In this case, the standard deviations were analogous to the measurement of the lubricant as shown above. Of course, more sites could be analyzed, but the overall number of sites is limited by the diameter of the shot which is several hundred µm to one millimeter. Thus, compared with the spatial resolution of TPI and NIR imaging, that of LIBS is worst.

5.4 Conclusion and Outlook

LIBS can be a useful tool for fast analyses when hetero-atoms or metals are present in the molecules or salts that should be analyzed in a matrix. If this is not the case, detection is difficult or impossible. For the studied products, TPI could give more exact information about the coating and NIR was able to determine the distribution of the API where LIBS could not provide information. However, LIBS was able to detect the lubricant at low concentrations without problems; this was not investigated by THz or NIR measurements but it is expected that those methods would have difficulties in detecting low concentrations of lubricants.

The study shows that, overall, LIBS can be useful for a first or rough estimation of coating thickness, and to a certain degree also coating uniformity and distribution of API and lubricant, depending on the product. The method is very fast, but as it is destructive it is not possible to analyze large quantities. This is a clear disadvantage compared with TPS/TPI and NIR imaging. The choice of the method depends of course on the problem and on the products that have to be analyzed. For the studied products the question was the analysis of coating thickness and uniformity and the API distribution in low-dosage tablets. Here, LIBS did not prove to be better than or even equivalent to TPI and NIR imaging. However, for other problems, especially for rough estimations, it can be a useful and fast analytical tool.

6

Conclusion and Outlook

In this work, different new and innovative technologies were used for analyzing solid dosage forms. The abilities of NIR spectroscopy, NIR imaging, TPS, TPI and LIBS to analyze different parameters of tablets or capsules were investigated. The techniques were compared, and the advantages and disadvantages were pointed out. It was evaluated if the techniques were able to analyze the wanted parameter in a laboratory environment, and the potential of the techniques for at- and on-line measurements was discussed. Six different products were used: one product was hard-gelatin capsules, two were low-dosage tablets, and three were film-coated tablets. The analyzed parameters were coating thickness and uniformity of the film-coated tablets, distribution of API and excipients mainly in the low-dosage tablets and presence of a briquette in the capsules. Additionally, the applications of NIR spectroscopy in a solids manufacturing environment were presented.

The overview of the applications of NIR spectroscopy in the full-scale manufacturing of solid dosage forms showed that NIR measurements are already applied in nearly all production steps. Most common are at-line analyses, but on-line and in-line measurements also exist. NIR measurements prove to be valuable for process control, also in a PAT context, and the number of applications is growing.

The capsules were analyzed by NIR spectroscopy and imaging. It was shown that non-destructive determination of the briquette was possible with NIR imaging. The hard-gelatin capsule shell was transparent to NIR radiation, and thus at a single wavelength it could be seen if a briquette was present or not. The briquette is important for correct dissolution of some products and, in this

case, its presence is checked in a destructive way. There, NIR imaging could enable fast, non-destructive in-process controls in the production area through the installation of a single-wavelength NIR camera and visual analysis of the NIR images, thus replacing the destructive in-process controls that are in use. A possible way to automation via edge and line detection algorithms was pointed out.

NIR imaging was also applied to study the distribution of API in a low-dosage tablet product. Images from tablet quarters and layers were compared qualitatively; the results were in accordance with classical wet-chemical results. The penetration depth of the NIR radiation into the tablets was investigated to estimate the analyzed sample size. The results of this study showed that NIR imaging has a certain potential for analyses of low-dosage tablets, however, the analysis was only qualitative. Quantitative analyses are not yet possible, but may become possible with further development of the technique and the computation tools. Overall, the method would probably be more useful in a development or up-scaling environment than in production.

Low-dosage tablets were also analyzed by TPS and TPI. In both cases, determination of the API was not possible. The content was below the limit of detection, or the measurement was saturated, and the influence of lactose was too strong. The experiments indicated that, at the moment, TPS and TPI are not adequate for the analysis of low-dosage tablets. However, as it depends on the characteristics of the products, i.e. the spectra of the API and the excipients, detection might nevertheless be possible for other low-dosage products; this would have to be investigated individually for each product.

TPI proved very valuable for analysis of coating thickness and uniformity. The fast and non-destructive method provided direct thickness values and was able to show inter- and intra-batch differences as well as inter- and intra-tablet differences. The monitoring of the coating process was possible. But limits of the technique were also shown: thin coating layers could not be detected, and owing to the rather low spatial resolution it was difficult to detect small cracks and to indicate the correct coating thickness on the embossing. Overall, TPI is a very promising technique with potential for at-line measurements.

NIR imaging was used to analyze the film-coat of tablets too. The results were compared with TPI results. Both techniques provided useful data for the monitoring of coating processes. The strength of TPI is surely that it provides direct thickness data whereas NIR imaging is an indirect method. But the resolution, both spatial and in depth, was better with NIR imaging. Thus, a combination of the two techniques could be very valuable. At-line or even on-line analysis in a production environment could be possible. However, both methods could be more valuable in development or up-scaling.

LIBS was not in the focus of this work; however, this destructive technique was investigated for comparison with the other methods. In a tablet, i.e. an organic matrix, LIBS is mainly able to detect hetero-atoms and metals. Thus, the information it provided on coating thickness and lubricant distribution was interesting, but it was not able to give information about the API in the low-dosage tablets as the molecule in the API did not contain hetero-atoms or metals. The results of this study indicated that the technique can be valuable for a fast, first estimation where hetero-atoms or metals are present, but for the presented questions, TPI and NIR imaging were superior.

This work demonstrated that each of the examined techniques has advantages and disadvantages; there is no technology that can solve everything. The choice of the technique depends very much of the question and the product. Therefore, the technique or device has to be tested according to the product and the question, and the results determine further action. It could be interesting, for example, to test TPI and NIR imaging systematically on different film-coated tablets to see how the detection limits vary according to the coating material, or to see which coating material is favored by which technique.

This work can also be the basis for further research on process understanding. It was shown that TPI and NIR imaging are both valuable tools to analyze coating thickness and uniformity, thus enabling monitoring of the coating process. In the named study, samples were taken out of a full-scale coater. One could also analyze samples from a lab-scale or medium-scale coating process. The results could then be compared. Possible differences could give information about differences in the coating process of equipment on

different scales. This would lead to a better process understanding and it would allow the detection of potential scale-up problems due to different equipment and parameters in advance. The same applies to NIR imaging: for example, tablets compressed on different tablet presses could be analyzed. By comparing the results, it might be possible to detect differences.

In the thesis, ideas for at-line and on-line applications are given. Those suggestions require further research. It would surely be interesting to investigate those methods and applications further and possibly proceed with implementation.

An interesting possibility would be the installation of a global central analytical unit within the company. Such a central competence center would be cost-effective and would allow the purchasing of expensive devices for methods like TPI or NIR imaging. The technologies would then be available and of use to all sites of the company. As the technologies are quite sophisticated, the unit would need specialists to work in it. On the one hand, those experts could develop the technologies and methods further, and on the other hand they could support the sites that are using the technologies, develop applications in collaboration with the sites, help with implementation and analyze samples on a service-provider basis.

7

Bibliography

[1] FDA, Guidance for Industry: PAT- A Framework for Innovative Pharmaceutical Development, Manufacturing, and Quality Assurance, (2004).

[2] W. Herschel, Philos. Trans. R. Soc. 90 (1800) 255-283.

[3] D.A. Burns, E.W. Ciurczak, Handbook of Near-Infrared Analysis, Second Edition, Revised and Expanded, Marcel Dekker, New York, 2001.

[4] H.W. Siesler, Y. Ozaki, S. Kawata, H.M. Heise, Near-Infrared Spectroscopy Principles, Instruments, Applications, Wiley -VCH, Weinheim, 2002.

[5] M. Donoso, E.S. Ghaly, Prediction of drug dissolution from tablets using near-infrared diffuse reflectance spectroscopy as a nondestructive method, Pharm. Dev. Technol. 9 (2004) 247-263.

[6] M.P. Freitas, A. Sabadin, L.M. Silva, F.M. Giannotti, D.A. do Couto, E. Tonhi, R.S. Medeiros, G.L. Coco, V.F.T. Russo, J.A. Martins, Prediction of drug dissolution profiles from tablets using NIR diffuse reflectance spectroscopy: A rapid and nondestructive method, J. Pharm. Biomed. Anal. 39 (2005) 17-21.

[7] A. Devay, K. Mayer, S. Pal, I. Antal, Investigation on drug dissolution and particle characteristics of pellets related to manufacturing process variables of high-shear granulation, J. Biochem. Biophys. Methods 69 (2006) 197-205.

[8] M. Otsuka, I. Yamane, Prediction of tablet hardness based on near infrared spectra of raw mixed powders by chemometrics, J. Pharm. Sci. 95 (2006) 1425-1433.

[9] J. Gottfries, H. Depui, M. Fransson, M. Jongeneelen, M. Josefson, F.W. Langkilde, D.T. Witte, Vibrational spectrometry for the assessment of active substance in metoprolol tablets: a comparison between transmission and diffuse reflectance near-infrared spectrometry, J. Pharm. Biomed. Anal. 14 (1996) 1495-1503.

[10] P. Chalus, Y. Roggo, S. Walter, M. Ulmschneider, Near-infrared determination of active substance content in intact low-dosage tablets, Talanta 66 (2005) 1294-1302.

[11] Y.-C. Feng, C.-Q. Hu, Construction of universal quantitative models for determination of roxithromycin and erythromycin ethylsuccinate in tablets from different manufacturers using near infrared reflectance spectroscopy, J. Pharm. Biomed. Anal. 41 (2006) 373-384.

[12] I. Malik, M. Poonacha, J. Moses, R.A. Lodder, Multispectral imaging of tablets in blister packaging, AAPS PharmSciTech 2 (2001) article 9.

[13] T. Herkert, H. Prinz, K.-A. Kovar, One hundred percent online identity check of pharmaceutical products by near-infrared spectroscopy on the packaging line, Eur. J. Pharm. Biopharm. 51 (2001) 9-16.

[14] M. Laasonen, T. Harmia-Pulkkinen, C. Simard, M. Rasanen, H. Vuorela, Determination of the thickness of plastic sheets used in blister packaging by near infrared spectroscopy: development and validation of the method, Eur. J. Pharm. Sci. 21 (2004) 493-500.

[15] J.D. Kirsch, J.K. Drennen, Near-Infrared Spectroscopic Monitoring of the Film Coating Process, Pharm. Res. 13 (1996) 234-237.

[16] M. Andersson, M. Josefson, F.W. Langkilde, K.-G. Wahlund, Monitoring of a film coating process for tablets using near infrared reflectance spectrometry, J. Pharm. Biomed. Anal. 20 (1999) 27-37.

[17] O.Y. Rodionova, L.P. Houmoller, A.L. Pomerantsev, P. Geladi, J. Burger, V.L. Dorofeyev, A.P. Arzamastsev, NIR spectrometry for counterfeit drug detection: A feasibility study, Anal. Chim. Acta 549 (2005) 151-158.

[18] J. Dubois, J.-C. Wolff, J.K. Warrack, J. Schoppelrei, E.N. Lewis, NIR chemical imaging for counterfeit pharmaceutical products analysis, Spectrosc. http://spectroscopymag.findpharma.com/spectroscopy (2007).

[19] D.J. Wargo, J.K. Drennen, Near-infrared spectroscopic characterization of pharmaceutical powder blends, J. Pharm. Biomed. Anal. 14 (1996) 1415-1423.

[20] S.S. Sekulic, H.W. Ward, II, D.R. Brannegan, E.D. Stanley, C.L. Evans, S.T. Sciavolino, P.A. Hailey, P.K. Aldridge, On-Line Monitoring of Powder Blend Homogeneity by Near-Infrared Spectroscopy, Anal. Chem. 68 (1996) 509-513.

[21] A.S. El-Hagrasy, H.R. Morris, F. D'Amico, R.A. Lodder, J.K. Drennen, Near-infrared spectroscopy and imaging for the monitoring of powder blend homogeneity, J. Pharm. Sci. 90 (2001) 1298-1307.

[22] O. Berntsson, L.-G. Danielsson, B. Lagerholm, S. Folestad, Quantitative in-line monitoring of powder blending by near infrared reflection spectroscopy, Powder Technol. 123 (2002) 185-193.

[23] M. Popo, S. Romero-Torres, C. Conde, R.J. Romanach, Blend uniformity analysis using stream sampling and near-infrared spectroscopy, AAPS PharmSciTech 3 (2002) article 24.

[24] E.T.S. Skibsted, H.F.M. Boelens, J.A. Westerhuis, D.T. Witte, A.K. Smilde, Simple assessment of homogeneity in pharmaceutical mixing processes using a near-infrared reflectance probe and control charts, J. Pharm. Biomed. Anal. 41 (2006) 26-35.

[25] P. Frake, D. Greenhalgh, S.M. Grierson, J.M. Hempenstall, D.R. Rudd, Process control and end-point determination of a fluid bed granulation by application of near infra-red spectroscopy, Int. J. Pharm. 151 (1997) 75-80.

[26] J. Rantanen, S. Lehtola, P. Ramet, J.-P. Mannermaa, J. Yliruusi, On-line monitoring of moisture content in an instrumented fluidized bed granulator with a multi-channel NIR moisture sensor, Powder Technol. 99 (1998) 163-170.

[27] J. Rantanen, O. Antikainen, J.-P. Mannermaa, J. Yliruusi, Use of the Near-Infrared Reflectance Method for Measurement of Moisture Content During Granulation, Pharm. Dev. Technol. 5 (2000) 209-217.

[28] J. Rantanen, E. Rasanen, J. Tenhunen, M. Kansakoski, J.-P. Mannermaa, J. Yliruusi, In-line moisture measurement during granulation with a four-wavelength near infrared sensor: an evaluation of particle size and binder effects, Eur. J. Pharm. Biopharm. 50 (2000) 271-276.

[29] J. Rantanen, E. Rasanen, O. Antikainen, J.-P. Mannermaa, J. Yliruusi, In-line moisture measurement during granulation with a four-wavelength near-infrared sensor: an evaluation of process-related variables and a development of non-linear calibration model, Chemom. Intell. Lab. Syst. 56 (2001) 51-58.

[30] W.P. Findlay, G.R. Peck, K.R. Morris, Determination of fluidized bed granulation end point using near-infrared spectroscopy and phenomenological analysis, J. Pharm. Sci. 94 (2005) 604-612.

[31] A. Gupta, G.E. Peck, R.W. Miller, K.R. Morris, Nondestructive measurements of the compact strength and the particle-size distribution after milling of roller compacted powders by near-infrared spectroscopy, J. Pharm. Sci. 93 (2004) 1047-1053.

[32] M. Brülls, S. Folestad, A. Spàren, A. Rasmuson, I*n-Situ* Near-Infrared Spectroscopy Monitoring of the Lyophilization Process, Pharm. Res. 20 (2003) 494-499.

[33] L.R. Hilden, C.J. Pommier, S.I.F. Badawy, E.M. Friedman, NIR chemical imaging to guide/support BMS-561389 tablet formulation development, Int. J. Pharm. 353 (2008) 283-290.

[34] M. Blanco, D. Serrano, On-line monitoring and quantification of a process reaction by near-infrared spectroscopy. Catalysed esterification of butan-1-ol by acetic acid, Analyst 125 (2000) 2059-2064.

[35] O. Berntsson, L.G. Danielsson, M.O. Johansson, S. Folestad, Quantitative determination of content in binary powder mixtures using diffuse reflectance near infrared spectrometry and multivariate analysis, Anal. Chim. Acta 419 (2000) 45-54.

[36] A.D. Trafford, R.D. Jee, A.C. Moffat, P. Graham, A rapid quantitative assay of intact paracetamol tablets by reflectance near-infrared spectroscopy, Analyst 124 (1999) 163-167.

[37] E. Räsänen, N. Sandler, Near infrared spectroscopy in the development of solid dosage forms, J. Pharm. Pharmacol. 59 (2007) 147-159.

[38] A. Candolfi, R. De Maesschalck, D.L. Massart, P.A. Hailey, A.C.E. Harrington, Identification of pharmaceutical excipients using NIR spectroscopy and SIMCA, J. Pharm. Biomed. Anal. 19 (1999) 923-935.

[39] J. Petri, A. Kaunzinger, A. Niemoller, M. Karas, Quality control of tablets by Near Infrared (NIR)-Spectroscopy, Pharmazie 60 (2005) 743-746.

[40] United States Pharmacopoeia USP 30 - National Formulary 25, United States Pharmacopeial Convention, 2007.

[41] K.H. Bauer, K.-H. Frömming, C. Führer, Lehrbuch der Pharmazeutischen Technologie, Wissenschaftliche Verlagsgesellschaft mbH, Stuttgart, 1999.

[42] J.C. Russ, The Image Processing Handbook, CRC Press, Boca Raton, 2002.

[43] European Pharmacopoeia, EDQM, 2008.

[44] P.R. Smith, D.H. Auston, M.C. Nuss, Subpicosecond photoconducting dipole antennas, IEEE J. Quantum Electron. 24 (1988) 255-260.

[45] C. Fattinger, D. Grischkowsky, Terahertz beams, Appl. Phys. Lett. 54 (1989) 490-492.

[46] D.E. Spence, P.N. Kean, W. Sibbett, 60-fsec pulse generation from a self-mode-locked Ti:sapphire laser, Opt. Lett. 16 (1991) 42.

[47] P.F. Taday, I.V. Bradley, D.D. Arnone, M. Pepper, Using Terahertz pulse spectroscopy to study the crystalline structure of a drug: a case study of the polymorphs of ranitidine hydrochloride, J. Pharm. Sci. 92 (2003) 831-838.

[48] C.J. Strachan, T. Rades, D.A. Newnham, K.C. Gordon, M. Pepper, P.F. Taday, Using terahertz pulsed spectroscopy to study crystallinity of pharmaceutical materials, Chem. Phys. Lett. 390 (2004) 20-24.

[49] C.J. Strachan, P.F. Taday, D.A. Newnham, K.C. Gordon, J.A. Zeitler, M. Pepper, T. Rades, Using terahertz pulsed spectroscopy to quantify pharmaceutical polymorphism and crystallinity, J. Pharm. Sci. 94 (2005) 837-846.

[50] J.A. Zeitler, D.A. Newnham, P.F. Taday, C.J. Strachan, M. Pepper, K.C. Gordon, T. Rades, Temperature dependent terahertz pulsed spectroscopy of carbamazepine, Thermochim. Acta 436 (2005) 71-77.

[51] P.F. Taday, Applications of terahertz spectroscopy to pharmaceutical sciences, Philos. Transact. A. Math. Phys. Eng. Sci. 362 (2004) 351-363; discussion 363-364.

[52] A.J. Fitzgerald, B.E. Cole, P.F. Taday, Nondestructive analysis of tablet coating thicknesses using terahertz pulsed imaging, J. Pharm. Sci. 94 (2005) 177-183.

[53] J.A. Zeitler, Y. Shen, C. Baker, P.F. Taday, M. Pepper, T. Rades, Analysis of Coating Structures and Interfaces in Solid Oral Dosage Forms by Three Dimensional Terahertz Pulsed Imaging, J. Pharm. Sci. 96 (2006) 330-340.

[54] L. Ho, R. Muller, M. Romer, K.C. Gordon, J. Heinamaki, P. Kleinebudde, M. Pepper, T. Rades, Y.C. Shen, C.J. Strachan, P.F. Taday, J.A. Zeitler, Analysis of sustained-release tablet film coats using terahertz pulsed imaging, J. Control. Release 119 (2007) 253-261.

[55] Y.C. Shen, P.F. Taday, D.A. Newnham, M. Pepper, Chemical mapping using reflection terahertz pulsed imaging, Semicond. Sci. Technol. 20 (2005) S254-S257.

[56] R.P. Cogdill, S.M. Short, R. Forcht, Z. Shi, Y. Shen, P.F. Taday, C.A. Anderson, J.K. Drennen, An efficient method-development strategy for quantitative chemical imaging using terahertz pulse spectroscopy, J. Pharm. Innov. 1 (2006) 63-75.

[57] R. Palermo, R.P. Cogdill, S.M. Short, J.K. Drennen III, P.F. Taday, Density mapping and chemical component calibration development of four-component compacts via terahertz pulsed imaging, J. Pharm. Biomed. Anal. 46 (2008) 36-44.

[58] G. Reich, Potential of Attenuated Total Reflection Infrared and Near-infrared Spectroscopic Imaging for Quality Assurance / Quality Control of Solid Pharmaceutical Dosage Forms, Pharm. Ind. 64 (2002) 870-874.

[59] M. Ruotsalainen, J. Heinamaki, H. Guo, N. Laitinen, J. Yliruusi, A novel technique for imaging film coating defects in the film-core interface and surface of coated tablets, Eur. J. Pharm. Biopharm. 56 (2003) 381-388.

[60] M.D. Mowery, R. Sing, J. Kirsch, A. Razaghi, S. Bechard, R.A. Reed, Rapid at-line analysis of coating thickness and uniformity on tablets using laser induced breakdown spectroscopy, J. Pharm. Biomed. Anal. 28 (2002) 935-943.

[61] S. Romero-Torres, J.D. Perez-Ramos, K.R. Morris, E.R. Grant, Raman spectroscopic measurement of tablet-to-tablet coating variability, J. Pharm. Biomed. Anal. 38 (2005) 270-274.

[62] S. Romero-Torres, J.D. Perez-Ramos, K.R. Morris, E.R. Grant, Raman spectroscopy for tablet coating thickness quantification and coating characterization in the presence of strong fluorescent interference, J. Pharm. Biomed. Anal. 41 (2006) 811-819.

[63] A.S. El-Hagrasy, S.-Y. Chang, D. Desai, S. Kiang, Raman spectroscopy for the determination of coating uniformity of tablets: assessment of product quality and coating pan mixing efficiency during scale-up, J. Pharm. Innov. 1 (2006) 37-42.

[64] J.F. Kauffman, M. Dellibovi, C.R. Cunningham, Raman spectroscopy of coated pharmaceutical tablets and physical models for multivariate calibration to tablet coating thickness, J. Pharm. Biomed. Anal. 43 (2007) 39-48.

[65] J.D. Kirsch, J.K. Drennen, Determination of film-coated tablet parameters by near-infrared spectroscopy, J. Pharm. Biomed. Anal. 13 (1995) 1273-1281.

[66] J.D. Pérez-Ramos, W.P. Findlay, G. Peck, K.R. Morris, Quantitative Analysis of Film Coating in a Pan Coater Based on In-Line Sensor Measurements, AAPS PharmSciTech 6 (2005) E127-E136.

[67] Y. Roggo, N. Jent, A. Edmond, P. Chalus, M. Ulmschneider, Characterizing process effects on pharmaceutical solid forms using near-infrared spectroscopy and infrared imaging, Eur. J. Pharm. Biopharm. 61 (2005) 100-110.

[68] R.C. Lyon, D.S. Lester, E.N. Lewis, E. Lee, L.X. Yu, E.H. Jefferson, A.S. Hussain, Near-Infrared Spectral Imaging for Quality Assurance of Pharmaceutical Products: Analysis of Tablets to Assess Powder Blend Homogeneity, AAPS PharmSciTech 3 (2002) article 17.

[69] F. Clarke, Extracting process-related information from pharmaceutical dosage forms using near infrared microscopy, Vib. Spectrosc. 34 (2004) 25-35.

[70] E.N. Lewis, J.E. Carroll, F. Clarke, A near infrared view of pharmaceutical formulation analysis, NIR news 12 (2001) 16-18.

[71] L. St-Onge, E. Kwong, M. Sabsabi, E.B. Vadas, Quantitative analysis of pharmaceutical products by laser-induced breakdown spectroscopy, Spectrochim. Acta B 57 (2002) 1131-1140.

[72] W.-B. Lee, J. Wu, Y.-I. Lee, J. Sneddon, Recent Applications of Laser-Induced Breakdown Spectrometry: A Review of Material Approaches, Applied Spectroscopy Reviews 39 (2004) 27-97.

[73] D.J.O. Orzi, G.M. Bilmes, Identification and Measurement of Dirt Composition of Manufactured Steel Plates Using Laser-Induced Breakdown Spectroscopy, Appl. Spectrosc. 58 (2004) 1475-1480.

[74] A.I. Whitehouse, Laser-induced breakdown spectroscopy and its application to the remote characterisation of hazardous materials, Spectrosc. Eur. 18 (2006) 14-20.

[75] L. St-Onge, J.-F. Archambault, E. Kwong, M. Sabsabi, E.B. Vadasc, Rapid quantitative analysis of magnesium stearate in tablets using laserinduced breakdown spectroscopy, J. Pharm. Pharm. Sci. 8 (2005) 272-288.

[76] R.L. Green, M.D. Mowery, J.A. Good, J.P. Higgins, S.M. Arrivo, K. McColough, A. Mateos, R.A. Reed, Comparison of Near-Infrared and Laser-Induced Breakdown Spectroscopy for Determination of Magnesium Stearate in Pharmaceutical Powders and Solid Dosage Forms, Appl. Spectrosc. 59 (2005) 340-347.

[77] J.-F. Archambault, A. Vintiloìu, E. Kwong, The Effects of Physical Parameters on Laser-Induced Breakdown Spectroscopy Analysis of Intact Tablets, AAPS PharmSciTech 6 (2005) E253-E261.

[78] M.C. Madamba, W.M. Mullett, S. Debnath, E. Kwong, Characterization of Tablet Film Coatings Using a Laser-Induced Breakdown Spectroscopic Technique, AAPS PharmSciTech 8 (2007) Article 103.